Quantum Phase Transition in a Low-Dimensional Weakly Interacting Bose Gas

THÈSE N^O 5205 (2011)

PAR

Luca FONTANESI

EPFL

ÉCOLE POLYTECHNIQUE
FÉDÉRALE DE LAUSANNE

Suisse
2011

To my family

ABSTRACT

This thesis is devoted to the study of the effect of disorder on low-dimensional weakly interacting Bose gases. In particular, the disorder triggers a quantum phase transition in one dimension at zero temperature that is investigated here through the study of the long-range behaviour of the one-body density matrix. An algebraic spatial decay of the coherence marks the quasicondensate, whereas, in the case of strong disorder, an exponential decay is recovered and it characterizes the insulating Bose-glass phase. This analysis is performed using an extended Bogoliubov theory to treat low dimensional Bose gases within a density-phase approach. A systematic numerical study allowed to draw the phase diagram of 1D weakly interacting bosons. The phase boundary obeys two different power laws between interaction and disorder strength depending on the regime of the gas where the transition occurs. These relations can be explained by means of scaling arguments valid in the white noise limit and in the Thomas-Fermi regime of the Bose gas. The phase transition to a quasicondensed phase comes along with the onset of superfluidity: the inspection of the superfluid fraction of the gas is consistent with these predictions for the boundary. The finite temperature case and the scenario in two dimensions are briefly discussed.

The quantum phase transition is caused by low-energy phase fluctuations that destroy the quasi-long-range order characterizing the uniform system. Within the approach presented here, the phase fluctuations are identified as the low-lying Bogoliubov modes. Their properties have been investigated in detail to understand which changes trigger the phase transition and we found that the transition to the insulating phase is accompanied by a diverging density of states and a localization length, measured through the inverse participation ratio, that diverges as a power-law with power -1 for vanishing energy.

The fragmentation of the gas is also studied: this notion is very often associated with the onset of the insulating phase. The characterization of the density fragmentation is performed by analyzing the probability distribution of the density. A density profile is defined as fragmented when the probability distribution at vanishing density is finite or divergent and this happens for a gas in the Bose-glass phase. On the contrary, the superfluid phase is characterized by a zero limiting probability of having vanishing densities. This definition is derived analytically, and confirmed by a numerical study. This fragmentation criterion is particularly suited for detecting the phase transition in experiments: when a harmonic trap is included, the transition to the insulating phase can be extracted from the statistics of the local density distribution.

RIASSUNTO

Questa tesi è dedicata allo studio dell'effetto del disordine su un gas di bosoni debolmente interagenti in bassa dimensionalità. In 1D non avviene condensazione di Bose-Einstein, ma a temperatura zero il gas è in una fase superfluida, nota come quasicondensato e caratterizzata da una matrice densità ad un corpo che decade con una legge di potenza in funzione della distanza. La presenza del disordine può innescare una transizione di fase quantistica da superfluido ad isolante e nel caso dominato dal disordine, la matrice densità ad un corpo presenta un decadimento esponenziale che contraddistingue la fase isolante, anche chiamata "Bose Glass". In questo lavoro, un gas di bosoni unidimensionale viene descritto tramite un approccio di campo medio espresso nel formalismo fase-densità: la transizione di fase viene individuata analizzando il comportamento a lunga distanza della matrice densità e quantificando la frazione superfluida del gas. Questo consente di tracciare un diagramma di fase in funzione di disordine ed interazione: la linea di demarcazione tra le due fasi quantistiche segue due diverse leggi di potenza che dipendono unicamente del regime in cui il gas si trova. Queste relazioni trovano un'elegante spiegazione utilizzando leggi di scala valide nel regime di disordine non correlato (rumore bianco) e nel regime di Thomas-Fermi.

Lo stato quasicondensato è caratterizzato dalla presenza di ordine a lunga portata che, in presenza di forte disordine, viene annullato dalle fluttuazioni di fase a bassa energia, responsabili della transizione di fase. Nel contesto fase-densità tali fluttuazioni sono identificate con i modi di Bogoliubov a bassa energia. Per comprendere in dettaglio cosa provoca la trasizione di fase ne abbiamo studiato le proprietà. L'analisi numerica ha rivelato che la transizione alla fase isolante è accompagnata dalla divergenza della densità di stati dei modi di Bogoliubov e che la loro lunghezza di localizzazione diverge con una legge di potenza con esponente -1 a bassa energia.

Infine abbiamo studiato la frammentazione del profilo di densità del gas. Questo concetto viene spesso associato all'insorgenza della fase isolante, ma fino ad ora non è stata fornita né una chiara definizione di frammentazione né una connessione con la transizione di fase. Un profilo di densità si definisce frammentato quanto la distribuzione di probabilità della densità ha un valore finito o divergente nel limite di densità zero e questo avviene per una gas nella fase isolante. Al contrario, la fase superfluida è caratterizzata da una probabilità nulla di avere densità zero. Tale definizione è derivata analiticamente e confermata da uno studio numerico. Questo criterio può essere utilizzato sperimentalmente per stabilire la transizione di fase grazie ad uno studio statistico sulla distribuzione di densità locale del gas di bosoni.

CONTENTS

INTRODUCTION

"We shall not cease from exploration
And the end of all our exploring
Will be to arrive where we started
And know the place for the first time."

T.S. ELIOT, *Little Gidding* in *Four Quartets*

The topic of Bose-Einstein condensation defines unquestionably one among the most active research domains both in experimental and theoretical physics. Since its first observation in 1995 [Davis et al., 1995, Anderson et al., 1995], realized with ultracold atoms, the scientific community has devoted growing attention to this subject.

In recent times, a special interest in low-dimensional systems was developed. The confinement of the system to reduced dimensionality allows to achieve strongly correlated regimes in dilute gases and to study configurations where the role of interaction and of the underlying potential are emphasized. In addition, the study of 1D physics can improve the understanding of the phenomenology in higher dimensionality thanks to the combination of analytical calculations and numerical results.

The Mermin-Wagner theorem states that there can be no long-range order in one and two dimensional systems, hence no condensation. This is due to large phase fluctuations at long wavelengths, which destroy long-range coherence. In the 2-D case, this happens at any finite temperature, while Bose-Einstein condensation still arises at zero temperature. At low temperature instead, *quasicondensation* (condensation with fluctuating phase) occurs, marked by a power-law decay of the one-body spatial correlation function. This system displays a phonon-like energy-momentum spectrum and thus superfluidity. At a finite critical temperature a transition, named after Berezinski-Kosterlitz-Thouless (BKT), is triggered by the spontaneous formation of vortex-antivortex pairs that destroy superfluidity [Hadzibabic et al., 2006, Schweikhard et al., 2007]. For a 1D Bose gas, the situation is even more restrictive, with quasicondensation occurring at zero temperature only, while an exponential decay of the spatial correlation occurs at any finite temperature. This scenario is valid for uniform systems in the thermodynamic limit. Spatial confinement or disorder are expected to dramatically change the critical behaviour.

The effect of disorder on quantum systems is a subject of both fundamental and practical interest. Since the seminal work of Anderson [Anderson, 1958], it has become

clear that what seems at first sight a nuisance is in fact a source of very rich physical behavior. Disorder is not just a perturbation of the wave functions: in 3D it produces localized single-particle states up to some critical energy called mobility edge. In lower dimensions, no mobility edge exists and all states are localized. In the context of solid state physics, the fermionic problem is the most relevant one, but thanks to the enormous progress in experimental control over ultracold atomic gases, culminated with the experimental observation of Anderson localization in 1D bosonic systems with vanishing interaction [Billy et al., 2008, Roati et al., 2008], the problem of the disordered Bose gas has become a subject of a vigorous research activity as well.

A single particle picture can be a good approximation of a dilute gas, but in practice interactions between particles play often a crucial role in the localization-delocalization of bosons. In presence of a lattice, for sufficiently strong interaction, bosons freeze on single lattice sites forming a Mott-insulator [Fisher et al., 1989]. This mechanism of localization, recently observed in optical lattices of different dimensionality [Greiner et al., 2002, Stöferle et al., 2004, Spielman et al., 2007], is due to the repulsive interaction between particles. On the other hand, many-body interactions, in the case of Bose particles, may also induce a phase transition to a superfluid state.

The theoretical interest in this phase transition dates back to the eighties and a variety of theoretical techniques have been used to tackle the problem. There are two main regimes that have been considered, one marked by weak disorder and arbitrary interactions, the other characterized by weak interactions and arbitrary disorder. The former has been the object of the first investigations: using a renormalization group analysis, Giamarchi and Schultz [Giamarchi & Schulz, 1988] were able to study the quantum phase transition in the limit of weak disorder in one dimension. The picture emerging from this analysis was that for a finite amount of disorder, a minimal strength of interactions is required to break the Anderson localization, but that for too strong interactions, the system is driven into a strongly correlated localized phase. Their renormalization group approach was able to study the latter phase transition quantitatively, but it could not be clarified whether the transition at the weak interaction side is of the same nature. The interplay between periodic and disordered potentials was first addressed in the seminal work by Fisher *et al.* [Fisher et al., 1989], where the insulating disordered phase, named *Bose glass*, was contrasted to the Mott insulator by its compressible nature and to the superfluid phase by its vanishing superfluid stiffness. Quantum Monte Carlo [Prokof'ev & Svistunov, 1998] and density matrix renormalization group [Rapsch et al., 1999] studies have investigated in detail the disorder-interaction phase diagram in the limit of strong interactions. The physics of low dimensional degenerate Bose gases and the notion of disorder are introduced in Chapter 1, together with a brief review of the state of the art on the role of disorder on interacting bosons.

The versatility and tunability of ultracold atomic systems have motivated, in recent years, the study of this fundamental phenomenon in low-dimensional disordered Bose gases (e.g. see [Modugno, 2010, Sanchez-Palencia & Lewenstein, 2010] and references therein), for which however neither the superfluid fraction nor the one-body density matrix are easily accessible in experiments. There were experimental efforts to reach the Bose

glass phase coming from the strongly correlated phase [Fallani et al., 2007, Pasienski et al., 2010]. On the other hand, several experimental works have recently addressed the quite different regime where the gas is in the weakly interacting limit and with many particles in each potential minimum [Deissler et al., 2010, Chen et al., 2008, Clément et al., 2008]. For this reason, the superfluid-insulator phase transition in the weakly interacting regime has been recently subject of intense theoretical analysis (see e.g. [Altman et al., 2004, Lugan et al., 2007a, Nattermann & Pokrovsky, 2008]), but a clear quantitative study of the phase diagram and of the phenomenology triggering the phase transition is still lacking. In this thesis we want to give a clear picture of the quantum phase transition occurring in the weakly interacting regime, studying quantitatively the disorder-interaction phase diagram. We will mainly restrict to the one dimensional case where the limit of weak interaction is attained for large bosonic densities [Lieb & Liniger, 1963].

Within the weak interaction limit, the theoretical description of the Bose gas can be performed in a first approximation by means of the Bogoliubov approach. On the theoretical side, due to the important role played by fluctuations, the low-dimensional Bose gas represents a very challenging problem, contrarily to the 3-D case where approximate symmetry-breaking models (e.g. Bogoliubov or Popov) are quite reliable. The pathologies that Bogoliubov shows in low dimensionality, due to the absence of a condensate, are solved by using an extended Bogoliubov method [Mora & Castin, 2003] presented in Chapter 2, developed to treat low dimensional Bose gases by defining the problem on a grid. Being a mean field model, its predictions become accurate for large densities and are exact for infinite densities and vanishing coupling constant. In this framework, the solution of the bosonic problem is given by a Gross Pitaevskii equation describing the ground state and two coupled Bogoliubov-de Gennes equations for the excitations.

The quantum phase transition is addressed in Chapter 3 by studying the long-range behaviour of the one-body density matrix. The quasicondensed state is marked by an algebraic decay, as opposed to an exponentially decaying coherence typical of the Bose glass phase. This distinction allows to draw the interaction-disorder phase diagram, also confirmed by the study of the superfluid fraction of the gas. The phase boundary is characterized by two power-law relations in the disorder-interaction phase diagram, depending on the regime of the gas where the transition occurs. In particular, when the correlation length is much smaller than the healing length the role of the disorder is analogous to that of a white noise potential and the critical disorder and interaction are related by a 3/4-power-law relation. In the opposite limit the gas enters the Thomas-Fermi regime and the relation becomes linear. These two dependencies can be explained through scaling arguments.

As the phase transition is triggered by long-range phase fluctuations, we focus on the behaviour of the low-energy Bogoliubov modes to understand which properties undergo substantial changes and cause the loss of long-range order. The density of states is constant in the superfluid phase, as for phonons in random chains [Ziman, 1982]; in the Bose glass phase, a divergence of the low energy density of states is numerically identified, in contrast to the common belief [Fisher et al., 1989]. The localization of the Bogoliubov modes is measured via the inverse participation ratio and it always exhibits a power-

law divergence at low-energy, E^α. The superfluid is characterized by $1 < \alpha < 2$, whereas $0 < \alpha < 1$ characterizes the Bose glass phase. The value $\alpha = 1$ marks the phase boundary, in agreement with recent results obtained via a renormalization group approach [Gurarie et al., 2008].

In chapter 4 the density-fragmentation criterion for the phase transition is presented. The notion of *fragmentation* has been widely used in relation to Bose-Einstein condensation [Nozières, 1995]. In the case of a disordered Bose gas, fragmentation has been frequently evoked as a criterion for the transition from superfluid to Bose glass phase [Lugan et al., 2007a, Deissler et al., 2010]. To our knowledge, however, a rigorous definition of fragmentation of the density profile, and a proof of its relation to the quantum phase of the gas, are still lacking. We define a state fragmented if the probability distribution of its density is non-zero in the limit of vanishing density. We link this criterion to the occurrence of the quantum phase transition with an analytical argument confirmed by numerical results. Several different ways of characterizing the phase transition have recently been discussed (see e.g. [Damski et al., 2003, Delande & Zakrzewski, 2009, Carrasquilla et al., 2010]), contrarily to most of them, this criterion is groundbreaking from the experimental point of view because it paves the way to a determination of the quantum phase of the gas through a local statistical study of the density. This would imply an averaging over disorder realizations to infer properties in the thermodynamic limit instead of requiring long-system sizes or transport measurements.

THE QUANTUM DEGENERATE BOSE GAS

Contents

The physics of ultracold atomic gases has received a growing attention by the scientific community since the first experimental observation of *Bose Einstein condensation* (BEC) in 1995 [Davis et al., 1995, Anderson et al., 1995]. This phenomenon was predicted by Einstein for non-interacting bosons in 1925 and extended to the weakly interacting gas by Bogoliubov, but it has remained very elusive experimentally because of the very low temperatures necessary to reach condensation. The impressive improvements of the cooling techniques has allowed to reach temperatures in the nanoKelvin range and, in 1995, condensation of alkali gases. BEC does not occur in reduced dimensionality because of the enhanced role of phase fluctuations [Mermin & Wagner, 1966]. Nevertheless, at very low temperature, the gas enters a quantum degenerate regime, where Bose statistics still shows an interesting phenomenology known as quasicondensation [Popov, 1972] that comes along with superfluidity.

In parallel, there has been a significant scientific effort in studying the interplay between disorder and quantum mechanics, mainly aimed at understanding the low temperature transport in metals. In particular, Anderson showed that diffusion breaks down for sufficiently strong disorder in 3D and this results in localized states and absence of transport [Anderson, 1958]. This investigation was of fundamental relevance to condensed matter physics because it first explained the notion of insulator. Even for what concerns the physics of disorder, low dimensionality shows some peculiarities and, as was first shown by means of the one-parameter scaling theory of localization, the presence of disorder in 1 and 2D always implies localized single-particle states [Abrahams et al., 1979].

The presence of inter-particle interaction is unavoidable in atomic Bose gases and, in addition, weak repulsion favours the onset of a coherent superfluid (SF) phase. Hence, a crucial point is to understand the interplay between disorder and interaction in determining the quantum phase of the gas. Ultracold Bose gases are an ideal ground to test these many-body quantum effects. In these gases the inter-particle interactions are highly controllable via Feshbach resonances, and allow to explore a variety of regimes ranging from the non-interacting gas – for which Anderson localization was recently observed [Billy et al., 2008, Roati et al., 2008] – to the strongly correlated regime. At the same time, disorder can be easily imprinted and controlled by means of optical potentials.

This thesis is devoted to the study of the interplay of disorder and weak repulsive interaction in low-dimensional Bose gases. To this end, in this introductory chapter the physics of degenerate Bose gases is reviewed in different dimensionalities in Sections 1.1 and 1.2. The notion of disorder is discussed in Section 1.3 by introducing the models of disorder relevant to the present analysis and to experiments with ultracold atoms. In Section 1.4 the present knowledge of the role of disorder on interacting bosons is illustrated.

1.1 BOSE-EINSTEIN CONDENSATION

BEC arises as the macroscopic occupation of a single quantum state. This phenomenon was initially predicted for non-interacting bosons, as presented in Section 1.1.1. The non-interacting case is singular and it was soon realized [Bogoliubov, 1947] that interactions are essential for a correct description of the Bose gas: the weakly-interacting case is analyzed in Section 1.1.2 within a perturbative approach.

An alternative and more general definition of BEC relies on the concept of off-diagonal long-range order (ODLRO) that translates into a one-body density matrix that does not decay to zero at infinite distance (see Section 3.1 for an exhaustive analysis). This criterion, named after Penrose and Onsager [Penrose & Onsager, 1956], holds equally for ideal and interacting gases. In this scenario, the order parameter of the Bose-Einstein phase transition is the lowest eigenvalue of the one-body density matrix, that becomes macroscopic in presence of a condensate [Leggett, 2001].

1.1.1   IDEAL BOSE GAS

Non-interacting bosons are the simplest system to show BEC. The occupation of the single-particle states is described by the Bose distribution

$$f(\epsilon) = \frac{1}{e^{\frac{\epsilon-\mu}{k_B T}} - 1}, \tag{1.1}$$

where ϵ is the energy of the state, μ is the chemical potential, k_B is the Boltzmann constant and T is the temperature. For this quantity to be well defined, the chemical potential has to be smaller than the single-particle ground state energy, E_0. The occupation can be related to the total number of particles N through the density of states (DoS) $D(\epsilon)$ as

$$N(\mu) = \int f(\epsilon)D(\epsilon)\mathrm{d}\epsilon = \int_{E_0}^{\infty} \frac{D(\epsilon)}{e^{\frac{\epsilon-\mu}{k_B T}} - 1}\mathrm{d}\epsilon, \tag{1.2}$$

that is an increasing function of the chemical potential μ. When μ approaches E_0 from smaller values, the occupation number $f(E_0)$ becomes increasingly large: this is the physical phenomenology behind the macroscopic occupation of a single-particle state, i.e. BEC.

Condensation occurs when $\mu \to E_0$ and it can be described by splitting the total number of particles into a sum of an occupation of the excited states N_{ex} and a component, N_0 populating the ground state. If one takes $E_0 = 0$ and inserts the expression for the density of states in three dimensions, $D(\epsilon) = \frac{Vm^{3/2}}{\sqrt{2}\pi^2\hbar^3}\sqrt{\epsilon} = C\sqrt{\epsilon}$, with m the bosonic mass and V the volume, Eq. (1.2) becomes

$$N_{ex}(\mu = 0) = C \int_0^{\infty} \frac{\sqrt{\epsilon}\mathrm{d}\epsilon}{e^{\frac{\epsilon}{k_B T}} - 1}\mathrm{d}\epsilon. \tag{1.3}$$

The critical temperature, below which BEC occurs, can be inferred by imposing that the population in the excited states equals the total number of particles. One then obtains

$$N = C\Gamma(\alpha)\zeta(\alpha)(k_B T_C)^\alpha, \quad \text{and} \quad k_B T_C = \left[\frac{N}{C\Gamma(\alpha)\zeta(\alpha)}\right]^{\frac{1}{\alpha}} \tag{1.4}$$

where $\alpha = 3/2$, $\Gamma(\alpha)$ is the Euler gamma function and $\zeta(\alpha) = \sum_{n=1}^{\infty} n^{-\alpha}$ is the Riemann zeta function. By lowering the temperature – or, alternatively, by increasing the total number of bosons at constant temperature – a finite number of particles goes into the ground state populating the condensate. The temperature dependence of the condensate fraction, $N_0(T) = N - N_{ex}(T)$, can be evaluated by computing the population of excited particles,

$$N_{ex} = C\Gamma(3/2)\zeta(3/2)(k_B T)^{3/2}, \qquad N_0 = N\left[1 - \left(\frac{T}{T_c}\right)^{3/2}\right]. \tag{1.5}$$

This model provides an easy intuitive introduction to the concept of BEC. However, the lack of interactions between particles leads to some inconsistencies in the theory, such

as infinite compressibility in presence of a condensate. Bogoliubov developed a theory that takes into account weak two-body interactions between particles in a perturbative way [Bogoliubov, 1947]. This approach is reviewed in the next section.

1.1.2 Weakly interacting gas

In the case of bosons, in the absence of Pauli exclusion, interactions have to be considered to avoid an unphysical collapse to infinite density. The starting point to describe a system of N interacting bosons is its many body Hamiltonian

$$\hat{H} = \int d\mathbf{r}\hat{\Psi}^\dagger(\mathbf{r}) \left[\frac{\hbar^2}{2m}\nabla^2 + V(\mathbf{r}) \right] \hat{\Psi}(\mathbf{r}) + \frac{1}{2}\int d\mathbf{r}d\mathbf{r}'\hat{\Psi}^\dagger(\mathbf{r})\hat{\Psi}^\dagger(\mathbf{r}')U(\mathbf{r}-\mathbf{r}')\hat{\Psi}(\mathbf{r}')\hat{\Psi}(\mathbf{r}), \quad (1.6)$$

where V is the external potential, U is the two-body interaction, $\hat{\Psi}^\dagger(\mathbf{r})$ and $\hat{\Psi}(\mathbf{r})$ are the boson creation and annihilation operators for a particle at a position $\mathbf{r}$, obeying the commutation relations

$$\left[\hat{\Psi}(\mathbf{r}), \hat{\Psi}^\dagger(\mathbf{r}')\right] = \delta(\mathbf{r} - \mathbf{r}'),$$
$$\left[\hat{\Psi}(\mathbf{r}), \hat{\Psi}(\mathbf{r}')\right] = \left[\hat{\Psi}^\dagger(\mathbf{r}), \hat{\Psi}^\dagger(\mathbf{r}')\right] = 0. \quad (1.7)$$

The basic idea behind Bogoliubov approach is the separation of the field operator in a classical macroscopic part representing the condensate Ψ_0 and a perturbative quantum correction accounting for fluctuations $\delta\hat{\Psi}$. Here we discuss directly a generalization of the Bogoliubov theory suitable to describe non-uniform configurations [Fetter, 1972].

The field operator can be written in second quantization in terms of the single particle wavefunctions, Ψ_α, as $\hat{\Psi}(\mathbf{r}) = \sum_\alpha \Psi_\alpha(\mathbf{r})\hat{a}_\alpha$, where the $\hat{a}_\alpha$'s are the single-particle annihilation operators that obey bosonic commutation rules, $[\hat{a}_\alpha, \hat{a}_\beta^\dagger] = \delta_{\alpha,\beta}$. A Bose condensed gas is characterized by a macroscopic occupation of a single-particle state, namely the condensed part $\Psi_0(r)\hat{a}_0$. In other words, BEC occurs when the population of this state, N_0, satisfies $N - N_0 \ll N_0$ and N_0 is of the order of the total number of particles N. In this limit, the unitary commutator between $\hat{a}_0$ and $\hat{a}_0^\dagger$ can be neglected with respect to $\hat{a}_0^\dagger\hat{a}_0 = N_0 \gg 1$ and these operators can be well approximated by c-numbers as $\hat{a}_0 = \hat{a}_0^\dagger = \sqrt{N_0}$. One can rewrite the field operator as

$$\hat{\Psi}(\mathbf{r}) = \Psi_0(\mathbf{r})\sqrt{N_0} + \sum_{\alpha\neq0} \Psi_\alpha(\mathbf{r})\hat{a}_\alpha. \quad (1.8)$$

In a uniform gas the problem can be equivalently formulated in k-space and condensation typically occurs in the zero-momentum state, i.e. $\Psi_0 = 1/\sqrt{V}$, that satisfies the normalization condition $\int |\Psi_0|^2 d\mathbf{r} = 1$. The general expression for the field operator becomes $\hat{\Psi}(\mathbf{r}) = \sqrt{N_0/V} + \delta\hat{\Psi}(\mathbf{r})$, where $\delta\hat{\Psi}(\mathbf{r})$ is the perturbation due to the excited states. Ψ_0 can be interpreted as the order parameter of the Bose-Einstein phase transition and vanishes above the critical temperature.

Provided that the perturbation entering the decomposition of the field operator is small, an equation for the field at the lowest order, Ψ_0, can be obtained. If the gas is dilute, one can consider only two-body collisions that are parametrized by the s-wave scattering length a, dominant in the dilute regime. This is equivalent to replacing the interaction term in Eq. (1.6) with an effective contact interaction potential of the form $U(\mathbf{r}-\mathbf{r}') = g\delta(\mathbf{r}'-\mathbf{r})$. In 3D, the coupling constant g is related to the scattering length via $g = 4\pi\hbar^2 a/m$. The minimization of the operator $\hat{H} - \mu\hat{N}$ results in the time-independent Gross-Pitaevskii equation for the ground state wavefunction [Pitaevskii, 1961, Gross, 1963]

$$-\frac{\hbar^2}{2m}\nabla^2\Psi_0(\mathbf{r}) + V(r)\Psi_0(\mathbf{r}) + gN_0|\Psi_0(\mathbf{r})|^2\Psi_0(\mathbf{r}) = \mu\Psi_0(\mathbf{r}). \tag{1.9}$$

This is a nonlinear Schrödinger equation, where the nonlinear term is given by the particle interaction and it is proportional to the condensate density $|\Psi_0(\mathbf{r})|^2$. The effective potential acting on the particles is the combination of the external potential and a non-linear term, that takes into account the mean-field effect of the other bosons.

As Ψ_0 minimizes the energy functional, the first order correction in the fluctuation term vanishes in the Hamiltonian (1.6). The lowest non-zero correction to the ground state comes from the quadratic term in the fluctuations: the eigenstates of the quadratic problem represent the elementary excitations of the system. This expansion is performed by looking for solutions of the form of plane waves. From the Gross-Pitaevskii equation, one obtains, to linear order, the set of Bogoliubov-de Gennes coupled equations for the excitations [De Gennes, 1966]

$$\left(\hat{H}_0 + 2gN_0|\Psi_0(\mathbf{r})|^2 - \mu\right)u_j(\mathbf{r}) + gN_0|\Psi_0(\mathbf{r})|^2 v_j(\mathbf{r}) = E_j u_j(\mathbf{r}),$$
$$-gN_0|\Psi_0(\mathbf{r})|^2 u_j(\mathbf{r}) - \left(\hat{H}_0 + 2gN_0|\Psi_0(\mathbf{r})|^2 - \mu\right)v_j(\mathbf{r}) = E_j v_j(\mathbf{r}). \tag{1.10}$$

Here $u_j(\mathbf{r})$ and $v_j(\mathbf{r})$ represent the Bogoliubov modes and E_j's are their energies. This procedure gives the same results as the diagonalization of the quadratic Bogoliubov Hamiltonian through the quasiparticle operators defined in terms of the Bose operators $\hat{\alpha}_j$ and $\hat{\alpha}_j^\dagger$ as

$$\delta\hat{\Psi}(\mathbf{r}) = \sum_{j\neq 0}[u_j(\mathbf{r})\hat{\alpha}_j + v_j^*(\mathbf{r})\hat{\alpha}_j^\dagger]. \tag{1.11}$$

Imposing the Bose commutation rules gives the normalization condition

$$\int d\mathbf{r}[u_i(\mathbf{r})u_j^*(\mathbf{r}) - v_i^*(\mathbf{r})v_j(\mathbf{r})] = \delta_{ij}. \tag{1.12}$$

In the uniform case, the excitation spectrum follows the typical linear Bogoliubov dispersion and the amplitudes $u_i(r)$ and $v_i(r)$ are plane waves [Bogoliubov, 1947]. Interactions between quasi-particles, involving higher order terms in the Hamiltonian, are neglected in the Bogoliubov approximation.

Within the Bogoliubov formalism one can easily write the expression for the one-body density matrix, that reads

$$
\begin{aligned}
G_{(1)}(\mathbf{r}, \mathbf{r}') &= \langle \hat{\Psi}^\dagger(\mathbf{r}) \Psi(\mathbf{r}') \rangle \\
&= \phi_0^*(\mathbf{r}) \phi_0(\mathbf{r}') + \sum_{j \neq 0} [u_j^*(\mathbf{r}) u_j(\mathbf{r}') p_j + v_j(\mathbf{r}) v_j^*(\mathbf{r}')(1 + p_j)]
\end{aligned}
\tag{1.13}
$$

where p_j denotes the thermal population of the Bose gas, $p_j = [e^{E_j/k_B T} - 1]^{-1}$. The diagonal of this matrix gives the density distribution of the Bose gas, while the off-diagonal terms represent the correlations.

DENSITY-PHASE FORMALISM

This problem can be reformulated in the so-called *density-phase* representation, completely equivalent to the one exposed in the previous section, that turns to be very useful in low dimensionality. In this formulation the field operator can be expressed as $\hat{\Psi}(r) = e^{i\hat{\theta}(r)} \sqrt{\hat{\rho}(r)}$, where $\hat{\rho}(r)$ and $\hat{\theta}(r)$ are respectively the density and the phase operators. Assuming small density fluctuation, as expected in the weakly interacting regime [Kane & Kadanoff, 1967], we can apply the Bogoliubov prescription to the density operator, obtaining

$$
\hat{\Psi}(\mathbf{r}) = e^{i\hat{\theta}\mathbf{r}} \sqrt{\rho_0(\mathbf{r}) + \delta\hat{\rho}(\mathbf{r})},
\tag{1.14}
$$

where $\rho_0(\mathbf{r})$ is a c-number representing the average density of bosons at the point $\mathbf{r}$. The bosonic operators are replaced by a density and a phase operator that can be expressed in terms of the previous quantities as

$$
\begin{aligned}
\delta\hat{\rho}(\mathbf{r}) &= \sum_j [f_j(\mathbf{r})\hat{b}_j + f_j^*(\mathbf{r})\hat{b}_j^\dagger], \\
\hat{\theta}(\mathbf{r}) &= \sum_j [\theta_j(\mathbf{r})\hat{b}_j - \theta_j^*(\mathbf{r})\hat{b}_j^\dagger],
\end{aligned}
\tag{1.15}
$$

where the factors f_j and θ_j are linked to the u_j and v_j of the Bogoliubov transformation by

$$
\theta_j(\mathbf{r}) = \frac{u_j(\mathbf{r}) - v_j(\mathbf{r})}{2i\sqrt{\rho_0}}, \qquad f_j(\mathbf{r}) = \sqrt{\rho_0}[u_j(\mathbf{r}) + v_j(\mathbf{r})].
\tag{1.16}
$$

In the density-phase representation the one-body density matrix takes the form

$$
\begin{aligned}
G_1(\mathbf{r}, \mathbf{r}') &= \langle \hat{\Psi}^\dagger(\mathbf{r}) \Psi(\mathbf{r}') \rangle \\
&= \langle \sqrt{\rho(\mathbf{r})} e^{-i\hat{\theta}(\mathbf{r})} e^{i\hat{\theta}(\mathbf{r}')} \sqrt{\rho(\mathbf{r}')} \rangle \simeq \sqrt{\rho_0(\mathbf{r})\rho_0(\mathbf{r}')} \langle e^{-i\hat{\theta}(\mathbf{r})} e^{i\hat{\theta}(\mathbf{r}')} \rangle,
\end{aligned}
\tag{1.17}
$$

where the last equality relies on the fact that density fluctuations are weak. As the Bogoliubov Hamiltonian is quadratic, we can apply Wick's theorem to compute the expectation

values of the observables and this gives the general property $\langle e^{ix} \rangle = e^{-\langle x^2 \rangle/2}$, where x is a generic linear combination of b-operators. Substituting in equation (1.17) we obtain the expression for the one-body density matrix in the density-phase formalism

$$G_1(\mathbf{r}, \mathbf{r}') = \sqrt{\rho_0(\mathbf{r})\rho_0(\mathbf{r}')} e^{\langle [\hat{\theta}(\mathbf{r}) - \hat{\theta}(\mathbf{r}')]^2 \rangle/2} = \sqrt{\rho_0(\mathbf{r})\rho_0(\mathbf{r}')} e^{\langle [\Delta\theta(\mathbf{r} - \mathbf{r}')]^2 \rangle/2} \tag{1.18}$$

where $\Delta\theta(\mathbf{r} - \mathbf{r}') = \hat{\theta}(\mathbf{r}) - \hat{\theta}(\mathbf{r}')$. The mean squared phase fluctuations appearing in the exponential of Eq. (1.18) can be evaluated at large distance and take the asymptotic form [Popov, 1972, Pitaevskii & Stringari, 2003, Bloch et al., 2008]

$$\frac{\langle [\Delta\theta(\mathbf{r})]^2 \rangle}{2} = \frac{m^2 c}{2\rho} \int \frac{\mathrm{d}^d k}{(2\pi\hbar)^d} \left(p_k + \frac{1}{2} \right) \frac{e^{ik\cdot\mathbf{r}/\hbar}}{k}, \tag{1.19}$$

where c is the sound velocity, $\beta = (k_B T)^{-1}$ and ρ is the total density. In the integral there is a contribution coming from thermal fluctuations linked to the thermal Bose distribution p_k and a term coming from quantum fluctuations. In three dimensions this integral is convergent, therefore, the one-body density matrix in Eq. (1.18) goes to a constant equal to the condensate density at infinite distance, proving the onset of BEC.

1.2   LOW DIMENSIONALITY

The analysis presented in this thesis is mainly concerned with one dimensional systems. Quantum physics in 1D is of particular interest both because some models can be solved analytically and because of the enhanced role played by fluctuations triggered by interaction [Giamarchi, 2004]. Moreover, 1D physics represents a perfect starting point to understand the phenomenology occurring in higher dimensions.

The formalism developed in the previous section can be extended to arbitrary dimensionality, in particular, it can be interesting to apply the previous arguments to the one and two-dimensional gases. For the non-interacting Bose gas, Eq. (1.2) still holds, but the DoS depends on the dimensionality, d, according to $D_d(E) \propto E^{\frac{d}{2}-1}$. It is easy to check that in 1 and 2D the integral in Eq. (1.2) diverges and no condensation is predicted for an ideal low-dimensional gas.

When dealing with weakly interacting low-dimensional Bose gases, because of the relevant role played by phase fluctuations, the density-phase formalism turns out to be very convenient. In this representation the behaviour of the one-body density matrix can be extracted from Eq. (1.18). In one dimension at zero temperature, considering only the quantum contribution, the quadratic quantum fluctuations diverge as a logarithm, implying an algebraic decaying one-body density matrix of the form [Pitaevskii & Stringari, 2003]

$$G_1(r - r') \propto \left(\frac{\xi}{|r - r'|} \right)^{\frac{mc}{2\pi\hbar\rho}}, \tag{1.20}$$

where ξ is the healing length. The algebraic decay of the coherence at long distance implies the absence of ODLRO: there is no condensation in 1D. On the contrary this

functional behaviour marks the onset of *quasicondensation*, i.e. a condensate with fluctuating phase [Popov, 1972] discussed in detail below. The inclusion of finite-temperature contributions induces an exponential decay of the coherence, typical of a gas in the normal phase. This agrees with the conclusions drawn by Yang & Yang who have found no singularities occurring in the thermodynamic functions of the 1D Bose gas, thus, no phase transition at non-zero temperature [Yang & Yang, 1969]. An analogous algebraic decay, with a more general validity, can be obtained from the Lieb-Liniger model and within the hydrodynamic approach described below.

In two dimensions – at low and finite temperature – a power law-decay of the one body density matrix is recovered marking a quasicondensed state, whereas at zero temperature the 2D Bose gas undergoes true condensation.

1.2.1 QUASICONDENSATION AND SUPERFLUIDITY

The algebraic decay of the coherence in one dimension at zero temperature and in 2D below a certain critical temperature is due to the long-range effect of low-energy phase fluctuations that prevent the formation of a BEC. To describe this phenomenon it has been introduced the idea of *quasi-condensate*, i.e. a condensate with fluctuating phase. The behaviour of its one-body density matrix – different from the one of a classical gas – is known as quasi-long range order. This notion found its origin in the seminal work by Popov [Popov, 1972] that studied low-dimensional bosons within a path integral formalism, separating the Bose field in a Bogoliubov-like way between fast and slow-modes. A quasicondensate is a Bose gas in the degenerate regime characterized by reduced density fluctuations and a coherence extending over a length larger than the thermal de-Broglie wavelength and decaying algebraically.

The relation between (quasi-)condensation and superfluidity has been subject of intense debate over the years and for interacting Bose gases these two phenomena are intimately linked [Leggett, 1973, Leggett, 2001]. The occurrence of condensation (or quasi-condensation) is a property based on the one-body density matrix. On the other hand, superfluidity is defined as the response of the fluid to a small velocity field (see Chapter 3.3 for a rigorous definition). Starting from the hydrodynamic Hamiltonian expressed in the density-phase formalism, it can be proven [Bloch et al., 2008] that a finite superfluid fraction, together with the assumption of finite compressibility are sufficient conditions for the existence of BEC (or quasicondensation in low-dimensionality). The presence of ODLRO, on the other hand, is a sufficient condition to have superfluidity (e.g. see [Leggett, 2001, Bloch et al., 2008]). It is important to stress that these statements does not imply that superfluid and quasicondensed fraction coincide. As superfluidity is both sufficient and necessary for quasicondensation, from now on, the words *quasicondensate* and *superfluid* will be used indiscriminately to denote the coherent phase.

On the other hand, an exponential and algebraic decay of $G_1(r)$ means that coherence drops to zero at infinite distance: this denotes the absence of ODLRO in low dimensional Bose systems and the impossibility of attaining BEC according to the Penrose-Onsager criterion. The absence of condensation in $d < 3$ is a manifestation of the Mermin-Wagner

theorem, briefly presented in the next section.

Mermin-Wagner Theorem

The first argument preventing the formation of long-range order in low dimensionality was given by Peierls in 1935 [Peierls, 1935]. A more rigorous argument has been extended to bosons [Hohenberg, 1967] and spin systems [Mermin & Wagner, 1966] and it claims that, in presence of short-ranged interaction, quantum and thermal fluctuations in reduced dimensions are strong enough to prevent the spontaneous break-down of a continuous symmetry (as the $U(1)$ symmetry marking the onset of BEC). An intuitive proof ad absurdum can be given for the two dimensional case. Starting from the hypothesis that at a finite very low temperature T a condensate exists in $\mathbf{k} = 0$, the number of particles in the excited states $\mathbf{k} \neq 0$ is

$$N' = \sum_{\mathbf{k} \neq 0} \tilde{n}_{\mathbf{k}} = \frac{L^2}{4\pi^2} \int \tilde{n}_{\mathbf{k}} \mathrm{d}^2\mathbf{k}, \tag{1.21}$$

where

$$\tilde{n}_{\mathbf{k}} + \frac{1}{2} \geq \frac{k_B T}{\hbar^2 k^2/m} \frac{\rho_0}{\rho}, \tag{1.22}$$

with ρ_0 the density of the condensate. When $k \to 0$ the lower term behaves as $1/k^2$ (from the Bogoliubov k^{-2}-theorem [Bogoliubov, 1960]) and, in 2D, this gives a logarithmic divergence in the integral (1.21) thus the initial assumption has to be wrong and no condensate exists. This argument rules out condensation at finite temperature in one and two dimensions. It can be proven that quantum fluctuations prevent the formation of a condensate in one dimensional systems even at zero temperature [Pitaevskii & Stringari, 1991].

Mean field model

The hypothesis on which Bogoliubov theory relies is invalidated by the absence of a macroscopic occupied state in low-dimensionality. Therefore, even if the standard Bogoliubov theory can be used to compute qualitatively asymptotic quantities in the limit of weak interaction and weak density fluctuations (as shown for the $G_1(r)$) it is corrupted by divergences in the density and phase operators (for a detailed discussion see [Castin, 2004]). Different approaches have tried to extend the Bogoliubov theory to low dimensional gases. First of all, Popov developed a functional integral approach separating the atomic field in a fast and a slow part [Popov, 1983]. Although this method allows to evaluate correctly some physical quantities it is only valid at low energies and the introduction of an arbitrary cutoff entails a loss of generality. The density-phase formalism can still be applied to compute some thermodynamic quantities such as the long-range behaviour of the one-body density matrix, but this method relies on a ultraviolet cutoff that makes its predictions reliable with logarithmic accuracy only at large distances and,

in addition, a non-careful definition of the operators bring some inconsistencies with the Bogoliubov theory in 3D [Shevchenko, 1992]. Some approaches solved the problem developing a theory based on the path integral formalism [Al Khawaja et al., 2002, Andersen et al., 2002].

To describe the Bose gas in this thesis, we adopt a method developed by Mora & Castin [Mora & Castin, 2003], that, expanding the Hamiltonian to the third order in density fluctuations and phase gradient, built a theory that deals properly with low-dimensional Bose gases. This method relies on the introduction of an unphysical grid that allows to correctly define density and phase operators and, differently from Popov's method, treats all the modes on the same footing. This method is successful in describing Bose gases in arbitrary dimensions and it is presented in detail in Chapter 2.

All the methods outlined so far are only valid in the limit of weak interactions. To describe the complete physics of the 1D bosonic systems, different approaches have to be used. In the following section some of the most common methods to describe one dimensional Bose gases are mentioned.

1.2.2 LIEB-LINIGER MODEL

The basic starting point to study one-dimensional bosons with contact interaction is the N-body Hamiltonian

$$H = -\frac{\hbar^2}{2m} \sum_i^N \frac{\partial^2}{\partial x_i^2} + g_0 \sum_{i<j} \delta(x_i - x_j). \tag{1.23}$$

This model is exactly solvable via Bethe ansatz as it has been shown by Lieb and Liniger [Lieb & Liniger, 1963]. They found that this problem is fully determined by the parameter

$$\gamma = \frac{g_0 \rho}{\hbar^2 \rho^2 / 2m} = \frac{m}{\hbar^2} \frac{g_0}{\rho}, \tag{1.24}$$

where $\rho = N/L$ is the density. This parameter measures the interaction strength of the gas, its value being proportional to the ratio between interaction and kinetic energy. The strongly interacting regime is achieved for large γ, i.e. for low densities – an opposite behaviour with respect to the 3D case. In the limit $\gamma \to \infty$ the Hamiltonian describes a gas of impenetrable bosons, also known as Tonks-Girardeau regime. The infinite repulsion imposes that any wavefunction vanishes whenever two particles meet at the same spatial coordinate [Girardeau, 1960]. This constraint is fulfilled by the wavefunction

$$\Psi_B(x_1, x_2, \ldots, x_N) \propto \prod_{i<j} |\sin(\pi |x_i - x_j|/L)|, \tag{1.25}$$

that coincides with the wavefunction of non-interacting spinless fermions: a system of impenetrable bosons can be mapped onto a system of non-interacting fermions and its properties can be extracted accordingly. The single-particle wavefunctions are spatially distinct and extend over a distance determined by the average inter-particle distance

$1/\rho$. The absence of fluctuations in the number of particles implies that the gas does not show long-range coherence and it resembles a gas of classical hard spheres. The chemical potential in this regimes approaches the value $\mu = \pi\hbar\rho^2/(2m)$, independent on the coupling strength, because the energy is of fully kinetic nature.

The opposite limit $\gamma = 0$ corresponds to the non-interacting Bose gas and the regime of weak interaction is attained for small γ that, quite counterintuitively, in 1D corresponds to the high-density limit. In this case the gas has a collective behaviour and can be successfully described by Bogoliubov perturbation theory [Lieb & Liniger, 1963], with a chemical potential taking its mean field value $\mu = g_0\rho$.

A characteristic length scale $\xi = \sqrt{\hbar^2/(m\mu)}$, named healing length, controls the crossover between collective and single-particle behaviour. In the weakly interacting regime the healing length extends over distances much longer than the average inter-particle separation, $\xi \gg 1/n$, whereas in the strong coupling regime these two lengths are comparable. In experiments, the value of γ can be tuned by varying the density or by tuning the scattering length by means of Feshbach resonances [Pollack et al., 2009].

Tomonaga-Luttinger liquid

A very general and convenient way to study the physics of quantum one-dimensional gases has been introduced by Haldane [Haldane, 1981] that gave a universal description of a range of 1D models known as Tomonaga-Luttinger liquids. For what concern bosons, this approach happens to be an hydrodynamic model also known as *bosonization*, based on the density-phase representation of the bosonic field, that parametrizes the problem with a single parameter, the Tomonaga-Luttinger parameter K. This allows to write an effective low-energy quadratic Hamiltonian for the bosonic problem that is valid at any interaction energy. This model revealed to be very effective in the computation of correlation functions and other physical observables, but also in treating the role of strong interaction in presence of an underlying potential, e.g. through perturbative techniques and renormalization [Giamarchi & Schulz, 1987]. The results given by this approach are consistent with the Lieb-Liniger model and the Bogoliubov approach.

1.2.3 Trapped case

Current experiments dealing with low-dimensional Bose gases are mainly performed by confining the ultracold atomic gas by means of magnetic or optical traps. When dealing with one-dimensional configurations, the condition of sufficiently strong transverse confinement guarantees the exclusion of any radial dynamics, while the longitudinal trapping has to be weak so not to affect the 1D phenomenology of the gas.

The Mermin-Wagner theorem prevents the formation of BEC in low dimensionality, but it is strictly valid only for phase transitions occurring in the thermodynamic limit. Current experiments deal with extremely non-ideal conditions, such as a finite number of particles, finite system size, the presence of a trap to confine the atomic cloud and finite temperature. In these conditions, the thermodynamic properties of the gas are subject to significant changes.

It was proved [Bagnato & Kleppner, 1991, Ketterle & van Druten, 1996] that a trapped non-interacting 1D gas can achieve true condensation under suitable conditions of trapping and temperature. This is due to the change in the DoS of the trapped gas and, in particular, to the discreteness of the energy levels introduced by the trap. The inclusion of interaction has been taken into account by Petrov *et.al.* [Petrov et al., 2000]: they found that the phase of an interacting Bose gas in a trap depends on interaction, temperature, trap frequency and number of particles and they obtained the crossover diagram reported in Fig. 1.1. A key parameter to determine the regime of the trapped gas can be defined as

$$\alpha = \frac{mg}{\hbar}\sqrt{\frac{\hbar}{m\omega}}, \tag{1.26}$$

where ω is the trapping frequency. This parameter provides the ratio between the interaction and the trapping energy and it replaces γ (see Eq. (1.24)) in the determination of the regime of the gas. The phases occurring at low-densities are, as in the homogeneous case, a classical gas and a Tonks gas depending on the temperature. At large densities, even if the system is at finite temperature, a quasicondensed phase exists and, at lower temperature, true condensation can be achieved. The crossover between these two is triggered by the enhancement of phase fluctuations due to the temperature. However, the constraint over the temperature turns out to be quite severe with respect to trapping and interaction energies.
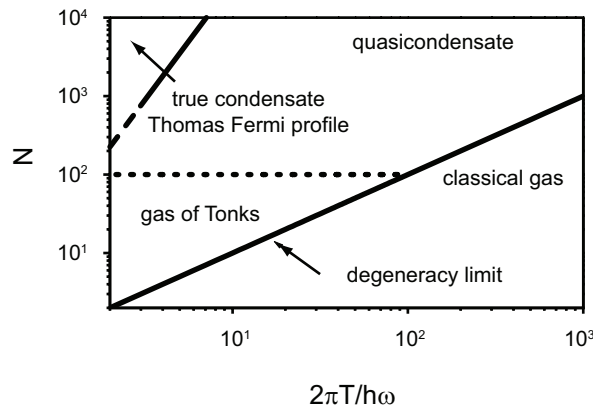
Figure 1.1: Crossover diagram of an interacting 1D Bose gas in presence of a trapping potential extracted from [Petrov et al., 2000].

To summarize, the presence of a trap radically changes the physical description of the Bose gas, allowing the achievement of BEC even in low dimensionality by quenching long-range phase fluctuations. A secondary effect of a confining harmonic potential is the introduction of a spatial inhomogeneity that locally modifies the density profile of the atomic cloud. Disorder has the same local effect of modulating the bosonic density, and, in addition, it can destroy long-range coherence by localizing the wavefunction of collective

excitations as it happens in the non-interacting case. Next section is devoted to the introduction of spatial disorder: some specific types of disorder, relevant to experiments and to the theoretical analysis that follows, are described in detail.

1.3 Disorder

After having discussed the physics of the uniform degenerate Bose gas, here, the notion of *disorder* is introduced. Disorder in quantum systems has received a wide attention by the scientific community mainly since the seminal work of Anderson where it was proven that in 3D below a certain mobility edge the single-particle states are localized because of constructive interference of multiply reflected waves [Anderson, 1958]. Perhaps the most comprehensive study of the effects of disorder is the scaling theory of localization [Abrahams et al., 1979], that confirms the result in 3D and asserts that all the eigenstates of the single-particle problem are localized in lower dimensionality in presence of disorder (even vanishingly small). This phenomenon manifests as the exponential decay of the eigenfunctions on length-scales of the order of the transport mean-free-path. Anderson localization has been recently observed for matter waves in ultracold atomic gases of bosons with vanishing interaction [Roati et al., 2008, Billy et al., 2008]. When dealing with ultracold atomic gases, disorder is usually imprinted externally through the creation of laser-generated optical potentials. Being highly controllable, these potentials are very efficient for the investigation of the physics of disorder, contrarily to its unavoidable presence in solid state systems.

Disorder is considered here as the value of potential energy defined over the spatial coordinate r and independent on time (quenched). It is a continuous variable $V(r)$ characterized by an average value, $\langle V(r) \rangle = 0$ for simplicity, a distribution $P[V]$ and a certain correlation function. The two-point correlation is defined as

$$\langle V(r)V(r') \rangle = \Delta^2 f(r - r') \tag{1.27}$$

where Δ is the amplitude of the potential and $\langle \ldots \rangle$ denotes the average over a statistical ensemble. The distribution $f(r - r')$, also known as autocorrelation function, satisfies $f(0) = 1$ and is characterized by the correlation length η over which f decays to zero (or rather it becomes exponentially small). This length-scale defines a corresponding energy, called *correlation energy*

$$E_c = \frac{\hbar^2}{2m\eta^2}, \tag{1.28}$$

that will turn out to be relevant for the study performed in Chapter 3.

Each disorder type that we consider is assumed to be spatially *homogeneous* in the sense that its properties are translationally invariant on average and, in addition, any statistical correlation within the random potential is supposed to vanish at infinite distance [Lifshitz et al., 1988].

For the sake of generality, most of the analysis in the following chapters is performed considering a gaussian-distributed and gaussian-correlated disorder, presented in Section 1.3.1. Current experiments aiming at the characterization of ultracold atomic gases usually deal with optically-realized disorder such as speckle patterns and quasiperiodic potentials that are described in detail respectively in Sections 1.3.2 and 1.3.3.

1.3.1 GAUSSIAN DISORDER

The numerical analysis presented throughout this thesis are mainly performed in presence of gaussian disorder. The potential is assumed to have zero average, $\langle V(r) \rangle = 0$, and an amplitude defined as $\Delta_g = \sqrt{\langle V^2 \rangle}$. The Gauss-distributed spatial correlation decays to zero at infinite distance and it can be expressed as

$$\langle V(r)V(r') \rangle = \Delta_g^2 e^{-\frac{(r-r')^2}{2\eta_g^2}}, \tag{1.29}$$

where η_g is the correlation length (the subscript g denotes the gaussian potential) and the variable $V(r)$ is Gauss-distributed in energy. In the limit $\eta_g \to 0$ one recovers a gaussian distributed uncorrelated potential

$$\langle V(r)V(r') \rangle = w\delta(r - r'), \tag{1.30}$$

also known as white-noise potential, widely employed to study the physics of disorder (see for instance [Halperin, 1965, Fisher et al., 1989]).

Most of the present experiments are carried out making use of optical potentials such as speckle and quasi-periodic potentials. The use of a gaussian potential for the present analysis is motivated only by a claim of generality, even though the gaussian correlation is consistent with certain experimental realizations [Chen et al., 2008]. This kind of potential reproduces faithfully the distribution of a large number of uncorrelated variables, thanks to the central limit theorem. As the external potential is only treated numerically any analysis could be easily extended to the potentials described below.

> The numerical implementation of the disordered potential is performed on a grid of step ℓ_N fine enough to reproduce the oscillation of the correlated potential ($\eta \gg \ell_N$). The disorder profile is the result of the convolution between an uncorrelated random potential, with a gaussian energy distribution of the amplitude Δ_g, and a spatial gaussian of standard deviation η_g.

> In Fig. 1.2**a**, a sample gaussian disordered profile is shown in units of the correlation energy. The energy distribution of the potential appears in Fig. 1.2**b**: the circles mark the numerical results, obtained by statistical averaging, and they are fitted with a gaussian distribution of standard deviation Δ_g, centered in $E = 0$ (the distribution has $\langle V \rangle = 0$). Fig. 1.2**c** shows the auto-correlation function $f(r - r')$: the numerical results are marked by the circles, while the solid line is a gaussian fit with standard deviation η_g. The spatial coordinate is measured in units of correlation lengths.
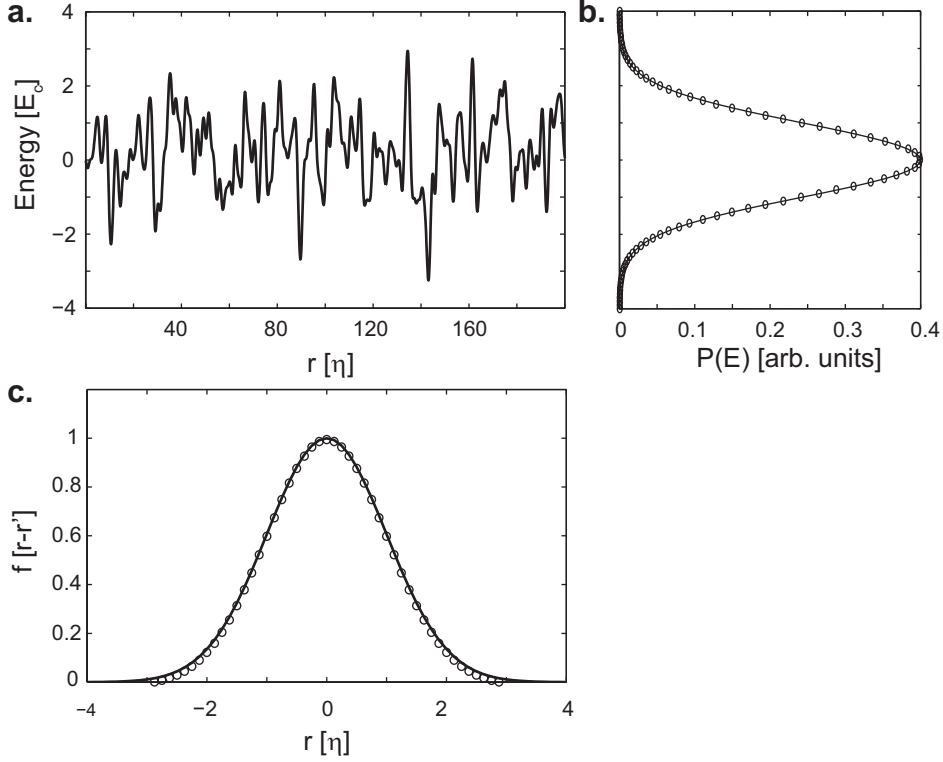
Figure 1.2: a. Sample of a gaussian disorder profile with unitary correlation length η_g and unitary amplitude Δ_g in a system of length $L = 200\ \eta_g$. **b.** Average spectral distribution of the potential: the circles are the results of a numerical average performed over many disorder realizations (equivalent to performing simulations on very large samples), whereas the solid line is a gaussian fit $\propto e^{-E^2/(2\Delta_g^2)}$. The standard deviation of this distribution, Δ_g, denotes the disorder amplitude. **c.** Autocorrelation function $f(r - r')$ in presence of gaussian disorder: the circles are the result of numerical simulations performed on a finite-size system ($L = 10^4\ \eta_g$), while the solid line is a gaussian fit of the form $e^{-r^2/(2\eta_g^2)}$.

Throughout this thesis the amplitude of the disorder, expressed by Δ, and the correlation length of the potential, marked as η, refer to gaussian disorder.

1.3.2 Speckle Disorder

Optical trapping is one of the most common technique to trap atomic gases in low dimensionality. As most of the disorder types presented below, it is an optical potential, i.e. it is generated by means of laser light and it exploits the fact that atoms interact with light through dipole interaction. Considering an atomic transition of frequency ω_T, slightly off-resonance with respect to the laser frequency ω_L ($\delta = \omega_L - \omega_T$ is the detuning), the

atoms experience a potential [Grimm et al., 2000]

$$V_{opt}(r) \propto \frac{I}{\delta},$$ (1.31)

where I is the intensity of the laser. The potential is proportional to the light intensity, but, more remarkably, it changes sign by tuning the laser frequency across the transition: the interaction is repulsive if the laser is blue-detuned ($\delta > 0 \rightarrow V > 0$), attractive in the case of red-detuned light ($\delta < 0 \rightarrow V < 0$).

Speckle patterns are a very common optical way to implement disorder when dealing with ultracold gases [Clément et al., 2006, Chen et al., 2008, Dries et al., 2010, Clément et al., 2008]. Speckle potentials are realized by collecting the coherent laser scattered by a rough plate. In this manner the light acquires spatially random phases and the recollection of the scattered light builds a random interference pattern. The intensity of the laser is linked to the electric field by

$$I = \frac{1}{2}\epsilon|\mathcal{E}(r)|^2,$$ (1.32)

where ϵ is the dielectric constant and $\mathcal{E}(r)$ is the complex electric field. The statistical properties of the intensity pattern can be derived from the distribution of the electric field. The central limit theorem guarantees that a large sum of uncorrelated scatterers gives rise to a gaussian probability distribution for the real and imaginary parts of the electric field, namely

$$P[\mathcal{R}(E), \mathcal{I}(E)] = \frac{1}{2\pi\sigma^2} e^{-\frac{\mathcal{R}(\mathcal{E})^2 + \mathcal{I}(\mathcal{E})^2}{2\sigma^2}},$$ (1.33)

where σ is the standard deviation of the real and imaginary part of the electric field. This reflects on the intensity distribution that takes the form

$$P[I] = \frac{e^{-I/\langle I\rangle}}{\langle I\rangle} \, \Theta[I],$$ (1.34)

where Θ is the Heaviside function. Performing an energy shift $V(r) = V_{opt}(r) - \langle V_{opt}(r)\rangle$ and defining $\Delta_s = \langle V_{opt}\rangle$, the potential $V(r)$ has zero average and a distribution with standard deviation $\sqrt{\langle V^2\rangle} = \Delta_s$, that is related to the intensity profile by $V(r) = \Delta_s(I(r)/\langle I\rangle - 1)$. Its probability distribution follows

$$P[V(r)] = \frac{1}{e|\Delta_s|} \exp\left[-\frac{V(r)}{\Delta_s}\right] \, \Theta\left[\frac{V(r)}{\Delta_s} + 1\right],$$ (1.35)

that is an exponentially decaying function truncated at $V = -\Delta_s$. The sign of the interaction can be controlled by the detuning, δ: this parameter strongly influences the distribution of the potential because a blue-detuned laser creates repulsive speckles, bounded from below, whereas a red-detuned laser gives an attractive disordered potential with an upper bound.

The autocorrelation of a speckle potential, formed from a square aperture, takes the form [Clément et al., 2006, Goodman, 2007, Sanchez-Palencia et al., 2007]

$$\langle V(r)V(r+a)\rangle = \Delta_s^2 \frac{\sin(a/\eta_s)^2}{(a/\eta_s)^2}, \tag{1.36}$$

where η_s is the correlation length. The correlation length and the shape of the correlation function are linked to the existence of a cutoff in k-space introduced by the focusing lens (dependent on the physical parameters of the apparatus) and will be discussed in detail below.

In accordance with the experimental realization, the speckle potential is generated starting from an electric field, defined in real space, with an uniformly distributed random phase (this is true as long as the distance between the scatterers is much longer than the wavelength of the impinging light)

$$E(x) = \sqrt{\frac{\mathcal{I}\pi}{k_c \mathcal{L}}} \sum_{k=-k_c}^{k_c} e^{ikx} e^{i\theta(k)}, \tag{1.37}$$

where $\mathcal{I}$ is the intensity of the impinging light, $\mathcal{L}$ is the length of the scattering plate that gives the quantization in k-space ($\Delta k = 2\pi/\mathcal{L}$), $\theta(k)$ are the random uncorrelated phases in the interval $(-\pi, \pi]$, the distribution in real space is defined on a one dimensional segment and the sum is extended to each point of the grid. The window, of width k_c, is applied on the distribution in Fourier space to obtain the distribution of the disorder as the square of the resulting field in real space. Its correlation length η_s is linked to the cutoff in k-space as $\eta_s = 1/k_c$: the correlation length can be experimentally tuned via the numerical aperture of the focusing lens. In the simulations that follow, η_s is taken as the unit of length, consequently k_c is the unit in Fourier space.

There are different procedures that allow to build computationally a speckle potential (see for instance [Huntley, 1989, Horak et al., 1998]). In the present work the scheme presented above has been followed strictly and it can be shown that in the limit of a large number of scatterers this method is equivalent to the one outlined in the above references [Goodman, 2007].

In what follows, speckle disorder is only treated in Chapter 4.3, where the fragmentation criterion is tested considering realistic conditions. For clarity, when dealing with a speckle potential, the quantities identifying the disorder are labeled by a subscript s (e.g. Δ_s and η_s).

1.3.3 QUASI-PERIODIC POTENTIALS

For completeness here the case of quasi-periodic potential is presented. This optical potential is largely used to study the effects of disorder on quantum systems [Diener

et al., 2001, Fort et al., 2005], even if it shows a phenomenology halfway between a lattice configuration and a disordered system with some peculiar properties linked to its quasi-periodicity.

This disorder is the result of the interference of two lattices with incommensurate wavelengths. Typically there is a primary lattice of amplitude V_1 with a certain periodicity, $d_1 = \pi/k_1$, and a secondary lattice, acting as a perturbation, of amplitude $V_2 \ll V_1$, with incommensurate periodicity $d_2 = \pi/k_2$, where $\beta = k_2/k_1$ is irrational. In finite size system it is sufficient that β is the ratio of two large relatively prime natural numbers. The resulting potential, also known as Harper potential [Harper, 1955], is the sum of these two fields

$$V_Q(r) = V_1 \sin^2(k_1 x) + V_2 \sin^2(k_2 x + \phi), \tag{1.38}$$

where ϕ is an arbitrary phase and the amplitudes of the single fields are controlled by the intensity of the lasers. The secondary lattice does not modify substantially the spatial positions of the minima $r_j \simeq j\pi/k_1$, whereas it shifts their energies in a non-periodic, although deterministic way.

Within the tight binding approximation the Hamiltonian

$$H = -\frac{\hbar^2}{2m}\nabla_r^2 + V_Q(r) \tag{1.39}$$

can be mapped onto the discrete Aubry-André Hamiltonian [Aubry & André, 1980, Modugno, 2009]

$$H = -J\sum_j (c_{j+1}^\dagger c_j + c_j^\dagger c_{j+1}) + \Delta_Q \sum_j \cos(2\pi\beta j + \phi)c_j^\dagger c_j, \tag{1.40}$$

where j labels the lattice site, c_j annihilates a boson on the site j, J is the tunneling energy and Δ_Q is an index of the amplitude of the disorder. These quantities can be linked to the experimental ones [Modugno, 2009, Modugno, 2010] appearing in Eq. (1.38) and, in particular,

$$\Delta_Q \simeq \frac{V_2}{2} e^{-\frac{\beta^2}{\sqrt{V_1/E_{r1}}}}, \tag{1.41}$$

where $E_{r1} = \hbar^2 k_1^2/2m$ is the recoil energy. The argument of the exponential is typically very small and the strength of the disorder is, in good approximation, linear in the amplitude of the secondary lattice. The distribution of the potential in Eq. (1.40), behaves as [Guarrera et al., 2007, Roux et al., 2008]

$$P[E] \propto \frac{1}{\sqrt{\Delta_Q^2 - E^2}}, \tag{1.42}$$

therefore, it is bound and symmetric around $E = 0$ and it diverges in $E = \pm\Delta_Q$.

The correlation function of this potential has an intermediate behaviour between a binary potential and a truly random one, indeed the correlation function is

$$\langle V(r)V(r - r')\rangle = \frac{\Delta_Q^2}{2\pi} \cos{(2\pi\beta r)}. \tag{1.43}$$

and it does not decay to zero when $|r - r'| \to \infty$, as it could be inferred being this potential completely deterministic.

In absence of the perturbing lattice, the solutions of the single-particle problem are known to be extended Bloch states. This feature survives also in presence of the secondary lattice, in fact, differently from the model studied by Anderson [Anderson, 1958], the single-particle problem in presence of a quasi-periodic potential requires a critical amount of disorder for localization [Aubry & André, 1980]. In the case $\beta = (\sqrt{5} - 1)/2$, it can be shown that the model presents a metal-insulator transition for $\Delta_Q/J = 2$. In this sense, quasiperiodic potentials have the peculiarity of showing an intermediate behaviour between commensurate and disordered ones.

1.4   Bosons in disordered media

At this point, all the ingredients to introduce the study of disorder on interacting Bose gases have been presented. The main physical content coming into play is the interplay between disorder and repulsive interaction in determining the quantum phase of the gas.

The interest in the role of disorder was initially triggered by the experimental realization of thin films of superfluid ^4He in porous Vycor glass [Crooker et al., 1983]. Several methods have been used to investigate the effect of disorder in interacting bosonic system. The results presented here have been mainly obtained through the study of Bose-Hubbard model, Josephson junctions model, Tomonaga-Luttinger liquid and mean-field theories.

This section is devoted to the introduction of the main models used to study disorder: the results and the physical phenomenology related to the presence of a non-uniform potential are briefly discussed.

Non-interacting case

Non-interacting one-dimensional bosons at zero temperature condense in the lowest single-particle energy state. Anderson showed that in presence of disorder this state is non-diffusive and localized. In this sense the mere presence of disorder drives a transition from an extended to a localized state. Anderson localization has been recently observed for ultracold bosonic gases with vanishing interaction in presence of speckle and quasiperiodic potentials [Billy et al., 2008, Roati et al., 2008]. The presence of interaction modifies substantially this scenario and the interplay between interaction and disorder in determining the quantum phase of the gas is a very active and open field of condensed matter physics both from the theoretical and the experimental points of view (see [Sanchez-Palencia & Lewenstein, 2010] and references therein).

In presence of interaction the localized single-particle state, where all the particle would condense in the non-interacting case, cannot accommodate a macroscopic number of particles (infinite in the thermodynamic limit) in a finite-size region. Any vanishingly small interaction would make this state unstable, therefore, the non-interacting limit cannot be adopted as a starting point for the description of the interacting case [Jaksch et al., 2008, Cazalilla et al., 2011].

BOSE-HUBBARD MODEL

A common starting point to study the physics of boson in disordered media is the Bose-Hubbard model. This model – defined on a lattice – is described by the Hamiltonian

$$H_{BH} = -J \sum_i \hat{a}_{i+1}^\dagger \hat{a}_i + \hat{a}_i^\dagger \hat{a}_{i+1} + \frac{1}{2}U \sum_i \hat{n}_i(\hat{n}_i - 1) - \sum_i (\varepsilon_i + \mu)\hat{n}_i, \qquad (1.44)$$

where $\hat{a}_i$ and $\hat{a}_i^\dagger$ are operators destroying and creating one boson at the ith lattice site and $\hat{n}_i = \hat{a}_i^\dagger \hat{a}_i$. First-neighbour interaction is taken into account by the tunneling term J, $U > 0$ denotes the on-site interaction, μ is the chemical potential. Disorder is considered in this model through the distribution of ε_i that gives an effective local shift to the chemical potential. A complete model may also include disorder into J and U, but this would not modify radically the present scheme, that already contains the relevant physics of the *dirty bosons problem*. Higher order on-site states can be neglected because at very low temperature only the lowest energy state will be populated. The model represented by the Hamiltonian (1.44) is not exactly solvable, but its phenomenology is quite well understood [Fisher et al., 1989].

This discrete model is well reproduced in experiments by ultracold bosons loaded onto optical lattices. The presence of a lattice is analogous to the discretization of the Bose-Hubbard Hamiltonian and the parameters such as tunneling energy and on-site interaction can be easily tuned by controlling the laser intensity and by means of Feshbach resonances [Jaksch et al., 1998, Bloch et al., 2008].

JOSEPHSON MODEL

Another commonly employed model to describe disordered bosonic media is the Josephson junctions model, also known as quantum rotor [Sachdev, 1999]. This model was initially introduced to describe a regular array of superconducting islands weakly coupled by tunnel junctions. It is described by the Hamiltonian

$$H_J = \sum_{\langle i,j \rangle} J_{ij} \cos(\hat{\phi}_i - \hat{\phi}_j) + \frac{1}{2}U \sum_i \hat{n}_i^2 - \sum_i (\varepsilon_i + \mu)\hat{n}_i, \qquad (1.45)$$

where J_{ij} are the Josephson coupling between the sites i and j and the operators $\hat{n}_i$ and $\hat{\phi}_i$ are the conjugated number and phase operators obeying the commutation relations $[\hat{\phi}_k, \hat{n}_j] = i\delta_{kj}$. In absence of disorder the Hamiltonian describes a periodic system with

a phase uniquely determined by the interplay between on-site energy U and tunneling J. This model can be mapped onto the Bose-Hubbard model by the transformations

$$\hat{a}_i^\dagger \leftrightarrow= \hat{n}_i^{1/2} e^{i\hat{\phi}_i}$$
$$\hat{a}_i \leftrightarrow= e^{-i\hat{\phi}_i} \hat{n}_i^{1/2}, \tag{1.46}$$

but they only agree in the limit of large average site occupancy $\langle \hat{n}_i \rangle \gg 1$.

In this thesis we will rely on this model and its analogy with disorder barriers in the case of a single bosonic Josephson junction (two coupled wells scenario) in Chapter 3.2.1 and in the discussion of fragmentation in Chapter 4. Indeed, we believe that the relevant physical content of disordered bosons is already contained in the phenomenology of the coupled-well problem, where repulsive interaction, tunneling and on-site energy compete in the determination of the thermodynamic properties. Now, we move to the discussion of the different quantum phases arising as solutions of the Bose-Hubbard model.

Superfluid phase

When the tunneling dominates, the bosons form a coherent delocalized state, ideally a SF, of the form

$$|\Psi_N\rangle(U=0) = \frac{1}{\sqrt{N}} \left(\frac{1}{\sqrt{N_L}} \sum_R \hat{a}_R^\dagger \right)^N |0\rangle, \tag{1.47}$$

where N is the number of bosons, N_L the number of lattice sites and $\hat{a}_R^\dagger$ creates a boson at the position R. The tunneling term has a delocalizing effect that affects the kinetic component of the bosons and that reduces the phase fluctuations. This coherent state is a BEC in $D > 1$ and a quasicondensate in $D = 1$. As long as the state is not strongly perturbed by the disorder ε_i or the interaction term U, the superfluidity survives.

Mott insulator

On the contrary, when the tunneling energy vanishes, particles tend to accommodate on different lattice sites: assuming unitary filling, each site has a well defined number of particles ($n = 1$ with no number fluctuations) fixed by the repulsive interaction and the long-range phase coherence is lost. For $J/U = 0$ there is a unit increase in filling at each integer value of μ/U (cfr. Fig. 1.3**a**&**b**). This phase, characterized by particles localized on single sites, is known as *Mott insulator* (MI), in analogy with electronic insulator with half-filled band, and for unitary filling ($N = N_L$) it reads

$$|\Psi_N\rangle(J=0) = \left(\prod_R \hat{a}_R^\dagger \right)^N |0\rangle, \tag{1.48}$$

a product of localized Fock states. This phase is incompressible, implying that a variation in the chemical potential does not entail a density change, and it is characterized by a

gap in the energy spectrum required to overcome the repulsion. In the case of non-integer filling the gas is in the SF phase as long as there is a finite tunneling term, in fact, the fraction of atoms exceeding the integer filling delocalize over the whole system.
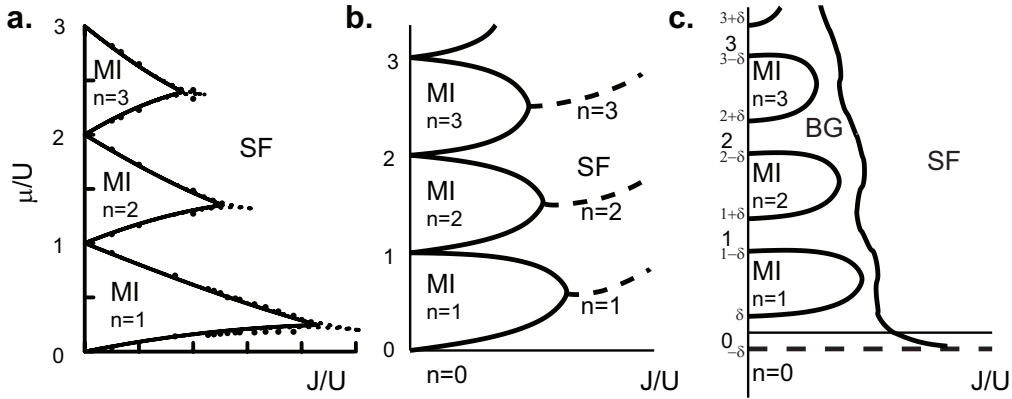

Figure 1.3: a. Phase diagram of the 1D Bose-Hubbard model extracted from [Freericks & Monien, 1996] computed from a third order strong coupling calculation and compared to the results of quantum Monte Carlo simulations [Scalettar et al., 1991]. **b.** Qualitative shape of the phase diagram of the 3D Bose-Hubbard model in absence of disorder first computed in [Fisher et al., 1989] and extracted from [Jaksch et al., 2008]. The Mott-insulator phase lies within lobes in the low J/U-part of the phase diagram that shrink for increasing μ/U. **c.** Qualitative shape of the phase diagram of the disordered 3D Bose-Hubbard model first computed in [Fisher et al., 1989] and extracted from [Jaksch et al., 2008]. An insulating Bose-glass phase intervenes at intermediate values of J/U between SF and MI: even at $J/U = 0$ a BG phase appears between the MI lobes with different filling factor.

This problem has been qualitatively studied via scaling arguments by Fisher *et.al.* in generic dimensions [Fisher et al., 1989] and their resulting phase diagrams are shown in Fig. 1.3**a**&**b** on the $\mu/U - J/U$ plane. Several numerical simulations [Scalettar et al., 1991, Krauth et al., 1991, Prokof'ev & Svistunov, 2004] and certain analytical arguments [Freericks & Monien, 1994, Freericks & Monien, 1996] have confirmed these predictions. The Mott-insulator lobes appear for low values of the tunneling and each of these lobes contains an integer and growing amount of bosons per site. Remarkably, these lobes shrink for larger chemical potential, meaning that largely populated Mott phases occupy a vanishingly small part of the phase-space (this fact has a close connection to the analysis performed in Chapter 3 for infinite density). These results were obtained for a periodic system and the inclusion of disorder, that enriches and complicates this scenario, is the subject of the next section.

DISORDERED CASE

Giamarchi & Schultz [Giamarchi & Schulz, 1987, Giamarchi & Schulz, 1988] studied the 1D problem treating disorder as a perturbation within a renormalization group approach.

They found a universal power law for correlation functions on the transition between a superfluid and a localized phase for a strongly interacting Bose gas. Their approach, based on the hydrodynamic description introduced by Haldane [Haldane, 1981] and known as bosonization, is only valid at large interaction, where weak disorder acts as a perturbation. Their findings are summarized in the schematic phase diagram of Fig. 1.4 in the interaction-disorder plane.
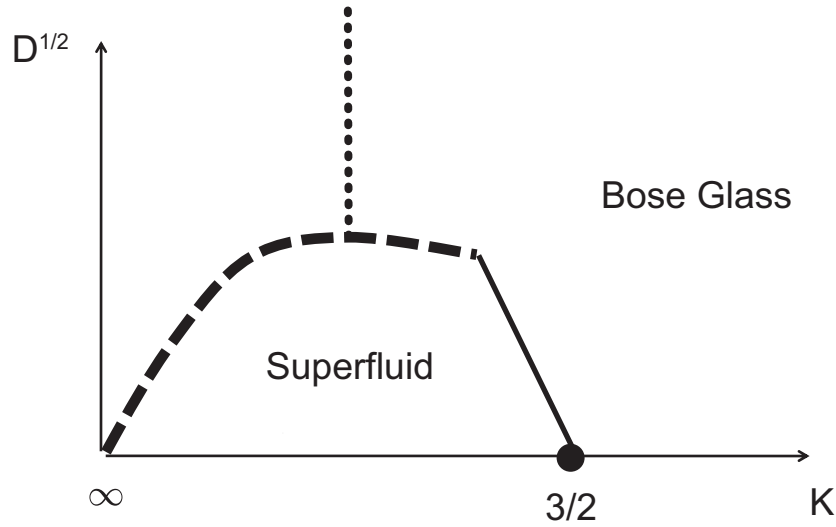

Figure 1.4: Schematic phase diagram of 1D interacting bosons for incommensurate filling derived in Ref. [Giamarchi & Schulz, 1987, Giamarchi & Schulz, 1988] and extracted from [Cazalilla et al., 2011]. K is the Tomonaga Luttinger parameter and is inversely proportional to the strength of interaction ($K = \infty$ for noninteracting bosons). D, on the vertical axis, denotes the disorder strength and it parametrizes an uncorrelated disorder with the autocorrelation $D\delta(r - r')$. The solid line is the universal transition line computed in [Giamarchi & Schulz, 1987] via renormalization group approach. The authors claim that the phase boundary has to bend down to the origin to be consistent with a localized state occurring in the non-interacting case (vertical axis $K = \infty$). The vertical dotted line separate two distinct localized phases (strongly interacting and strongly disordered): whether their nature is different or not it is still under debate.

Relying on these results, Fisher *et.al.* [Fisher et al., 1989] performed a scaling analysis aimed at giving the qualitative effect of the inclusion of disorder in bosons on a lattice. They considered the Bose-Hubbard Hamiltonian of Eq. (1.44) in presence of an uncorrelated uniformly distributed bound disorder and an unbound gaussian-distributed disorder. Their results are sketched in Fig 1.3**c**.

BOSE-GLASS

The main conclusion that can be drawn from the analysis listed above is that the SF coherent phase can be destroyed by disorder. In presence of an underlying periodic structure the transition to the MI takes place through a glassy phase named *Bose-glass*

(BG) (see Fig. 1.3**c**). This phase differentiates from the MI in the fact that it is gapless and that its density can be varied continuously, therefore the phase is compressible. On the other hand, the phase is not SF, in fact, it does not show any (quasi-)long-range order and it has no superfluid fraction. As it was initially studied [Giamarchi & Schulz, 1987], the SF-BG is a localization-delocalization phase transition (as for MI-SF). It occurs because of an enhanced role of the phase fluctuation, in particular phase flips (known in literature also as phase slips) that are low-energy long-range fluctuations that act reducing the coherence over large distances. In the case of zero tunneling, $J = 0$, disorder opens a BG window between the Mott lobes at different filling factor. The phenomenology occurring in the disordered case is the formation of incoherent droplets of bosons: by increasing the tunneling energy at a certain threshold the droplets percolate and restore the overall coherence, driving the system into a SF phase. The disorder-interaction phase diagram of the Bose-Hubbard model has been studied, among others, via quantum Monte Carlo techniques [Prokof'ev & Svistunov, 1998] and via density matrix renormalization group [Rapsch et al., 1999]: some of these results are presented and commented in Chapter 3.4.

A very debated question concerns whether the BG phase completely surrounds the MI lobes or if a direct MI-SF transition is possible. After controversial results and theories, this issue apparently came to a solution [Pollet et al., 2009, Gurarie et al., 2008] proving that a direct transition in presence of disorder is not possible, in agreement with previous arguments [Fisher et al., 1989, Freericks & Monien, 1996].

When an underlying periodic structure lacks, the SF phase simply moves to the BG phase for sufficiently strong disorder. This transition occurs at weak interaction when disorder-interaction ratio is large, otherwise it is driven by strong interaction when the gas is in the strongly correlated regime and the disorder just acts as a small perturbation (see Fig. 1.4). Consistently with this argument, in this regime the uniform Bose gas moves into the Tonks-Girardeau regime and it loses its long-range coherence.

Quantum Phase Transition

The Mermin-Wagner theorem prevents the occurrence of a phase transition associated to the breaking of a continuous symmetry in one and two dimensions. Even if there is no BEC, a topological phase transition still occurs in 2D: below a critical temperature T_{KT} the one body density matrix of a 2D boson gas decays algebraically and the gas is superfluid. Above this temperature the gas behaves as a normal fluid, with no superfluid component and an exponentially decaying one-body density matrix. The occurrence of the phase transition is associated with the proliferation of vortex-antivortex pairs, destroying quasi-long-range order, and with a universal jump in the superfluid fraction [Nelson & Kosterlitz, 1977, Prokof'ev et al., 2001]. This phase transition, initially predicted for the XY model in 2D, is known as Berezinskii-Kosterlitz-Thouless transition (BKT) [Berezinskiĭ, 1972, Kosterlitz & Thouless, 1973]. Note that the occurrence of BKT does not violate the Mermin-Wagner theorem because there is no breaking of a continuous symmetry.

Phase transitions are defined as phenomena occurring at finite temperature in the thermodynamic limit. No phase transition takes place in one-dimensional bosonic system. On the contrary, at zero temperature, as presented above, interaction and disorder can destroy the quasi-long range order of the system. A phase transition occurring at zero temperature driven by some auxiliary parameters is known as a *quantum phase transition*. The role of topological excitations in one dimension is played by *phase flips*, long range fluctuations originating from a non-zero modulation of the potential, that are detrimental to long-range coherence (for a detailed analysis see Chapter 3). As discussed above, the B-H Hamiltonian at integer filling shows a quantum phase transition, driven by J/U, caused by phase fluctuations and associated with the loss of long-range coherence in the one-body density matrix. Its universality class in d-dimensions is the one of the $(d + 1) - XY$ model [Fisher et al., 1989, Sachdev, 1999]: in 1D this transition is of the Kosterlitz-Thouless type, therefore it shows a jump in the superfluid fraction [Nelson & Kosterlitz, 1977]. The quantum MI-SF phase transition can also be triggered by tuning the chemical potential (i.e. the density): in this scenario the transition is caused by density fluctuations and it belongs to a different universality class (mean field) with respect to the J-driven transition described above [Fisher et al., 1989]. Even the occurrence of this phase transition does not violate the Mermin-Wagner theorem, because, given the underlying potential, the symmetry that is being broken is the discrete invariance under lattice translations, which is possible at zero temperature even in 1D.

In presence of disorder we have shown that a BG phase appears as a consequence of phase fluctuations. The SF-BG transition at strong disorder, analyzed in detail in [Giamarchi & Schulz, 1988, Fisher et al., 1989], is of the BKT-type, even if it shows different properties with respect to the SF-MI. Also in the case of strong disorder the transition appears to be of the same kind [Altman et al., 2004, Altman et al., 2010], even if the authors found exponentially diverging length and time scales. To conclude, the MI-BG transition is entirely local and it is of the Griffiths type [Griffiths, 1969, Fisher et al., 1989, Gurarie et al., 2009].

The phase transition to a Mott-insulating phase has been experimentally observed with ultracold atoms in optical lattices in 3D [Greiner et al., 2002, Jaksch et al., 2008] and subsequently in lower dimensions [Stöferle et al., 2004, Spielman et al., 2007, Spielman et al., 2008]. In the disordered case, the experimental observation of a superfluid-insulator transition in the strongly interacting regime, has been recently claimed [Pasienski et al., 2010].

Quasiperiodic potential

The role of interaction has been studied also in presence of quasiperiodic potentials. As commented in Section 1.3.3, in this case a critical interaction strength is necessary to localize the single-particle wavefunctions. This feature survives even including interaction between bosons, as it has been found in several theoretical investigations [Roth & Burnett, 2003b, Roscilde, 2008, Roux et al., 2008, Schmitt et al., 2010]. These bichromatic potentials have been proposed to study the SF-BG-MI phase transition [Damski et al., 2003]. In the

opposite regime (weakly interacting), a good evidence of a superfluid-insulator transition has been recently obtained for an atomic gas of ^{39}K [Deissler et al., 2010, Deissler et al., 2011].

MOTIVATION

Recent developments of the experimental techniques, following the first observation of BEC in ultracold atomic systems, have brought to the creation of quantum systems of unparalleled precision and controllability. This brought to the observation of Anderson localization in 1D bosonic gases with vanishing interaction [Billy et al., 2008, Roati et al., 2008]. The realization of 1D Bose gases in the weakly interacting regime has renewed the attention into the superfluid-insulator transition occurring at low inter-particle coupling. The insulating phase arising at weak interaction has a different nature with respect to the strongly correlated one and it is often referred as *Anderson glass* [Scalettar et al., 1991]. Interaction plays an opposite role in the two regimes. When the transition occurs at large U, the repulsion tends to localize the N-particle wavefunction, whereas at small U it competes with disorder in restoring coherence bringing the system towards the superfluid phase. It is still not clear whether these two phases are physically different or if they are connected by a crossover [Giamarchi & Schulz, 1988, Batrouni et al., 1990].

As shown in Section 1.2.2, the weakly interacting limit in 1D correspond to the limit of large densities: many of the methods listed above present difficulties in this regime. Indeed, disorder cannot be included as a perturbation any longer and even exact numerical methods, such as Monte Carlo and DMRG, are strongly limited when dealing with a large number of particles. Many theoretical approaches have attacked this problem with different methodologies. The phase transition has been addressed using real-space renormalization group [Altman et al., 2004, Altman et al., 2008, Altman et al., 2010, Vosk & Altman, 2011], studying the density distribution via a mean field theory [Lugan et al., 2007a, Lugan, 2010] or analyzing the scaling of the N-body Hamiltonian in arbitrary dimensions [Falco et al., 2009b, Falco et al., 2009a, Nattermann & Pokrovsky, 2008]. Some of the results of these analysis are shown and commented in Chapter 3.

Despite the interest received by the scientific community, a precise description of the phase boundary in the weakly interacting limit has not been given. First, this is due to the difficulties in obtaining exact analytical results. On the other hand, an accurate prediction of the phase transition is a subtle numerical problem. In addition, the exact phenomenology that triggers the phase transition in this regime, where interaction is not sufficient to overcome the disorder and the density fragments into mutually incoherent puddles, is still poorly understood. For these reasons, in this thesis we aim at characterizing the weakly interacting phase transition via an extended Bogoliubov method, presented in Chapter 2, and we focus on the properties of the quantum gas to understand which are the significant changes across the phase boundary. This is intended to deepen the understanding of the SF-BG quantum phase transition and to give some experimentally useful hints to characterize the phase diagram in a regime that nowadays is currently realized.

1D BOSE GAS: FORMALISM

Contents

In Chapter 1 the physics of quantum degenerate Bose gases was presented. It has been shown that the standard Bogoliubov approach has strong limitations in describing the weakly interacting regime in low dimensionality. Here an extended version of the Bogoliubov model, that allows to correctly describe low-dimensional systems, is presented in detail for the one-dimensional case. This formalism has been developed by Mora & Castin [Mora & Castin, 2003]. In this thesis we apply this model to analyze the properties of a low-dimensional Bose gas in presence of disorder and focussing on the behaviour of the one-body density matrix computed within this formalism. In addition, we investigate the implications of the validity conditions of this formalism stressing in which limit the predictions of the mean-field theory are reliable. In Section 2.1 the weakly interacting regime where the Bogoliubov approach is valid is discussed; the results of the perturbative expansions are shown in Section 2.2, whereas the validity conditions of the model are reviewed in Section 2.3.

This chapter is intended to give all the ingredients to understand the theoretical framework used throughout this thesis. More details on this theoretical approach can be found in the references [Mora & Castin, 2003, Castin & Dum, 1998, Mora, 2006].

2.1 WEAKLY INTERACTING LIMIT

The many-body Hamiltonian for a 1D system of N bosons, assuming a contact interaction of the form $U(r - r') = g_0\delta(r - r')$, is

$$\hat{H} = \sum_{i=1}^{N}\left[\frac{\hat{p}_i^2}{2m} + V(\hat{r}_i)\right] + \sum_{i<j=1}^{N} g_0\delta(\hat{r}_i - \hat{r}_j), \tag{2.1}$$

where g_0 is the bare coupling constant, m is the mass of the particles, V is the external potential and $\hat{r}_i$ and $\hat{p}_i$ are respectively the position and momentum operators of the i-th particle. This model, in absence of an external potential, has been solved exactly by Lieb and Liniger using the Bethe ansatz [Lieb & Liniger, 1963]. They showed that the physics of the 1D Bose gas is uniquely determined by the parameter γ (see also Chapter 1.2.2), defined as

$$\gamma = \frac{mg_0}{\hbar^2\rho}, \tag{2.2}$$

that marks the regime of the gas. $\gamma = 0$ corresponds to the ideal case of non-interacting bosons, whereas $\gamma = \infty$ denotes the hard-core or Tonk Girardeau limit [Girardeau, 1960], where the bosonic system acquires fermionic properties. The parameter γ gives information about the ratio between the average inter-particle distance $1/\rho$ and the correlation length $l_c = 1/\sqrt{mg_0n}$: the weakly interacting regime is attained when the correlation spreads over a large number of bosons, i.e. for $\gamma \ll 1$, a situation achieved for small values of the interaction constant or for large densities,

$$\rho \gg \frac{mg_0}{\hbar^2}. \tag{2.3}$$

This counterintuitive behaviour is peculiar of the 1D case. In this regime the gas allows for a perturbative solution, such as Bogoliubov approach, as originally shown in Ref. [Lieb & Liniger, 1963].

Yang and Yang [Yang & Yang, 1969] have extended this approach to finite temperatures, proving that a phase transition is absent at $T \neq 0$. However, at sufficiently low temperature the Bose gas is in the quantum degenerate regime and it behaves differently from the high-temperature case, where it retrieves the properties of a classical gas. In order to describe the Bose gas within a perturbative approach even at finite T, the temperature has to fulfill the constraint of quantum degeneracy, i.e.

$$\rho\sqrt{\frac{2\pi\hbar^2}{mk_BT}} \gg 1, \tag{2.4}$$

that guarantees a macroscopic occupation of states at low energy. The quantum phase transition investigated in this thesis occurs at zero temperature, where the condition of quantum degeneracy is automatically fulfilled.

From these conditions of applicability it is evident that a large density is necessary for the Bogoliubov theory to hold: this topic is analyzed in detail in Section 2.3. Within this range of validity, the mean-field approach presented in the next section correctly describe the properties of the Bose gas.

2.2   Bogoliubov model for Quasi-condensates

Provided that the gas is weakly interacting, it can be described by means of a perturbative approach [Lieb & Liniger, 1963]. The lack of an actual condensed state in low dimensionality, however, invalidates the assumptions of the standard Bogoliubov method: in fact the condition of small quantum correction $\delta\hat{\Psi}$ to a macroscopically occupied condensate with wavefunction Ψ_0 ceases to hold. Bogoliubov's idea can still be adapted to quasi-condensates in the case of weak density fluctuations, relying on the density-phase representation [Popov, 1972], by rewriting the expression for the field as $\hat{\Psi} = e^{i\hat{\theta}}\sqrt{\hat{\rho}}$. This representation allows to separate the term describing the amplitude of the field from the fluctuating term, related to the phase, responsible for the absence of coherence at large distances. Therefore, in the absence of a condensate, a perturbation theory is built by splitting the density operator into a main c-component ρ_0 and a small fluctuation term $\delta\hat{\rho}$. A straightforward definition of the density and phase operators can however lead to divergences in the theory [Shevchenko, 1992, Pitaevskii & Stringari, 2003] and to some inconsistencies with the standard Bogoliubov theory in 3D. These problems arise because of the difficulties in dealing with density and phase variables defined on a continuous variable r [Shevchenko, 1992, Wu & Griffin, 1996]. According to Mora and Castin [Mora & Castin, 2003], the definition of the system on a grid can overcome such a problem. In fact, this allows to have small and finite density fluctuations inside each grid element (whose divergence is instead unavoidable in a continuous model). A Bogoliubov-like theory is recovered by carrying out a perturbative expansion in powers of the density fluctuations $\delta\hat{\rho}$ and of the phase gradient $\nabla\hat{\theta}$. In this section this extended Bogoliubov theory, adapted for dealing with low dimensional Bose gases, is presented (the complete derivation of the theory can be found in [Mora & Castin, 2003]).

The system under study is a one-dimensional continuous bosonic chain of length L subject to periodic boundary conditions, that make it equivalent to a ring. The extended Bogoliubov model requires the introduction of a discretization of the space so that every single bin – of size ℓ – is largely occupied and the density operator does not vanish in any lattice site. The aim of this model is to reproduce the properties of the gas in the continuum. Hence, the ultraviolet cutoff introduced by the lattice has to be large compared to the other energy scales entering the problem: this makes the theory effective only at low energies (a detailed analysis of the regime of validity is presented in Section 2.3). The 1D bosonic Hamiltonian defined on a grid reads

$$H = \sum_r \ell\left[-\frac{\hbar^2}{2m}\hat{\Psi}^\dagger(r)\Delta\hat{\Psi}(r) + [V(r)-\mu]\hat{\Psi}^\dagger(r)\hat{\Psi}(r) + \frac{g_0}{2}\hat{\Psi}^\dagger(r)\hat{\Psi}^\dagger(r)\hat{\Psi}(r)\hat{\Psi}(r)\right], \quad (2.5)$$

where $\hat{\Psi}^\dagger(r)$ and $\hat{\Psi}(r)$ are field operators satisfying bosonic commutation rules, the sum is extended to every lattice site labeled by its position and a contact interaction potential is assumed, $U(r_1 - r_2) = g_0\delta_{r_1,r_2}/\ell$, with g_0 defining the bare coupling constant. The kinetic term includes a discrete version of the Laplacian that couples neighbouring sites

as

$$\Delta\Psi(r) = \frac{\Psi(r+\ell) + \Psi(r-\ell) - 2\Psi(r)}{2\ell}. \tag{2.6}$$

The bosonic commutation relations for the field in the discrete model translate into

$$[\hat{\Psi}(r), \hat{\Psi}^\dagger(r')] = \frac{\delta_{r,r'}}{\ell}. \tag{2.7}$$

Hamiltonian (2.5) can be rewritten in terms of the conjugated variables $\hat{\rho}$ and $\hat{\theta}$ by substituting the field as $\hat{\Psi} = e^{i\hat{\theta}}\sqrt{\hat{\rho}}$. In low dimensionality, repulsive interactions moderate the density fluctuations around the average value [Carusotto & Castin, 2001]. Hence, the density operator can be rewritten as $\hat{\rho}(r) = \rho_0(r) + \delta\hat{\rho}(r)$, with a macroscopic classical part ρ_0 and a fluctuation term $\delta\hat{\rho}$ and, in accordance with Bogoliubov prescription, the Hamiltonian can be expanded in terms of the small parameter $\varepsilon_1 = |\delta\hat{\rho}|/\rho_0$. To correctly describe the Hamiltonian at higher orders, the exponential has to be taken into account in the expansion and an exponential of the phase difference appears: this defines the second perturbative parameter as $\varepsilon_2 = |\ell\nabla\hat{\theta}|$ [Mora & Castin, 2003].

2.2.1   Ground state and excitations

The expansion of the Hamiltonian (2.5) at zeroth order takes into account only the classical component of the density, ρ_0. At the lowest order, in analogy with the derivation of the Bogoliubov theory presented in the previous chapter, a Gross-Pitaevskii-like equation (GPE) is found

$$\left[-\frac{\hbar^2}{2m}\Delta_r + V(r) + g_0 N_0 |\phi_0(r)|^2 \right] \phi_0(r) = \mu\phi_0(r). \tag{2.8}$$

$\phi_0(r)$ is the positive-defined, normalized ground-state wavefunction and it is related to the ground-state density via $\rho_0(r) = N_0|\phi_0(r)|^2$. Equation (2.8) has the form of a non-linear Schrödinger equation where the non-linear term is proportional to the local density of the ground state. From now on, we will refer to $U_0 = g_0 N_0/L$ as the interaction energy, whereas $U(r)$ will denote the spatial distribution of the interaction energy, namely $U(r) = g_0 N_0|\phi_0(r)|^2 = g_0\rho_0(r)$.

Introducing the dimensionless variable $x = r/\eta$, the distances can be measured in units of correlation length and the Laplacian transforms as $\Delta_r = \Delta_x/\eta^2$. All the energies can then be rescaled by the correlation energy, $E_c = \hbar^2/(2m\eta^2)$. Equation (2.8) can be rewritten as

$$\left(-\Delta_x + \tilde{V}(x) + \tilde{U}_0|\phi_0(x)|^2 \right) \phi_0(x) = \tilde{\mu}\phi_0(x), \tag{2.9}$$

where the $\sim$ denotes the energies in units of E_c. This scaling invariance will be applied throughout this thesis.

The numerical code to solve the Gross-Pitaevskii equation is based on the Crank-Nicholson algorithm that performs an evolution in imaginary time of a sample wavefunction (typically the normalized uniform wavefunction $1/\sqrt{L}$). This algorithm evolves the wavefunction, relaxing iteratively to the solution of the non-linear problem as explained in Appendix B.

The first order correction to the Hamiltonian vanishes because the solution of Eq. (2.8) minimizes the energy functional. The first correction in terms of the small perturbative parameters is therefore given by the second order: at that level, the Hamiltonian can be cast in the Bogoliubov form by defining the field operators

$$\hat{B}(r) = \frac{\delta\hat{\rho}(r)}{2\sqrt{\rho_0(r)}} + i\sqrt{\rho_0(r)}\hat{\theta}(r), \tag{2.10}$$

that obeys the bosonic commutation rules $[\hat{B}(r), \hat{B}^\dagger(r')] = \delta_{r,r'}/\ell$. The second-order term in the Hamiltonian reads

$$\hat{H}_2 = \ell\sum_r \hat{B}^\dagger(r)\left(-\frac{\hbar^2}{2m}\Delta_r + V(r) + U(r) - \mu\right)\hat{B}(r) + U(r)\left[\hat{B}^\dagger(r)\hat{B}(r) + \frac{1}{2}(\hat{B}^2(r) + \hat{B}^{\dagger 2}(r))\right] \tag{2.11}$$

and can be diagonalized as the standard Bogoliubov Hamiltonian. The normal eigenmodes of the Bogoliubov-de Gennes equation (BdGE), namely $u_j(r)$ and $v_j(r)$ can be obtained by diagonalizing the matrix

$$\begin{pmatrix} -\frac{\hbar^2}{2m}\Delta + V(r) - \mu + 2U(r) & U(r) \\ -U(r) & \frac{\hbar^2}{2m}\Delta - V(r) + \mu - 2U(r) \end{pmatrix}\begin{pmatrix} u_j \\ v_j \end{pmatrix} = E_j\begin{pmatrix} u_j \\ v_j \end{pmatrix}, \tag{2.12}$$

where the Bogoliubov modes u_j and v_j obey the normalization

$$\sum_r \ell[|u_j(r)|^2 - |v_j(r)|^2] = 1. \tag{2.13}$$

Equation (2.12) is a $2n \times 2n$ matrix that is linear once equation (2.8) for the ground state density has been solved. The lowest-energy solution of these equations, with eigenvalue 0, has the shape of the ground state, i.e. $u_0(\mathbf{r}) = v_0(\mathbf{r}) \propto \phi_0(\mathbf{r})$. Moreover, for any solution (u_j, v_j) with positive energy E_j, a solution (v_j^*, u_j^*) with negative eigenvalue $-E_j$ exists.

The operators $\hat{B}$ can be expressed in terms of these modes as

$$\hat{B}(r) = i\hat{Q}\sqrt{\rho_0(r)} + \hat{P}\partial_{N_0}\sqrt{\rho_0(r)} + \sum_j \hat{b}_j u_j(r) + \hat{b}_j^\dagger v_j^*(r), \tag{2.14}$$

where $\hat{b}_j$ and $\hat{b}_j^\dagger$ are bosonic operators obeying $[\hat{b}_i, \hat{b}_j^\dagger] = \delta_{i,j}$, whereas $\hat{Q}$ and $\hat{P}$ appear as a consequence of the non-fixed number of particles [Lewenstein & You, 1996, Mora & Castin,

2003, Castin & Dum, 1998]. They commute with $\hat{b}_j$ and $\hat{b}_j^\dagger$ and represent respectively a global choice of the phase and the fluctuations of the total number of particles. Eq. (2.14) can be rewritten by separating the *canonical* part into a component along the quasicondensate mode $\hat{\alpha}\phi_0(r)$ and an orthogonal part $\hat{\Lambda}(r)$ as

$$\hat{B}(r) = i\hat{Q}\sqrt{\rho_0(r)} + \hat{P}\partial_{N_0}\sqrt{\rho_0(r)} + \hat{\alpha}\phi_0(r) + \hat{\Lambda}(r), \tag{2.15}$$

with

$$\hat{\Lambda}(r) = \sum_j u_{j\perp}(r)\hat{b}_j + v_{j\perp}(r)\hat{b}_j^\dagger. \tag{2.16}$$

where the subscript $\perp$ denotes the component orthogonal to ϕ_0. The $\hat{\Lambda}$-operators describe the excitations orthogonal to the quasicondensate (for an exhaustive discussion see Ref. [Castin & Dum, 1998]), they obey the commutation rules

$$[\hat{\Lambda}(r), \hat{\Lambda}^\dagger(r')] = \delta_{r,r'}/\ell - \phi_0(r)\phi_0(r'), \tag{2.17}$$

and the expectation value $\langle\hat{\Lambda}^\dagger(r)\hat{\Lambda}(r)\rangle$ gives the density of non-condensed particles at position r.

The link to the density-phase operators in this approach is given by the relations

$$\delta\hat{\rho}(r) = \sum_j [f_j(r)\hat{b}_j + f_j^*(r)\hat{b}_j^\dagger] + \hat{P}\partial_{N_0}\rho_0,$$

$$\hat{\theta}(r) = \sum_j [\theta_j(r)\hat{b}_j - \theta_j^*(r)\hat{b}_j^\dagger] - \hat{Q}, \tag{2.18}$$

where the factors f_j and θ_j are linked to the u_j and v_j of the Bogoliubov transformation by

$$\theta_j(\mathbf{r}) = \frac{u_j(\mathbf{r}) - v_j(\mathbf{r})}{2i\sqrt{\rho_0}}, \qquad f_j(\mathbf{r}) = \sqrt{\rho_0}[u_j(\mathbf{r}) + v_j(\mathbf{r})] \tag{2.19}$$

An expression for the total density $\rho(r) = \rho_0(r) + \langle\delta\hat{\rho}(r)\rangle$ can be extracted by evaluating the expectation value of the density fluctuations. In order to obtain the first non-vanishing correction to the GP density one has to expand the Hamiltonian to the third order [Mora & Castin, 2003] and, in the canonical treatment of the theory, this gives

$$\langle\delta\hat{\rho}(r)\rangle = 2\phi_0(r)\chi(r) + \langle\hat{\Lambda}^\dagger(r)\hat{\Lambda}(r)\rangle, \tag{2.20}$$

where χ describes the depletion of the ground state and the corrections due to the interaction with the non-condensed particles, whereas the last term is the density of the particles occupying excited states. It can be shown [Castin, 2004] that the relative density fluctuations are inversely proportional to the ground-state density

$$\frac{\langle\delta\hat{\rho}(r)\rangle}{\rho_0(r)} \propto \frac{1}{\sqrt{\rho_0(r)}\ell}, \tag{2.21}$$

therefore the relative density fluctuations decrease by increasing ρ_0.

With the formalism developed in this section, the physical quantities relevant to the analysis that will be performed in the next chapter can be computed.

2.2.2 Observables

The physical properties of the $1D$ Bose gas can be inspected through the study of its observables. Some of them are relevant to the physics of the phase transition and here their analytic expressions are computed within the extended Bogoliubov model. Among them, the ground state energy and the correlation functions are of particular interest for the analysis that follows.

The zeroth order contribution to the energy can be extracted from the Gross-Pitaevskii energy functional. For a system of N_0 particles with density profile $\rho_0(r)$ it reads

$$E_0(N_0) = \sum_r \ell \left[-\frac{\hbar^2}{2m} \sqrt{\rho_0(r)} \Delta \sqrt{\rho_0(r)} + V(r)\rho_0(r) + \frac{g_0}{2}\rho_0^2(r) \right]. \tag{2.22}$$

The first correction to this prediction comes from the second order term in the Hamiltonian and takes the form

$$E_2 = -\frac{1}{2}\sum_r \ell U_0 \phi_0(r)^2 - \sum_j E_j \langle v_{j\perp}|v_{j\perp}\rangle. \tag{2.23}$$

The ground state energy can then be computed as

$$E_{ground} = N_0 \sum_r \ell \left[-\frac{\hbar^2}{2m}\phi_0(r)\Delta\phi_0(r) + V(r)\phi_0^2(r) + \frac{g_0}{2}(N_0-1)\phi_0^4(r) \right] - \sum_j E_j \langle v_{j\perp}|v_{j\perp}\rangle, \tag{2.24}$$

and this prediction for the ground state energy is consistent with the standard Bogoliubov theory.

Another useful quantity to characterize the phase transition is the one body density matrix, that can be extracted from the Bogoliubov theory at second order. The definition of $G_1(r,r')$ in the density-phase formalism reads

$$G_1(r,r') = \langle \hat{\Psi}^\dagger(r)\hat{\Psi}(r')\rangle = \langle \sqrt{\hat{\rho}(r)}e^{i[\hat{\theta}(r')-\hat{\theta}(r)]}\sqrt{\hat{\rho}(r')}\rangle. \tag{2.25}$$

By inserting the perturbative expansion of the operators one obtains [Mora & Castin, 2003] the general expression

$$G_1(r,r') = \sqrt{\rho(r)\rho(r')}\exp\left[-\frac{1}{2}\langle :(\Delta\theta)^2:\rangle_2 - \frac{1}{8}\langle :(\Delta\delta\tilde{\rho})^2:\rangle_2 \right], \tag{2.26}$$

where $\Delta\theta = \hat{\theta}(r) - \hat{\theta}(r')$, $\Delta\delta\tilde{\rho} = \delta\hat{\rho}(r)/\rho_0(r) - \delta\hat{\rho}(r')/\rho_0(r')$ and the normal ordering is taken with respect to the Λ-operators as defined in Appendix A (a rigorous derivation of this expression can be found in ref. [Mora & Castin, 2003]). As shown in Appendix A, $G_1(r,r')$ can be rewritten as a function of the Bogoliubov modes and it takes the form

$$G_1(r,r') = \sqrt{\rho(r)\rho(r')}\times$$
$$\exp\left[-\frac{1}{2}\sum_j (1+p_j)\left| \frac{v_{\perp j}(r)}{\sqrt{\rho_0(r)}} - \frac{v_{\perp j}(r')}{\sqrt{\rho_0(r')}} \right|^2 + p_j \left| \frac{u_{\perp j}(r)}{\sqrt{\rho_0(r)}} - \frac{u_{\perp j}(r')}{\sqrt{\rho_0(r')}} \right|^2 \right], \tag{2.27}$$

where $p_j = [e^{E_j/k_B T} - 1]^{-1}$ is the thermal Bose factor. At $T = 0$ there is no thermal population and Eq. (2.27) reduces to

$$G_1(r, r') = \sqrt{\rho(r)\rho(r')} \exp\left[-\frac{1}{2}\sum_j \left|\frac{v_{\perp j}(r)}{\sqrt{\rho_0(r)}} - \frac{v_{\perp j}(r')}{\sqrt{\rho_0(r')}}\right|^2\right], \quad (2.28)$$

where the only contributions to the decay of spatial correlation come from quantum fluctuations. In an inhomogeneous system it is convenient to introduce the reduced one-particle density matrix $g_1(r, r')$ defined as $g_1(r, r') = G_1(r, r')/\sqrt{\rho(r)\rho(r')}$ [Bloch et al., 2008]. This expression for the one-body density matrix, obtained within the extended Bogoliubov approach, does not coincide with the prediction of the Bogoliubov theory: this is due to the correct treatment of the fluctuations that avoids the onset of divergences in the theory.

The study presented in this thesis concerns the influence of disorder on a bosonic system. The one-body density matrix, as defined in Eq. (2.28) is a two-point property that is strongly affected by the specific disorder realization. Hence, this quantity is typically irregular and not translationally invariant (see Figs. 2.4**c** and 2.4**d**). For this reason, an averaged version of the one-body density matrix is introduced: it is known as *degree of coherence* and is defined as

$$\mathcal{G}_1(a) = \frac{1}{L}\int dr' g_1(r', r' + a). \quad (2.29)$$

This quantity behaves smoothly and it is translationally invariant (see Figs. 2.4.**e** and .**f**), thus it represents a good parameter to characterize the phase transition by identifying its functional long-range behaviour. This analysis is performed in Chapter 3.

2.2.3 The uniform case

The approach developed so far can be applied to investigate the spatially homogeneous case ($V(r) = 0$). The problem in absence of an external potential has an analytical solution, hence it represent a good candidate to understand how the presence of disorder affects the physical properties of the system. In this section the results for the uniform one-dimensional Bose gas are presented and analyzed in detail.

In the disorderless case, the solution of the GPE (2.8) is uniform and it takes the constant value $\phi_0 = 1/\sqrt{L}$, that gives for the chemical potential $\mu = U_0$. The problem is then mapped onto the original one solved by Bogoliubov [Bogoliubov, 1947] and the solutions for the excitations are the Bogoliubov modes u_k and v_k. The quadratic Hamiltonian can be diagonalized, obtaining

$$u_k(r) = \bar{u}_k \frac{e^{ikr}}{\sqrt{L}}, \quad v_k(r) = \bar{v}_k \frac{e^{ikr}}{\sqrt{L}}. \quad (2.30)$$

The modes behave like plane waves with increasing k-vector, with amplitudes, $\bar{u}_k$ and $\bar{v}_k$, that satisfy

$$\bar{u}_k - \bar{v}_k = \left[\frac{\hbar^2 k^2/2m + 2\mu}{\hbar^2 k^2/2m}\right]^{1/4} \quad (2.31)$$

and

$$\bar{u}_k + \bar{v}_k = \left[\frac{\hbar^2 k^2/2m}{\hbar^2 k^2/2m + 2\mu} \right]^{1/4}. \tag{2.32}$$

In the uniform case the excitations are orthogonal to the GP solution ϕ_0 and the corresponding eigenenergies are

$$E_k = \sqrt{\frac{\hbar^2 k^2}{2m} \left(\frac{\hbar^2 k^2}{2m} + 2\mu \right)}, \tag{2.33}$$

representing the well-known Bogoliubov dispersion relations.

Moving to the observables, the asymptotic behaviour of the one-body density matrix at $T = 0$ in the weakly interacting limit, $g/\rho \to 0$, has been computed by Popov [Popov, 1980] making use of the path integral formalism and it takes the form

$$g_1(0,r) \simeq \left(\frac{1.037\xi}{r} \right)^{\frac{1}{2\pi\rho_0\xi}}, \tag{2.34}$$

where ξ is the healing length. The same quantity can be extracted from the extended Bogoliubov model [Mora & Castin, 2003] and the two predictions coincide in the long-range limit. The numerical results obtained within the mean-field model are plotted in Fig. 2.1 for $U_0 = 0.8$ and $N_0/L = 8$ (red solid curve) together with the asymptotic prediction of equation (2.34) (red dashed line). In the intermediate range the two power-law decays coincide, but, in addition, the result obtained within the extended Bogoliubov model gives the correct value for g_1 at short distances (larger than the discretization length ℓ). The numerical result is affected by periodic boundary conditions ($\Psi(L) = \Psi(0)$) at distances comparable to L. In fact, the one dimensional system becomes equivalent to a ring and the point at distance L coincides with the point at zero distance, thereby leading to a coherence growth for distances larger than $L/2$. The calculation can be extended to finite temperature where an exponential decay is recovered [Kane & Kadanoff, 1967, Schwartz, 1977, Popov, 1983].

In expression (2.34) the dependencies of the one-body density matrix on the variables entering the problem are explicit. The reduced one-body density matrix has a dependence on ρ_0 and at the same time on $U_0 = g_0\rho_0$ via $\xi = \hbar/\sqrt{m\mu} = \hbar/\sqrt{mU_0}$. The exponent of Eq. (2.34) is proportional to $\sqrt{g_0/\rho_0}$ and it turns out that the slope of the algebraic decay is determined by the parameter $\gamma \propto g_0/\rho_0$, as in the Lieb and Liniger problem [Lieb & Liniger, 1963]. An increase of the coupling constant leads to a decrease of the spatial correlation, whereas density acts in the opposite direction. This is a peculiarity of one-dimensional bosonic systems and it explains why the gas enters the Tonk-Girardeau regime in the low-density limit.

This notion is better displayed by plotting $g_1(0,r)$ for a larger interaction constant and a larger density in Fig. 2.1, denoted by the green and black lines respectively. For the analysis that follows it is important to stress that an increase of the interaction energy
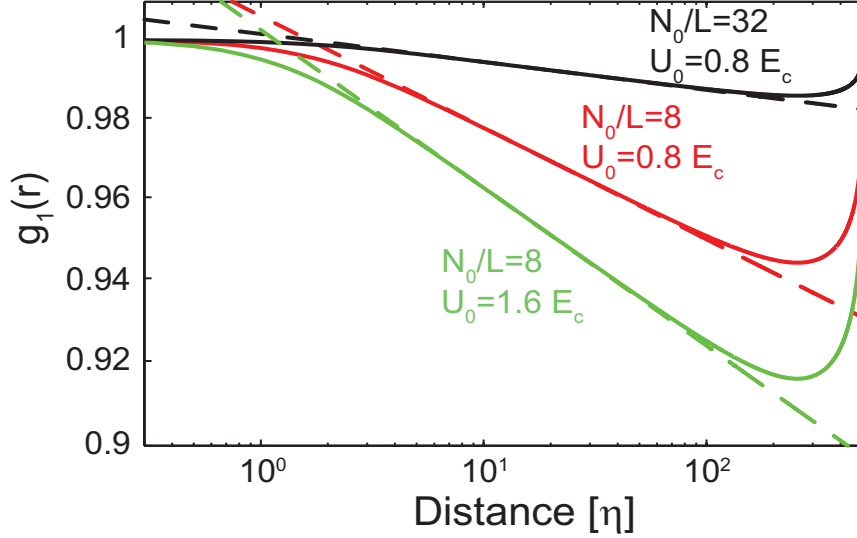
Figure 2.1: Reduced one-body density matrix plotted in log-log scale, $g_1(r_0 - r)$, in absence of disorder, for a system of length 512 η, $U_0 = 0.8\ E_c$ and $N_0/L = 8$ (red lines). The green lines denote $g_1(0, r)$ for a larger value of the interaction energy, $U_0 = 1.6\ E_c$, whereas the black lines are computed for a larger value of the density $N_0/L = 32$. The solid lines are the numerical solutions obtained from the extended Bogoliubov model and the dashed lines are the normalized asymptotic expressions reported in formula (2.34). The two models overlap in a large intermediate range of distances.

$(U_0 \propto 1/\xi^2)$ at fixed density corresponds to a reduction of coherence. This will turn out to be a key-feature to understand the quantum phase transition occurring for increasing U_0 at fixed disorder strength.

From now on, all analyses will be carried out at fixed density and varying interaction energy. As it will be explained in Sec. 2.3 this is not relevant in the limit where the prediction of the extended Bogoliubov model for the phase transition is exact, i.e. for constant U_0 and $g \to 0$.

2.2.4   THE DISORDERED CASE

The model presented in the previous sections extends to the case where an external potential is present. In this section some numerical results obtained in presence of gaussian disorder are shown: this allows to illustrate the qualitative effect of an underlying potential on the 1D Bose gas.

In Fig. 2.2, typical numerical results for the ground state wavefunction in a disordered environment are shown for two different interaction energies. The density tends to be larger where the disorder potential is low and adds to the bare potential $V(r)$ through the non-linear term. By increasing the interaction strength, the modulation of the GS decreases and its distribution becomes smoother, more similar to the homogeneous solution.

In the weakly interacting regime disorder tends to localize bosons, whereas interaction acts in the opposite direction. In a case dominated by disorder, the ground state separates into fragments linked by regions with an exponentially vanishing wavefunction that here are defined as "*weak links*". It is worth pointing out that the ground state wavefunction is always positive and does not vanish even in case of strong disorder.
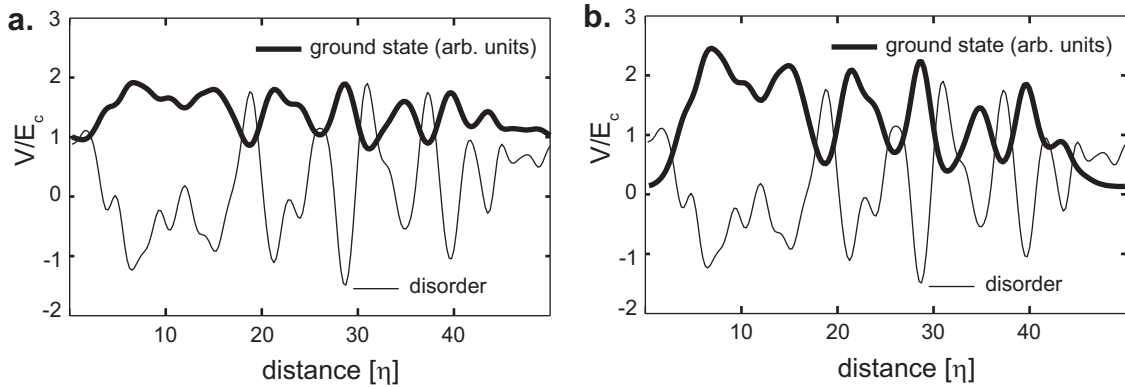

Figure 2.2: Ground state wavefunctions (thick lines) for the same disorder realization ($\Delta = 0.8\ E_c$) and two values of interaction energy: $U_0 = 1.44\ E_c$ (panel **a**) and $U_0 = 0.48\ E_c$ (panel **b**). A larger interaction energy tends to make the ground state smoother, thus closer to the constant solution of the uniform problem.

Starting from the GP solution the shape of the excitations can be computed from equation (2.12): the relevant quantities for the computation of the observables are the Bogoliubov modes and in particular the low-energy $v_{\perp j}$-modes that constitute the quantum fluctuations entering the expression (2.28) at $T = 0$. In Fig. 2.3 the first two orthogonalized $v_\perp$-modes are shown for the same realization of disorder appearing in Fig. 2.2 and for the same two values of U_0.

Low-energy excitations follow the modulation of the ground-state wave function, but, differently from ϕ_0, they show a phase character with a number of nodes that increases for increasing energy. As long as the disorder represents a small perturbation, the phase fluctuations preserve a plane-wave profile, only slightly modulated by the underlying disordered potential (cfr. Fig. 2.3**a**). On the other hand, as the ratio Δ/U_0 increases (Fig. 2.3**b**), disorder starts to compete with interaction and the $v_{\perp j}(r)$ modes lose their regular shape, developing nodes in correspondence with low-density zones (high barriers of the potential). This is shown in Fig. 2.3**b**, together with an example of an excitation at higher energy that displays a fast-oscillating behaviour and does not contribute in determining long-range properties.
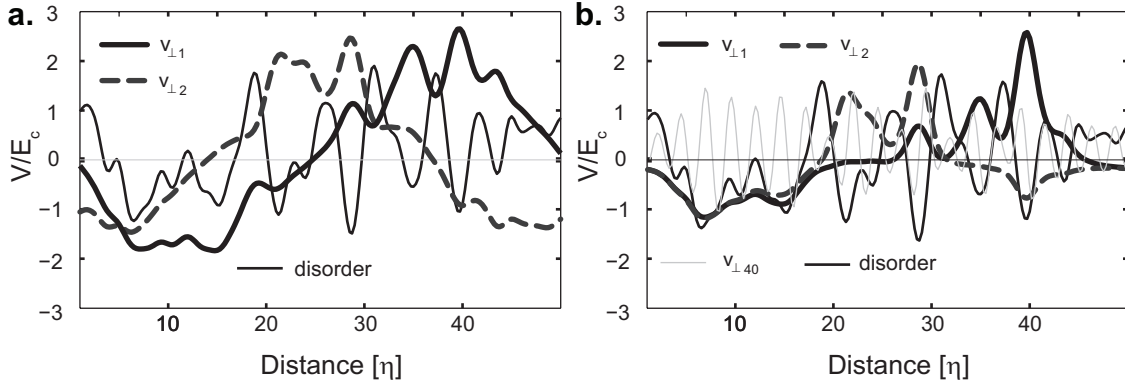
Figure 2.3: First two $v_{\perp j}$ excitations ($j = 1, 2$) for the same disorder realization ($\Delta = 0.8\,E_c$) and two values of the interaction energy: $U_0 = 1.44\,E_c$ (panel **a**) and $U_0 = 0.48\,E_c$ (panel **b**). An excitation at higher energy is shown in panel **b**: this mode is highly oscillating and has a poor effect on long-range properties. The magnitude of $v_{\perp j}$ is represented in arbitrary units.

2.3   VALIDITY OF THE APPROACH

In this section the conditions of validity of the extended Bogoliubov model are summarized, both from the numerical and physical point of view. The constraints and the limits where the theory is effective are analyzed in detail.

2.3.1   NUMERICAL CONSTRAINTS

A correct description of a low-dimensional Bose gas can be carried out by discretizing the space on an unphysical grid of step ℓ to avoid divergences in the density fluctuations. The numerical simulations of the continuous problem are, in turn, performed on a grid that has to be dense enough to reproduce the continuous model. As both these grids are unphysical, they are chosen to be the same, with a bin-size ℓ that introduces a corresponding energy cutoff $t = \hbar^2/(2m\ell^2)$.

Intuitively, the spatial resolution of the simulation needs to be smaller than the length-scales that have to be sampled, namely the correlation length of the disordered potential and the healing length[1]. These conditions can be translated into corresponding bounds on energy scales as

$$\ell \ll \eta, \xi \qquad \Longrightarrow \qquad t \gg E_c, \mu, \tag{2.35}$$

and this ensures that the lattice model reproduce faithfully the low energy properties of the continuous model.

---

[1] These conditions guarantees that ℓ is smaller than the single particle localization length l_0

2.3.2 PHYSICAL CONSTRAINTS

The Bogoliubov theory can be successfully applied to systems in the weakly interacting regime, whereas it fails in describing strongly correlated systems. In one dimension this condition (see Section 2.1) is expressed by

$$\frac{1}{\gamma} = \hbar \sqrt{\frac{\rho}{mg_0}} \gg 1, \tag{2.36}$$

that translates into the constraint of a small coupling constant or large densities. The condition of quantum degeneracy requires that the average inter-particle distance is larger than the de-Broglie wavelength λ_{th} [Castin et al., 2000], i.e.

$$\rho \lambda_{th} \gg 1 \qquad \Longrightarrow \qquad \rho \gg \sqrt{\frac{mk_B T}{2\pi \hbar^2}}, \tag{2.37}$$

that is guaranteed by the temperature equal to zero.

Finally, for the Bogoliubov approach to be valid, the perturbative parameters have to be small, i.e. small density fluctuations and slow phase variations

$$\frac{|\delta \hat{\rho}|}{\rho_0} \ll 1, \qquad |\ell \nabla \hat{\theta}| \ll 1. \tag{2.38}$$

These last conditions hold if each element of the grid is largely occupied [Mora & Castin, 2003],

$$\rho(\mathbf{r})\ell \gg 1, \tag{2.39}$$

and this condition is guaranteed by a large density of the ground state in each lattice site. It can be shown that both the perturbative parameters in Eq. (2.38) can be chosen of the order $1/\sqrt{\rho_0 \ell}$ [Castin, 2004].

The validity conditions can be summarized as

(I). $\ell \ll \xi, \eta$ (III). $|\delta \hat{\rho}/\rho_0| \ll 1$ (V). $\rho_0 \ell \gg 1$

(II). $\rho \ell \gg 1$ (IV). $|\ell \nabla \hat{\theta}| \ll 1$ (VI). $\rho \xi \gg 1$

Provided that ℓ is the shortest length scale entering the problem, conditions (I) are fulfilled. The validity of the model relies on having a large density of particles in each bin of the grid (II): this is guaranteed by condition (V), thereby conditions (III) and (IV) are fulfilled. The combination of the previous constraints validates the last (VI). Therefore, these constraints reduce to

$$\ell \ll \xi, \eta \qquad\qquad \rho_0 \ell \gg 1$$

Is the extended Bogoliubov model appropriate in describing the $1D$ Bose gas for any value of disorder and interaction? Repulsive interaction has the important role of

moderating density fluctuations, a key-ingredient for the application of Bogoliubov theory. In fact, the ideal non-interacting gas cannot be described within mean field theory at any finite temperature. The reason is that the requirement of small density fluctuations entails a minimum interaction energy to suppress the density fluctuations at finite temperature [Mora, 2006, Carusotto & Castin, 2001]. At $T = 0$, as long as disorder is absent, the gas can be described by a mean-field model for any finite value of the interaction strength U_0 provided that $\gamma \ll 1$ (the role of the density in the mean field limit is investigated in the next section).

On the other hand, the presence of disorder can invalidate the applicability of the Bogoliubov model in certain circumstances. In fact, it has been recently argued [Lugan et al., 2007a] that in the regime of very weak interactions (much weaker than the disorder amplitude), when the chemical potential lies in the Lifshitz tail of the single-particle spectrum, bosons occupy only low-energy Lifshitz states – solutions of the single-particle problem – that are strongly localized. On the contrary, the Bogoliubov approximation assumes that an extended N-particle ground-state wavefunction exists and, in this scenario, the theory cannot correctly describe the physical system. The Lifshitz-glass phase is expected to appear deep in the insulating phase and, for this reason, this argument does not invalidate the study of the quantum phase transition via the extended Bogoliubov theory.

2.3.3 The role of the density

In the two previous sections the conditions of validity of the model in term of the physical quantities has been discussed. The aim of the present section is to explain and prove that the density itself does not enter in the determination of the phase transition in the pure mean-field limit. In fact, the validity conditions impose that the general properties related to the phase transition are extrapolated for $\rho_0 \to \infty$ for fixed U_0 [Castin & Dum, 1998]. The foundation of this proof relies on the form of the GPE (2.8) and the BdGE (2.12) within the extended Bogoliubov model: these equations, that are the basis for the computation of the observables, do not depend on the average density (N_0/L) alone, but only on the interaction energy, $U_0 = g N_0/L$. This implies that, for a given U_0, the ground state wavefunction ϕ_0 and the excitations are not affected by a change in density. The phase transition is defined through the reduced one-body density matrix (cfr. Section 3.1), that within the extended Bogoliubov model reads

$$g_1(r, r') = \exp\left[-\frac{1}{2}\sum_j \left|\frac{v_{\perp j}(r)}{\sqrt{\rho_0(r)}} - \frac{v_{\perp j}(r')}{\sqrt{\rho_0(r')}}\right|^2\right]. \tag{2.40}$$

Recalling that $\rho_0(r) = N_0|\phi_0(r)|^2$ this equation can be rewritten as

$$g_1(r, r') = \exp\left[-\frac{1}{2}\frac{1}{N_0}\sum_j \left|\frac{v_{\perp j}(r)}{\phi_0(r)} - \frac{v_{\perp j}(r')}{\phi_0(r')}\right|^2\right] = \left[\exp\left(-\frac{1}{2}\sum_j \left|\frac{v_{\perp j}(r)}{\phi_0(r)} - \frac{v_{\perp j}(r')}{\phi_0(r')}\right|^2\right)\right]^{\frac{1}{N_0}}.$$

$$(2.41)$$

The dependence of g_1 on the density has been traced out in the exponent $1/N_0$ and appears as a scaling factor, that can affect the absolute value of the g_1, but cannot change its functional form (cfr. numerical simulations below). This means that the long-range behaviour of the one-body density matrix does not depend on the density alone, upon a scaling factor, and that the phase boundary extracted from this model is independent of the number of particle N_0. At the same time, the theory is accurate only for large occupation of each lattice bin. From this we can draw the conclusion that the mean field theory gives results that are exact in the limit of infinite density, regardless of the density modulation occurring in the condensate wavefunction. A key point to confirm this analysis is that, in presence of disorder, ϕ_0 does not vanish. It can suffer from strong modulation, but, as a solution of a quantum mechanical problem, would not be identically zero: in the limit $\rho \to \infty$ this guarantees that any cell of the grid is occupied by a large number of bosons.

In this example, the coherence between two wells separated by Gaussian barriers is studied: this simple analysis is performed to illustrate the role of the density on the one-body density matrix in presence of an external potential. The barriers have the form

$$V(r) = \frac{A}{\sqrt{2\pi\sigma^2}} e^{-\frac{(r-r_0)^2}{2\sigma^2}} \qquad (2.42)$$

where r_0 is the center of the Gaussian, σ is the standard deviation and A gives the amplitude of the Gaussian barrier. The scale of energy for this problem is defined through the width of the Gaussian $E_\sigma = \frac{\hbar^2}{2m\sigma^2}$.

The coherence analysis is performed at fixed $U_0 = E_\sigma$ for two different densities $N_0^{(a)}/L = 4/\sigma$ and $N_0^{(b)}/L = 16/\sigma$ for two amplitudes of the central Gaussian barrier, while the barrier on the edge is assumed very large to avoid coherence effects due to the periodic boundary conditions. In Figs. 2.4**a** and 2.4**b** the two potentials $V(r)$ are shown together with the profile of the interaction energy $U(r)$, coming from the solution of the GPE. Figs. 2.4**c** and 2.4**d** show the coherence of a point – located in the center of the first well (r_0) – with the rest of the system, measured through the reduced one-body density matrix $g_1(r_0 - r)$. The corresponding averaged correlations are reported in Figs. 2.4**e** and 2.4**f**. In these last four figures the discrepancy between the absolute values of the correlation for different densities is evident. Making use of equation (2.41) the mapping between the two curves, characterized by different densities can be easily computed as

$$g_1(r_0, r_1; N_0^{(a)}) = \left[g_1(r_0, r_1; N_0^{(b)}) \right]^{\frac{N_0^{(b)}}{N_0^{(a)}}}. \qquad (2.43)$$

This mapping has been numerically tested and it is reported in Fig. 2.4 by the red dashed lines. This comparison confirms that the change in density

only affects the absolute value of the coherence (lower density corresponds to lower coherence), whereas the shape of the correlation function is totally unchanged and only depends on $V(r)$ and U_0. The relevant feature that emerges is that, as argued from analytic consideration, the choice of a density does not affect the prediction of the phase boundary in the mean-field limit: in fact, the functional behaviour of the one-body density matrix (algebraic or exponential) is conserved by this mapping.

The analysis performed so far mainly involved the ground state density $\rho_0(r)$. A crucial question to understand how the fluctuations affect the density is the dependence of the density fluctuations $\langle \delta \hat{\rho} \rangle$ on the number of particles. The expectation value of the density fluctuations can be chosen of the order [Castin, 2004]

$$\frac{\langle \delta \hat{\rho} \rangle}{\rho_0} \sim \frac{1}{\sqrt{\rho_0 \ell}}, \tag{2.44}$$

hence, the relative weight of the fluctuations becomes negligible in the limit of large density and does not contribute in the limit $\rho_0 \to \infty$. This implies that the relevant contribution in the mean-field limit comes from the ground-state and this justifies that the fragmentation study, in Chapter 4, is performed by studying the ground-state density rather than the total density.

The reduction of the relative contribution coming from the excitations also explains the increase in coherence for large densities. Nevertheless, the qualitative role of the fluctuations is independent of the density (cfr. Fig. 2.4) and this guarantees the consistency of the theory even in the large density limit, where the coherence is almost completely preserved across the system.

To summarize, the quantum phase transition in the pure mean-field limit, $\gamma \to 0$ and $\rho \to \infty$, will be studied using the model described in this chapter. This is not just a mathematical curiosity but rather a good approximation of a bosonic $1D$ system at ultra-low temperatures in the case of very large population. Several recent experiments operate in this regime of very weak interactions [Deissler et al., 2010, Chen et al., 2008, Clément et al., 2008]. It is reasonable to argue that the effects of a finite density represent a small perturbation with respect to the exact mean-field result.
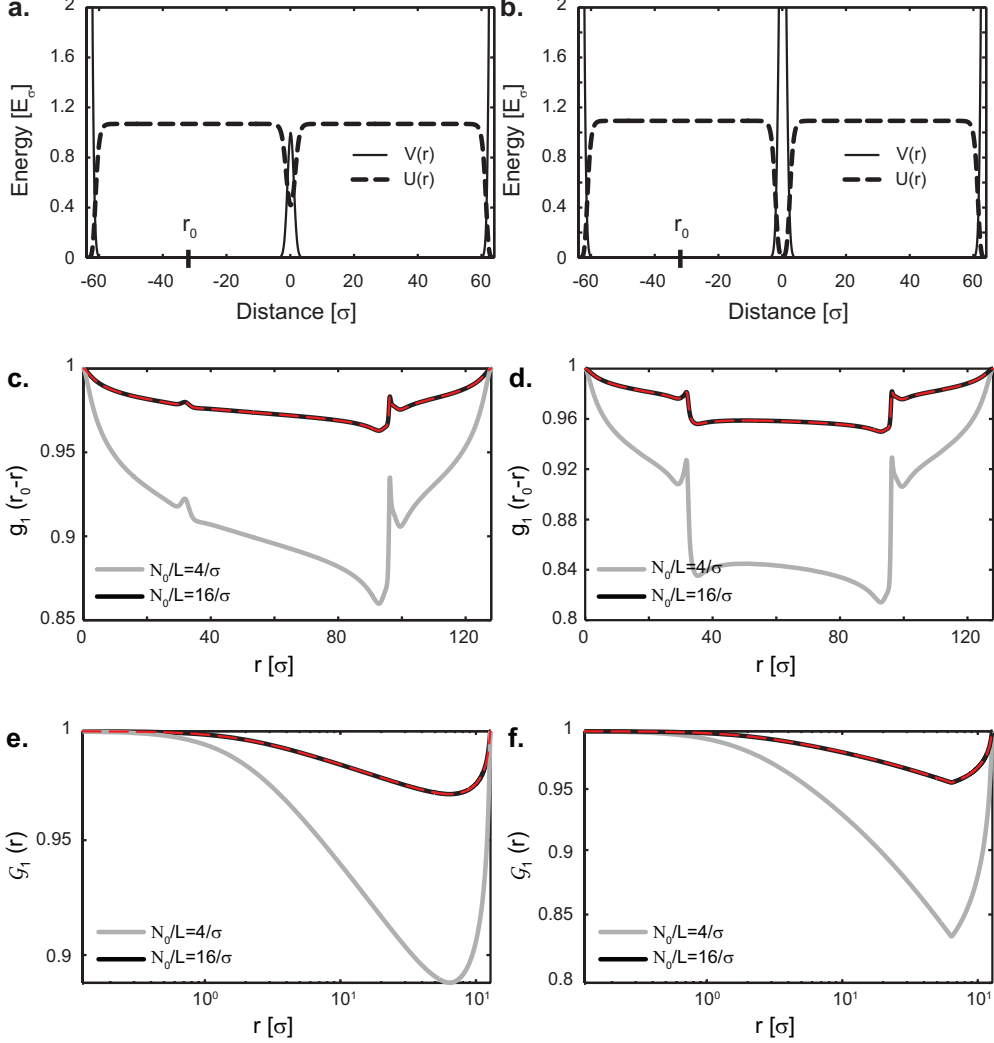
Figure 2.4: Coherence study of a double-well system created by two gaussian barriers. This analysis is performed at fixed $U_0 = E_\sigma$ and two different densities $N_0^{(a)}/L = 4/\sigma$ (grey solid lines) and $N_0^{(b)}/L = 16\sigma$ (black solid lines). The external potential and the interaction energy, solution of Eq. (2.8), are shown in the panels **a** and **b**. The barrier on the edge ($A/\sigma = 100\ E_\sigma$) is significantly larger than the one in the center to avoid the propagation of coherence due to the periodic boundary conditions. The amplitude of the central barrier changes between the panels on the left ($A/\sigma = 5\ E_\sigma$) and the ones on the right ($A/\sigma = 20\ E_\sigma$), tuning the system between a situation of weak perturbation to a more relevant separation between the two wells. The length of the system is $128\ \sigma$, measured in units of the standard deviation of the two Gaussian barriers. The reduced one body density matrix $g_1(r_0 - r)$, is shown in panels **c** and **d**. The reference point r_0 is chosen at the center of the first well, as shown in the upper panels. The degree of coherence is shown in panels **e** and **f**. The red dashed lines represent a mapping of the result obtained for $N_0^{(a)}/L = 4/\sigma$ onto the result for $N_0^{(b)}/L = 16\sigma$ made through Eq. (2.43), and they numerically prove that the mapping is exact.

THE SUPERFLUID-INSULATOR QUANTUM PHASE TRANSITION

Contents

In the previous chapter a theoretical method to describe low-dimensional Bose gases in the weakly interacting regime was presented. Here the extended Bogoliubov formalism is applied to investigate the properties of a 1D Bose gas at zero temperature in presence of disorder. In particular, this gas, that is superfluid in the uniform case, is expected to undergo a quantum phase transition to the insulating Bose-glass phase for sufficiently strong disorder. The transition is investigated by inspecting the long-range coherence of the gas and its superfluid component. Disorder diminishes the coherence and the superfluid component of the gas by triggering phase fluctuations responsible for driving the system to the normal phase: these fluctuations are identified in the low-energy Bogoliubov modes.

In this thesis we characterize the phase transition by studying the long-range behaviour of the one-body density matrix and by computing the superfluid component of the gas. We find numerical evidence for a change in the behaviour of the DoS at low energy across the phase boundary, namely a DoS that diverges going into the BG phase. The numerical analysis also shows a peculiar behaviour of the localization properties of the Bogoliubov modes. This study allows to draw the exact phase diagram in the limit of vanishing interaction – where mean-field theory is effective. This prediction is compared with results obtained for the disordered Bose-Hubbard model and with equivalent Bogoliubov-like approaches. In this chapter, the phase transition is inspected in Section 3.1 by studying the behaviour of the one-body density matrix. The properties of the Bogoliubov excitations, such as density of states (DoS) and localization length, are analyzed in Section 3.2. The superfluid component of the gas is investigated in Section 3.3 by studying the response of the system to an external velocity field. The study of all these features allows to draw the disorder-interaction phase diagram of the disordered weakly interacting Bose gas in 1D. This phase diagram is presented and discussed in Section 3.4.

To our knowledge, this is the first theoretical work that addresses the quantum phase transition by analyzing the long-range behaviour of the one-body density matrix. In fact, the study of the 1D Bose gas has been mainly performed by investigating two-body properties, localization and transport. In analogy with Anderson localization, these quantities allow to distinguish a superfluid behaviour as opposed to an insulating one. In the disorder-dominated phase, condensation and superfluidity are both absent, therefore, a natural question concerns whether one deals with a normal (diffusive) fluid or an insulating phase. From the one-body density matrix it is not possible to infer the diffusive or insulating nature of the phase, property that derives from two-body correlations (as the response function). On the other hand, literature is unanimous in reckoning that the Bose glass phase is insulating [Fisher et al., 1989, Aleiner et al., 2010] and that a single phase transition takes place in 1D bosonic systems. For this reason, the words *quasicondensate* and *superfluid* are used indistinctly in this thesis to refer to the coherent state (cfr. also Section 1.2.1).

3.1   ONE BODY DENSITY MATRIX

As we have seen in Chapter 1.1, according to the Penrose-Onsager criterion, the phase transition to a condensed or quasicondensed phase can be characterized through the behaviour of the one-body density matrix, defined as $G_1(r, r') = \langle \hat{\Psi}^\dagger(r') \hat{\Psi}(r) \rangle$ [Penrose & Onsager, 1956, Popov, 1972]. This quantity contains information about the probability amplitude of removing a particle at r and re-creating one at r', namely the one-particle Green function [Popov, 1980]. In simple terms, it expresses the correlation between two spatial points r and r' [Glauber, 1963].

The long-range behaviour of $G_1(0, r)$, in a uniform 1D bosonic system at zero temperature, has been initially studied within an hydrodynamic approach [Schwartz, 1977, Haldane, 1981]. Its asymptotic expression in the weakly interacting limit has been ob-

tained by means of a path integral formalism by Popov [Popov, 1980] and it reads

$$g_1(0, r) \simeq \left(\frac{1.037\xi}{r} \right)^{\frac{1}{2\pi\rho_0\xi}},$$ (3.1)

where $g_1(0, r)$ is the reduced one-body density matrix as defined in Chapter 2, ρ_0 is the quasicondensed density and ξ the healing length. The algebraic decay of the correlation, also defined as quasi-long-range order, characterizes the quasicondensed state. As checked in Chapter 2, the extended density-phase formalism gives results that are consistent with Popov's expression at long range and, additionally, they are trustworthy even at short distances [Mora & Castin, 2003]. The presence of a sufficiently strong disorder can destroy quasi-long-range order, triggering a quantum phase transition to a BG phase characterized by an exponential decay of the one-body density matrix [Fisher et al., 1989]. In the next section this change is inspected by studying the reduced one-body density matrix defined in Section 2.2.2.

3.1.1 Reduced one-body density matrix

Studying the behaviour of the one-body density matrix as a function of interaction, disorder and correlation energy allows to identify the quantum phase transition between the quasicondensed phase and the Bose-glass. The first analysis performed here focuses on the overall coherence of a single point, located at the position r_0, with the rest of the system for a specific disorder realization. In Fig. 3.1 the quantity $g_1(r_0, r)$ is shown for $\Delta = 0.8\, E_c$ and two values of interaction, respectively deep in the superfluid and in the insulating phase. This quantity is numerically calculated using Eq. (2.28), by solving the BdG problem on a domain of length $512\, \eta$ with periodic boundary conditions. This explains the unphysical increase of $g_1(r_0, r)$ for $r - r_0 > L/2$. As discussed in Section 2.2.4, the irregular shape of the reduced one-body density matrix confirms that this quantity is strongly affected by the presence of disorder and, thus, it is not an ideal marker for the phase transition. As shown in the next section, the criterion used to distinguish the quantum phases is based on the average of this quantity: it is nevertheless interesting to understand which features are responsible for the functional change of its averaged counterpart $\mathcal{G}_1$.

The decay of g_1 in the superfluid phase is algebraic on average, but its trend is noisy because it is affected by disorder. In the Bose glass phase, in addition to the disorder-induced modulation, this quantity shows abrupt jumps (see Fig 3.1**a**). These drops in coherence mark the separation between mutually incoherent regions. Pictorially, they are the consequence of the presence of weak links between two islands of condensate caused by large barriers of the underlying potential (see Fig. 3.1**c** for a direct comparison). An analogous step-like behaviour has been found in presence of quasiperiodic potentials [Cetoli & Lundh, 2010].

It is instructive to compare this spatial coherence with the shape of the Bogoliubov $v_\perp$-modes, as quantum fluctuations into these modes are responsible for the lack of long-range coherence. Comparing Figs. 3.1**a** and 3.1**b** it appears that these drops in $g_1(r_0, r)$ coincide

with the nodes of the lowest-lying Bogoliubov modes. The amount of the reduction in coherence is related to the amplitude of the excitations that increases for low energies as $|v_\perp(E)|^2 \propto 1/E$ all across the phase diagram (this statement is discussed in detail in Section 3.2.1). This analysis underlines the fundamental role played by weak links in
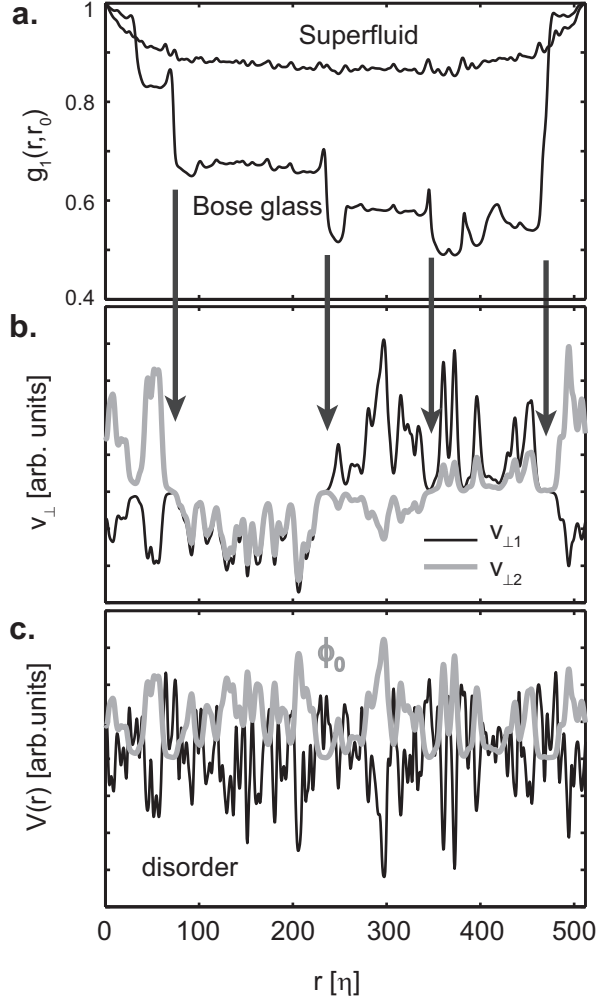

Figure 3.1: a. $g_1(r_0, r)$ in the superfluid and in the Bose glass phases, computed for $\Delta = 0.8\ E_c$ and $U_0 = 0.32$ and $1.6\ E_c$. At distances $\gtrsim L/2$ the coherence grows because of the periodic boundary conditions employed in the numerical simulations. **b.** Corresponding low-energy $v_\perp(r)$ excitations in the Bose glass phase, in the case $U_0 = 0.32\ E_c$. The arrows highlight the link between the jumps in $g_1(r_0, r)$ and the nodes of the low-energy excitations. **c.** Corresponding disorder realization (black line) and ground state wavefunction (grey thick line) obtained as a solution of the GPE.

triggering the phase transition. This will be investigated in more detail in relation to the Bogoliubov excitations (Section 3.2.1) and, in particular, in the context of fragmentation

(Chapter 4). The next section is devoted to the characterization of the quantum phase transition through the degree of coherence, that, contrarily to $g_1(r, r_0)$, allows a precise distinction between the two quantum phases.

3.1.2 DEGREE OF COHERENCE

Being the reduced one-body density matrix not a good indicator, the phase transition is inspected by studying the average of $g_1(r, r')$, namely the degree of coherence $\mathcal{G}_1(r)$, defined in equation (2.29) and recalled here: $\mathcal{G}_1(a) = \int \mathrm{d}r' g_1(r', r' + a)/L$. This quantity is expected to behave smoothly and it is translationally invariant in the thermodynamic limit. It should therefore allow to distinguish the quasicondensed phase from the BG, simply through the study of its long-range decay. Assuming an ergodic system, the running average on the spatial coordinate coincides with the average on a statistical ensemble of the disorder realizations. This implies that there is no dependence on the disorder realization and, given a disorder amplitude and distribution, this quantity only depends on the distance.

Three parameters enter the determination of the quantum phase of the gas: the disorder amplitude Δ, the interaction energy U_0 and the correlation energy E_c, therefore the problem can be rescaled to two parameters, Δ/E_c and U_0/E_c. In Fig. 3.2, $\mathcal{G}_1(r)$ is shown for a fixed value of interaction, $U_0 = 0.8 \ E_c$, and for varying disorder amplitude Δ. As it could be expected, disorder has a detrimental effect on the overall coherence of the gas, in fact the value of $\mathcal{G}_1$ is maximum in the uniform case (solid line in Fig. 3.2) and it monotonically decreases for increasing disorder. It decays algebraically for $\Delta = 0$ (linear in log-log scale) and, as long as the disorder only represents a small perturbation, it preserves this functional shape. When the ratio Δ/U_0 becomes significant, an exponential decay is instead observed, and the quasi-long range order is destroyed marking the onset of the BG phase.

An equivalent analysis performed at fixed disorder amplitude ($\Delta = 0.8 \ E_c$) and tuning U_0 is shown in Fig. 3.3. From this plot it emerges that, differently from the previous case, the degree of coherence at a fixed distance shows a non-monotonous behaviour as a function of U_0. In the uniform case the one-body density matrix is algebraic at large distances and, as expressed by Eq. (3.1), its value decreases by increasing the interaction energy ($U_0 \propto 1/\xi^2$), even though it keeps the same functional shape. Interactions cause stronger quantum fluctuations and therefore a loss of coherence, this trend is a sign that the system is moving towards the Tonks-Girardeau regime, where the coherence is limited to single bosons. By analogy, in presence of disorder, a 1D Bose gas in the SF phase decreases its coherence range when it becomes more interacting. On the other hand, it is reasonable to argue that values of disorder much larger than U_0 destroy long-range order and drive the system to a glassy phase. In these two limits of very large and very small interaction-to-disorder ratio, the coherence is lower than in the intermediate region where the transition occurs: this explains the non-monotonous behaviour of the degree of coherence (the same conclusion was drawn in seminal studies performed on the discrete Bose-Hubbard model [Scalettar et al., 1991]).
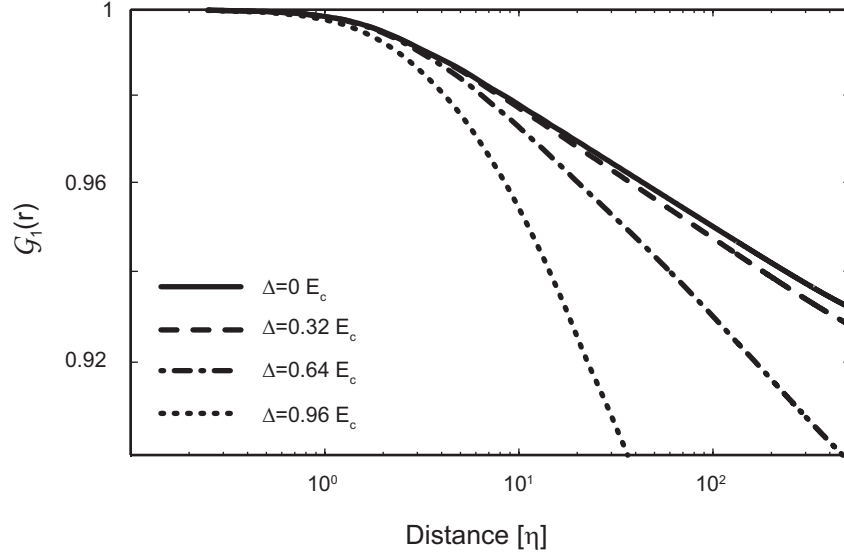
Figure 3.2: Degree of coherence $\mathcal{G}_1(r)$ for fixed interaction energy $U_0 = 0.8\ E_c$ and different values of disorder $\Delta = 0,\ 0.32,\ 0.64,\ 0.96\ E_c$. The solid line shows the degree of coherence in the uniform case. The presence of disorder decreases the overall coherence of the Bose gas, but as far as it only represents a small perturbation does not destroy the quasi-long-range order (dashed line). On the contrary, when disorder dominates (dotted line), the degree of coherence decays exponentially.

Going back to Fig. 3.3 the build-up of coherence occurs by increasing the interaction energy: at a certain threshold the coherence attains its maximum: this happens when interaction between particles is strong enough to overcome the underlying disorder. From there on, a phenomenology analogous to that of the uniform gas takes place, and $\mathcal{G}_1(r)$ still displays a power-law decay but falls off more rapidly as a function of distance. This non-monotonous behaviour makes easier a correct estimate of the critical interaction energy for a given disorder amplitude and, therefore, of the occurrence of the quantum phase transition.

The 1D system under study has periodic boundary conditions. This makes the $\mathcal{G}_1(r)$ symmetric on the interval $[0, L]$ and a proper size scaling is necessary to extract thermodynamic properties. In Figs. 3.2 and 3.3 we show only the spatial interval $[0, L/4]$ that reflects the behaviour in the thermodynamic limit. The numerical methods that we use for these simulations – mainly the diagonalization of the Bogoliubov matrix (2.12) – limit the achievable size to $L \sim 6000\eta$ sampled with 4 points per correlation length. This analysis have been performed for a large interval of values of disorder and interaction. The resulting phase diagram is shown in Fig. 3.4 in the $U_0/E_c - \Delta/E_c$ plane. It is evident that two different power laws characterize the boundary depending on the value of U_0/E_c at which the transition occurs. In the following sections
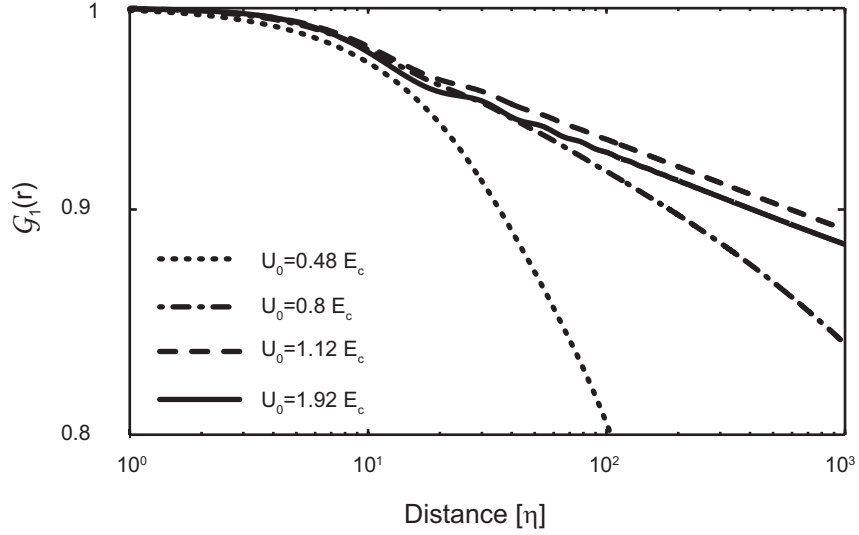
Figure 3.3: Degree of coherence, $g_1(r)$, for fixed disorder strength $\Delta = 0.8\ E_c$ for different values of interaction $U_0 = 0.48,\ 0.8,\ 1.12,\ 1.92\ E_c$. The trend of the coherence at fixed distance is non-monotonous as a function of interaction: by increasing the interaction strength, $\mathcal{G}_1$ attains its maximum for $U_0 = 1.12\ E_c$ and decreases for larger values of U_0, while still maintaining an algebraic decay.

an accurate analysis of the properties of the gas across the phase transition is performed. The discussion of the phase diagram will be resumed at the end of this chapter.

3.2   Bogoliubov excitations

In low dimensionality, the main mechanism of decoherence are fluctuations of the quantum phase, affecting the long-distance properties of the gas. The proliferation of these excitations, also known as phase flips, may destroy the superfluid phase. As explained in Section 3.1, the fluctuations responsible for the loss of coherence have been identified here in the low-lying Bogoliubov $v_{\perp j}$-modes. They are good candidates because they have a phase-character, they act over long distances – differently from fast-oscillating density fluctuations – and their relative weights, $|v_{\perp j}|^2$, give the main contribution to decoherence (see Fig. 3.6). Given this crucial role in triggering the phase transition, it is interesting to understand which of their properties undergo a significant change across the phase boundary. This section is devoted to the analysis of the properties of the Bogoliubov modes in the different phases. In particular, the DoS and the localization properties are investigated.
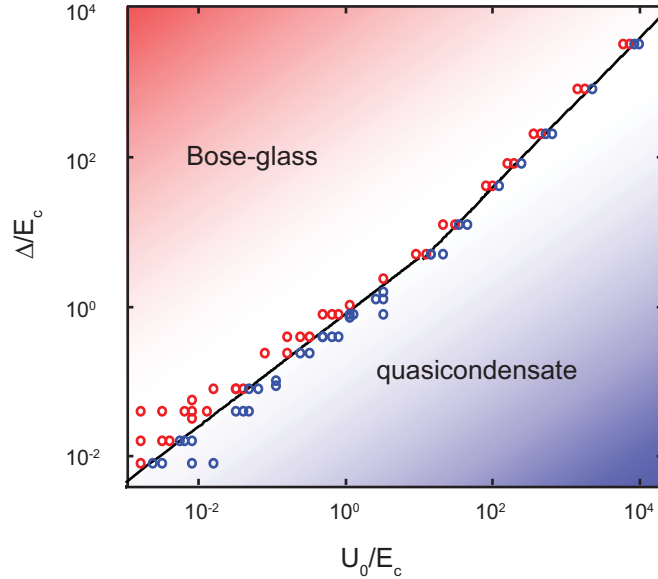
Figure 3.4: Quantum phase diagram of a 1D weakly interacting Bose gas in presence of gaussian disorder. The vertical axis Δ denotes the disorder strength whereas the horizontal axis indicates the interaction energy U_0. Both quantities are rescaled with respect to the correlation energy E_c. The red circles mark states in the Bose-glass phase whereas the blue ones corresponds to states in the quasicondensed phase. The black line is a guide for the eye that approximately shows the phase boundary.

3.2.1 DENSITY OF STATES

The solution of the Bogoliubov problem gives direct access to the spectrum of the excitations. This quantity plays a fundamental role in determining key physical properties such as compressibility and specific heat. Let us introduce their DoS, which counts the number of excitations $\mathrm{d}\mathcal{N}$ in an interval of energy $\mathrm{d}E$ around the energy E, namely

$$D(E) = \frac{\mathrm{d}\mathcal{N}}{\mathrm{d}E}. \tag{3.2}$$

As the phase transition is triggered by the low-energy fluctuations, here, the DoS of the low-lying Bogoliubov excitations is studied in presence of disorder. The behaviour of the DoS across the phase transition is the object of a long-standing debate. The excitations of the interacting Bose gas in the uniform case (such as in the SF phase) are sound-like and the DoS is known to approach a constant value for $E \to \mu$, in analogy with phonons in random elastic chains [Ziman, 1982]. On the other hand, the behaviour of the DoS in the insulating phase is still controversial even if several works argued that it has to be constant for $E \to \mu$ throughout the whole phase diagram. In this section, the numerical evidence of a diverging DoS of the Bogoliubov excitations in the BG phase is reported, together with a hand-waving argument supporting this behaviour.

In this numerical scheme the DoS is defined as

$$D(E) = \frac{1}{L} \sum_j \delta(E - E_j), \tag{3.3}$$

where the E_j are the positive Bogoliubov energies, directly extracted from the eigenvalues of the matrix (2.12). Given the nature of the Bogoliubov problem from now on we assume $\mu = 0$. The results shown in Figs. 3.5 and 3.6 are averaged over thousands of realizations. A consequence of the spatial homogeneity of the disorder is that quantities such as the DoS are self-averaging, in other words, the system under investigation is ergodic. In particular, the limiting behaviour can be equivalently extracted by performing an average over the different configurations of disorder for a system of finite size. The only inconvenience of finite size simulation is the introduction of an infrared cutoff in the spectrum.
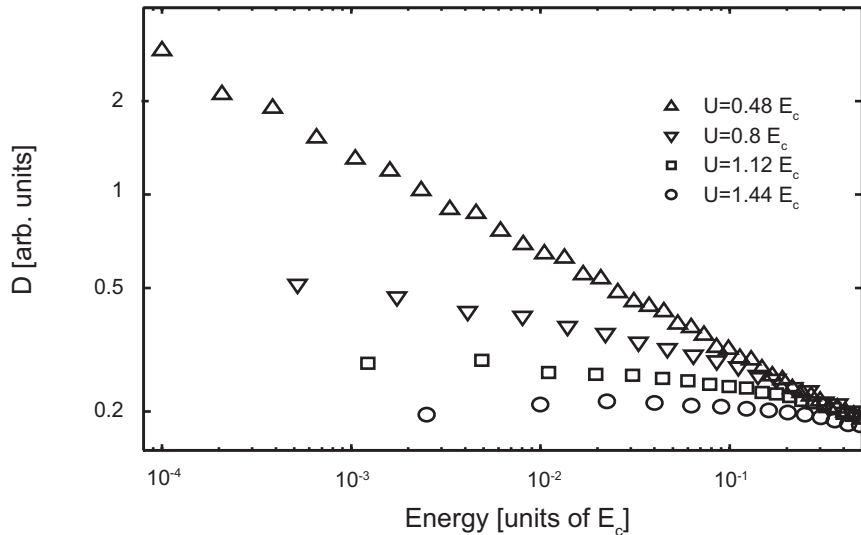

Figure 3.5: Averaged $D(E)$ at fixed $\Delta = 0.8\,E_c$ for various interaction energies. The triangles denote two Bose glass cases ($U_0 = 0.48 - 0.8\,E_c$), whereas squares and circles mark two superfluid phases ($U_0 = 1.12 - 1.44\,E_c$). The energy of the low-lying Bogoliubov excitations goes to lower values in the strongly disordered case because of the finite size of the system. In fact, with periodic boundary conditions in absence of disorder, the lowest energy excitation is a plane wave with wavelength L. In the strongly disordered case, on the contrary, the lowest energy can be extracted by analyzing a simple two wells system: the energy of the lowest mode – a phase flip – is proportional to the tunneling across the barrier [Gati & Oberthaler, 2007]. Strong disorder corresponds to high barriers, thereby small tunneling and small excitation energies. In both cases, the spectrum becomes gapless in the thermodynamic limit ($L \to \infty$).

As shown in Fig. 3.5, $D(E)$ approaches a constant value at low energy in the SF case. However, within the accuracy of the numerical investigation, it seems to develop a power-law divergence in the BG phase. In fact, by decreasing the interaction at fixed disorder, the DoS for $E \to 0$ increases and it starts diverging following a power-law

beyond the phase boundary with a slope that increases monotonically, when going deeper into the insulating phase. In other words, the density of Bogoliubov modes increases when approaching the chemical potential. This feature is peculiar of interacting bosonic systems, where the excitation spectrum is bound from below by μ and the spectrum is gapless in both the quantum phases investigated here. In fact, the non-interacting problem shows a $1/\sqrt{E}$ divergence in the uniform case that, in presence of disorder, turns into the so-called *Lifshitz tail* in the negative part of the spectrum of the excitations [Lifshitz, 1963, Lifshitz, 1964, Lee & Gunn, 1992].

The constant DoS in the SF phase agrees with the theoretical predictions [Gurarie & Altland, 2005, Gaul et al., 2009] and it is analogous to the DoS of random phononic chains [Ziman, 1982]. For what concerns the insulating phase, the conclusions drawn here are in contrast with what is stated in some previous theoretical studies [Fisher et al., 1989, Nisamaneephong et al., 1993, Ma et al., 1993, Lee & Gunn, 1990], arguing that the low-energy DoS should remain constant in the insulating phase. Can this behaviour be related to the change in the first-order correlation function? Inspection of the reduced one-body density matrix – in equation (2.28) – gives insight about the role of the spectral distribution of the excitations. We recall the expression for the reduced one-body density matrix

$$g_1(r, r') = \exp\left(-\frac{1}{2}\sum_j \left[\frac{|v_{j\perp}(r)|^2}{\rho_0(r)} + \frac{|v_{j\perp}(r')|^2}{\rho_0(r')} - \frac{v_{j\perp}^*(r)v_{j\perp}(r') + v_{j\perp}^*(r')v_{j\perp}(r)}{\sqrt{\rho_0(r)\rho_0(r')}}\right]\right).$$
(3.4)

At large distance, the crossed terms cancel and the main contribution is given by $\sum_j |v_{\perp j}(r)|^2 + |v_{\perp j}(r')|^2$. This expression can be rewritten in terms of energy, by using the DoS and it reads

$$g_1(r, r_0) \sim \exp\left[-\int |v_{\perp E}(r)|^2 D(E)\mathrm{d}E\right] = \exp\left[-\delta m\right],$$
(3.5)

where $|v_{\perp E}(r)|^2$ is defined as the local density of Bogoliubov excitations per unit energy, i.e.

$$|v_{\perp E}(r)|^2 = \frac{\sum_j |v_{\perp j}(r)|^2\delta(E - E_j)}{\sum_j \delta(E - E_j)}.$$
(3.6)

An expression analogous to (3.5) has been derived by Ma & coworkers [Ma et al., 1993], who have found, within a *spin wave approximation*, that a crucial role in determining the phase transition is played by

$$\delta m = \int D(E)v^2(E)\mathrm{d}E.$$
(3.7)

Let us now discuss the quantity $|v_{\perp E}|^2$ in the spatially homogeneous case. In one dimension without disorder $D(E)$ is constant, and the value of $v_{\perp E}$ can be computed

analytically. The Bogoliubov v-modes are

$$v_k = \sqrt{\frac{\frac{\hbar^2 k^2}{2m} + gn}{2\varepsilon(k)} - \frac{1}{2}} \tag{3.8}$$

where $\varepsilon(k)$ is the Bogoliubov dispersion, i.e.

$$\varepsilon(k) = \sqrt{\frac{gn}{m}\hbar^2 k^2 + \left(\frac{\hbar^2 k^2}{2m}\right)^2}. \tag{3.9}$$

At small k the dispersion is linear in k and results in $|v(E)|^2 \propto 1/E$, that, combined with a constant DoS entails δm diverging as $\ln N$ for $N \to \infty$ (consistently with the algebraic decay of g_1).

Expression (3.5) is valid even in the case of strong disorder: as a consequence the transition has to be contained in this exponent, and therefore δm has to diverge faster than in the uniform case. The behaviour of $|v(E)|^2$ in the strongly disordered case can be obtained from the analogy with Josephson physics, considering a Josephson junction connected via a weak link. The two-well system contains the same phenomenology of the disordered Bose gas under analysis and the weak link prevents the creation of coherence over the whole system. In this scenario, the energy dependence of the Bogoliubov modes can be extracted analytically [Paraoanu et al., 2001, Gati & Oberthaler, 2007] and, in the case of weak tunneling in Eq (1.45) it displays a divergence $|v(E)|^2 \sim 1/E$, as in the SF phase. The value of $|v(E)|^2$ is shown in Fig. 3.6: the numerical results for the uniform case are computed using the extended Bogoliubov approach, and coincide with the analytical expression extracted from Eq. (3.8). As argued above, the presence of a strong disorder does not distort the functional dependence of $|v(E)|^2$, hence, the change in $g_1(r)$ has to be linked to a change in $D(E)$ from constant to power-law divergent for $E \to 0$.

In spite of the identical assumptions, Ma *et.al.* drew opposite conclusions, attributing the triggering of the phase transition to a change in the term $v^2(E)$. Their argument relies on the fact that excitations at infinitely strong disorder in a spin chain are single spin flips with energies distributed as the underlying disorder. Their conclusion is that this distribution is finite for $E \to 0$ and it is supported by numerical simulations performed on small-scale systems. Here, a clear numerical evidence and an analytical argument are brought to prove that the amplitudes $v_\perp(E)$ do not play any role in determining the phase transition and, on the contrary, the numerics shows that a key role is played by the DoS. An intuitive explanation can be found by going back to the phenomenology of weak links analyzed in Section 3.1. Strong disorder entails a proliferation of weak links that comes along with a large amount of phase fluctuations destroying the quasi-long-range order. These low-energy excitations change their phase between weakly coupled neighbouring islands. The DoS is therefore directly related to the statistics of the strength of the weak links investigated in Ref. [Altman et al., 2008, Altman et al., 2010]. In this analysis the authors find a diverging DOS in the so-called *random-singlet phase*. We have no clear proof that the phase that we observe is a random-singlet, we just report that the two
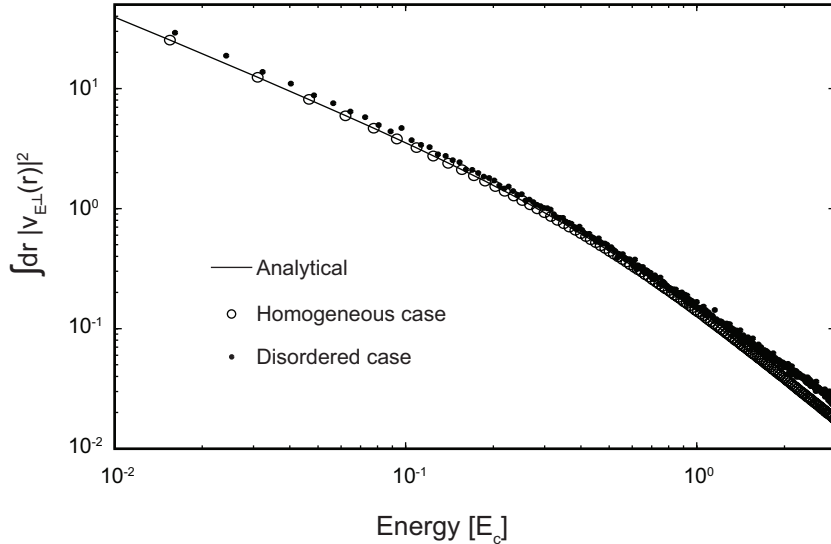
Figure 3.6: Comparison of the values of $|v(E)|^2 = \int \mathrm{d}r |v_{E\perp}(r)|^2$ in a uniform system and in a disorder-dominated case. The analytic prediction (solid line) and the numerical results in absence of disorder (circles) coincide and behave as $1/E$ for $E \to 0$. The results of realization average performed in case of strong disorder are shown by the black dots. Despite a small displacement, the two cases show the same analytical dependence at small energies, i.e. they diverge as $1/E$.

models agree in finding a diverging DoS. The random-singlet phase is specific of systems with particle-hole symmetry, as it is the case in the large density limit [Huber et al., 2007], that looks like the one described by the Bogoliubov model. On the contrary, this assumption is violated in the limit of low filling. On this point, there is the possibility that the divergence is an artifact of the infinite density and that the DoS for any finite density would bend to a finite value.

The discrepancy between our results and former predictions [Fisher et al., 1989, Ma et al., 1993] could also be due to a different nature of the phase transition in the weakly and strongly interacting regimes, as initially guessed [Giamarchi & Schulz, 1988, Scalettar et al., 1991] and recently suggested by a renormalization group analysis [Altman et al., 2010]. In particular the analysis by Altman *et al.* claims that the phase transition at strong disorder could belong to a different universality class with respect to the one at weak disorder.

3.2.2 PROPERTIES OF THE GAS

The behaviour of the DoS has important consequences on many physical properties of the gas such as speed of sound, compressibility and specific heat. In addition, the DoS plays a relevant role in the determination of some statistical averages and can be related to the proliferation of weak links when disorder dominates.

From the results of the previous section, it emerges that disorder acts increasing the

DoS at low energy. An immediate consequence is that the linear Bogoliubov dispersion becomes less steep [Gaul & Müller, 2011] and consequently the speed of sound of the gas decreases and finally vanishes in the insulating phase where the DoS diverges. An infinite DoS at low energy also implies a diverging compressibility, defined as $\kappa = \partial\rho/\partial\mu$. The compressibility is nonzero both in the quasicondensed and Bose-glass phase, but the glassy phase found in this work, being marked by a diverging compressibility, is qualitatively different from the one described by Fisher *et.al.* in their seminal work [Fisher et al., 1989].

Going deeper in the analysis of the DoS one can observe that the Bogoliubov spectrum is not modified by going to finite temperatures. Bogoliubov theory is however valid as far as the temperature is very low. One could object that the phenomenology that destroys long range order in the disorder-dominated case is substantially different from the uniform phase at finite temperature, although they show an analogous behaviour in the first order correlation function. The specific heat is a useful quantity to investigate the discrepancies between the two scenarios. The fate of the specific heat and its implications are discussed in detail in Chapter 5 where the finite temperature case is considered.

3.2.3 Localization

Since the recent observation of Anderson localization in atomic gases [Roati et al., 2008, Billy et al., 2008], the localization-delocalization transition – due to interaction – polarized the attention of the scientific community. These investigations concern the localization of both the ground state wave-function [Sanchez-Palencia et al., 2007, Scalettar et al., 1991] and the Bogoliubov quasi-particles [Lugan et al., 2007b, Bilas & Pavloff, 2006, Gurarie et al., 2008] and they are mainly aimed at recovering the exponential decay characterizing the tails of an Anderson localized wavefunction.

As pointed out in the previous sections, in presence of interaction, delocalized low-energy phase fluctuations are the main mechanism that reduces the coherence. For this reason, this section is devoted to the analysis of the localization properties of the Bogoliubov excitations. Most of the previous studies were restricted to the weak disorder case, describing the quasicondensed phase. The aim here is to study the extent of the low-energy Bogoliubov modes in both the superfluid and insulating phases and determine whether there is a significant change across the phase transition. In order to characterize the localization, the inverse participation ratio (IPR) of the $v_\perp$-modes is studied. This quantity directly gives an estimate of the spatial extent of their wavefunction and, for a generic normalized wavefunction, $\phi(r)$, it is defined as

$$I = \frac{1}{\int |\phi(r)|^4 \mathrm{d}r}. \tag{3.10}$$

I has the dimensionality of a length and it measures the portion of space where the wavefunction is substantially different from zero. In a finite system, it attains its maximum value (coincident with the system size) if the wavefunction is constant, $\phi(r) = 1/\sqrt{L}$. An IPR that diverges in the thermodynamic limit may be considered as a marker of an extended state. The IPR can be very different from other quantities characterizing

the localization as, for instance, the exponential decay length of the wavefunction tails related to Lyapunov's exponent [Kramer & MacKinnon, 1993]. It is nevertheless the most relevant characterization for our purposes, in fact, a phase change occurring over long distances can only be produced by an excitation whose wave function is significantly non-zero at points very far apart in space (even if it has rapidly decaying exponential tails outside these regions [Kramer & MacKinnon, 1993]). The IPR for the Bogoliubov excitations reads

$$I_j = \frac{\left(\int \mathrm{d}r |v_{\perp j}(r)|^2\right)^2}{\int \mathrm{d}r |v_{\perp j}(r)|^4}, \tag{3.11}$$

and the corresponding realization-averaged quantity investigated here is

$$L_a(E) = \frac{\sum_j I_j \delta(E - E_j)}{D(E)}. \tag{3.12}$$

In Fig. 3.7**a** the results are shown for fixed disorder and varying interaction strength. As it can be noticed, the IPR always shows a power-law divergence $E^{-\alpha}$ for $E \to 0$, with α increasing when going deeper in the superfluid phase and L_a diverges in both the limits $E \to \infty$ and $E \to 0$ with a minimum at intermediate energy. This different behaviour is symptomatic of the different nature of the excitations: phase-like with a phononic character at low-energies and density-like, behaving as free particles, at large energies.

In the low energy limit the exponent α characterizing the divergence varies continuously across 1, and it crosses that value in correspondence with the phase boundary computed through the correlation length (Fig. 3.7**b**). In the quasicondensed phase $\alpha > 1$, whereas $\alpha < 1$ in the BG phase. It decreases by lowering the interaction strength, apparently linearly vanishing for $U_0 \to 0$ as predicted for the non interacting case, where the localization goes to a constant value at low energy [Kramer & MacKinnon, 1993]. The phase transition inspected via the IPR gives the phase boundary with high accuracy as evident in Fig. 3.7**b**.

The localization of the excitations was studied by Bilas & Pavloff [Bilas & Pavloff, 2006] that found a localization diverging as E^{-2} at low energy in the quasicondensed phase and, instead, behaving as in the free particle case ($\propto E$) at large energies, because the BdG equations decouple. The two diverging behaviours for $E \to 0$ and $E \to \infty$ are qualitatively analogous to our findings, but the functional laws do not coincide. Our results instead agree fairly well with the theoretical predictions by Gurarie *et.al.* [Gurarie et al., 2008] that, through a renormalization group study, determined that at low energy the localization of the Bogoliubov modes in the SF phase diverges as $E^{-\alpha}$ with $1 < \alpha < 2$, where $\alpha = 1$ at the phase boundary. Here, a full agreement with this prediction is found, although it is not possible to reach the case with exponent $\alpha = 2$ because of the limitations due to the finite size of the simulations. This limits the analysis for large U_0, where the IPR saturates, and does not allow to catch the full extent of the excitations: the shaded zone in Fig. 3.7**a** marks this region affected by the finite size of the numerical sample. At large energies (not shown here) the IPR diverges as in the non-interacting case, that, for

the IPR, is known to differ from the prediction made by Bilas & Pavloff [Bilas & Pavloff, 2006].

This analysis deserves a comment in relation to the nature of the disordered potential. In fact, the energy dependence of the localization length in the non-interacting case depends on the disorder distribution. In the case of repulsive speckles the potential is bounded from below and its distribution decays exponentially at large energy. The energy of a single particle state is related to the probability of occurrence of spatially large minima as

$$E = \frac{\hbar^2}{2mL_S^2},\tag{3.13}$$

where L_S is the spatial extension of the minimum, a measure of the localization length. The inversion of this relation gives for the energy dependence of the localization

$$L_S = \sqrt{\frac{\hbar^2}{2mE}}.\tag{3.14}$$

The localization in presence of speckles diverges as $E^{-1/2}$, hence $\alpha = 1/2$ for $E \to 0$. This statement points out a dependence of the asymptotic behaviour of α for vanishing interaction on the statistics of disorder, nevertheless it does not contradict the prediction of $\alpha = 1$ at the phase transition, which thus takes a universal meaning.
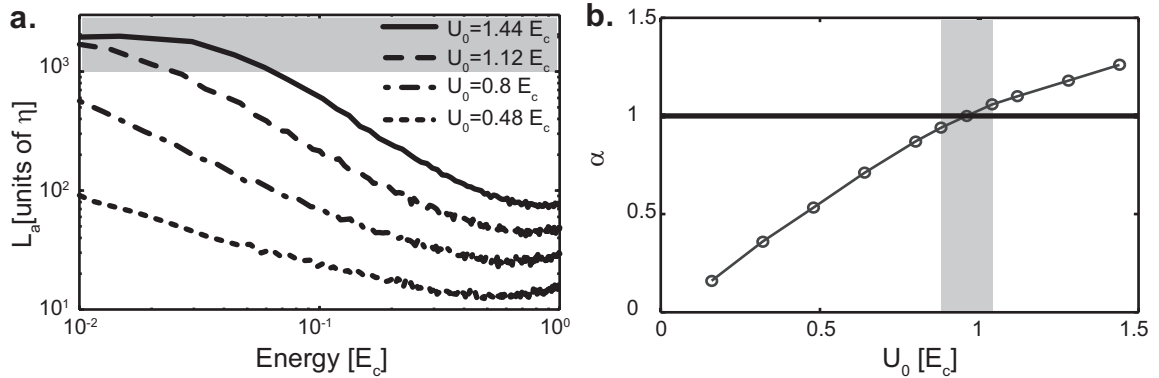
Figure 3.7: a. Averaged IPR for fixed $\Delta = 0.8\,E_c$ and varying U_0. The cases with $U_0 = 0.48 - 0.8\,E_c$ are in the BG phase, whereas for $U_0 = 1.12 - 1.44\,E_c$ are superfluid. A saturation of the IPR occurs at large lengths because of the finite size of the simulated system; the shaded zone represents a confidence limit. **b.** Computed exponents of the power-law divergence of $L_a(E)$ for different values of U_0; the shaded zone marks the phase boundary computed through the one-body density matrix.

For what concerns the ground state wavefunction, the results of such an analysis can be predicted theoretically. In fact, ϕ_0 always has an extended nature [Hertz et al.,

1979, Singh & Rokhsar, 1994] and this can be proven by assuming that the condensate wavefunction is localized. In this case, a macroscopic number of bosons N_0 would occupy a finite portion of space L_ℓ where $\phi_0(r)$ extends. The Gross-Pitaevskii energy of such a state can be written as (see Eq. (2.22))

$$E_{GP}(N) \simeq \int \mathrm{d}r N_0 \frac{\hbar^2}{2m} \phi_0^*(r) \nabla^2 \phi_0(r) + N_0 V(r) \phi_0^2(r) + \frac{1}{2} g_0 N_0^2 \phi_0^4(r), \qquad (3.15)$$

where the last term represents the interaction energy. The integral $\int \phi_0^4(r) \mathrm{d}r$, in the case of a localized wavefunction, is directly related to the IPR, i.e. it gives $1/L_\ell$ independently of the system size. As a consequence, the interaction energy would vary as the square of the number of particles and the total energy in equation (3.15) would not be an extensive quantity. The original assumption has to be incorrect and ϕ_0 must thus be extended. This does not prevent the condensate wavefunction from being vanishingly small in some regions that connect two "islands" where the condensate is localized.

The GP equation can be seen as a Schrödinger equation where the effective external potential is the sum of the disordered potential and of the interaction term. In this scenario one can wonder how this argument matches with the fact that all eigenstates of a disordered potential in one and two dimensions are localized [Anderson, 1958]. Interaction between particles is the explanation of this apparent paradox: in fact, the effective potential is the result of a nonlinear equation built so to have an extended ground state. Indeed, ϕ_0 acts on the disordered potential smoothing its original shape [Singh & Rokhsar, 1994].

3.3   SUPERFLUID FRACTION

The computation of the superfluid fraction of the gas is an alternative way to identify the quantum phase transition. In fact, the conducting phase in bosonic systems at zero temperature is believed to be always superfluid [Leggett, 1973, Leggett, 1998]. A non-zero superfluid fraction comes along with the establishment of quasi-long-range order across the system and, for this reason, the study of superfluidity represents an ideal check of the predictions of the previous sections.

Superfluidity denotes the ability of the fluid to flow without friction through the suppression of dissipation due to viscosity. The conceptual difference between a superfluid and a normal fluid can be inspected by embedding the fluid into a slowly rotating annulus: a normal fluid rotates in equilibrium with the container, whereas, a superfluid stays at rest in the laboratory frame, a phenomenon known as Hess-Fairbank effect [Hess & Fairbank, 1967, Leggett, 1973].

3.3.1   TWO-FLUID MODEL

In order to quantify the superfluid fraction of a gas, its response to the application of a small velocity field can be studied [Fisher et al., 1973, Roth & Burnett, 2003a, Lieb et al., 2002]. As the superfluid and normal components respond differently to the application

of a velocity field, the fluid can be depicted within a two-fluid scheme: a normal density component ρ_N, that is dragged by the field, and a superfluid one ρ_S, staying at rest. The energy difference between a system with an applied velocity field and one at rest, is given by the kinetic energy of the superfluid component and hence, via its velocity, by the total superfluid fraction. The energy difference, computed in the moving frame, applying a small velocity $\mathbf{v}$, reads

$$E_\Theta - E_0 = \frac{\rho_S}{\rho} \frac{1}{2} N m \mathbf{v}^2, \tag{3.16}$$

where E_Θ is the ground state energy of the system with the applied velocity field, E_0 is the energy of the system at rest, ρ is the total density, m is the mass of the particles, N is the number of particles. The superfluid is the fraction of the gas responding to the applied phase by flowing at the velocity $\mathbf{v}$ in the moving frame. An equivalent way to perform this task [Lieb et al., 2002] is by applying twisted boundary conditions to the system ($\Psi(L) = \Psi(0)e^{i\Theta}$) and evaluating the energy difference between the twisted system and the one with periodic boundary conditions.

From a microscopic point of view, the velocity field is associated to the spatial variation of the phase of the condensate as [Leggett, 2001]

$$\mathbf{v} = \frac{\hbar}{m} \nabla \theta(x). \tag{3.17}$$

If one imposes a total phase twist Θ linearly distributed over the length L as $\theta(x) = \Theta x/L$, then the total phase twist is connected to the velocity by

$$\Theta = \frac{\mathbf{v} L m}{\hbar}. \tag{3.18}$$

Therefore the relation between the energy difference and the superfluid fraction, $f_S = \rho_S/\rho$ reads

$$f_S = \frac{2mL^2}{\hbar^2 N} \lim_{\Theta \to 0} \frac{E_\Theta - E_0}{\Theta^2}, \tag{3.19}$$

where the limit of small velocity is taken in order to not underestimate the superfluid fraction [Roth & Burnett, 2003a]. This definition of superfluidity, as a dynamical response to an applied phase twist, is not unique [Prokof'ev & Svistunov, 2000], although it is commonly used in literature [Fisher et al., 1973], within mean field approaches [Singh & Rokhsar, 1994], Monte Carlo simulations [Batrouni et al., 1990] and DMRG calculations [Rapsch et al., 1999].

In the absence of disorder the SF fraction can be computed analytically. The velocity field would appear in the GP energy functional of equation (2.22) as a term $i\hbar\mathbf{v}\phi_0^*\partial_x\phi_0$, that brings an additional term in the GPE of the form $i\hbar\mathbf{v}\partial_x\phi_0$. Considering a plane wave solution of the form

$$\phi_0(x) = \frac{1}{\sqrt{L}} e^{i\Theta x/L}, \tag{3.20}$$

this solution can be written in the form $\sqrt{\rho}e^{i\theta(x)}$: here the link between the velocity field and the phase twist becomes explicit (it will be investigated in detail in Section 3.3.2). The twisted GP energy acquires an additional term

$$E_{\Theta,GP}(\mathbf{v}) = E_{0,GP} - \frac{1}{2}Nm\mathbf{v}^2 \implies \Delta E = \frac{1}{2}Nm\mathbf{v}^2, \tag{3.21}$$

that from Eq. (3.16) implies $\rho_S = \rho$ and the uniform interacting gas is totally superfluid at the GP level. As the contribution to the ground state energy coming from the Bogoliubov excitations cancels in the difference because of Galilean invariance [Carusotto & Castin, 2004, Leggett, 2001], the uniform gas is fully superfluid in the dilute limit, where the mean-field description is effective [Lieb et al., 2002].

In the simulations that follow, the total phase twist, distributed over the length L, is chosen to be small ($\Theta = \pi/32 \ll \pi$), to avoid level crossing and excitations. With a gauge transformation $\Psi(x) \to \tilde{\Psi}e^{i\Theta x/L}$, the twisted boundary problem is mapped on a problem with periodic boundary conditions and shifted momentum $p \to p + \hbar\Theta/L$, so that $\nabla \to \nabla + i\Theta/L$. This substitution enters the kinetic operator both in the GPE (2.8) and the BdGE (2.12). In the homogeneous case, Galilean invariance ensures that these latter give no contribution to the energy difference [Carusotto & Castin, 2004, Leggett, 2001], whereas, in the disordered case, they can develop a finite contribution [Roth & Burnett, 2003a], as also emerged from numerical simulations. The superfluid fraction is not a property of the ground state, but it rather depends on the excitation spectrum: this is expected if one considers the fundamental role of excitations in determining the quantum phase transition. At any finite density, the superfluid fraction extracted from the GP energy difference represents an upper bound of ρ_S because the second order contribution to the energy always lowers the SF fraction [Paramekanti et al., 1998]. As proven in the previous chapter, in the limit $\rho \to \infty$ the contribution of excitations to the total density becomes negligible compared to ρ_0 and the fluctuations play no-role in determining the total density in this limit, thus for large values of ρ_0 the contribution of Bogoliubov excitations to the SF fraction becomes negligible. In the limit of large densities, one could wonder if considering just the GP solution means restricting to zeroth order and missing the excitations that are fundamental to describe superfluidity. The solution of this apparent paradox is that the GP solution with an applied velocity field is already beyond the zeroth order in the perturbative expansion.

3.3.2   AVERAGING PROCEDURE

The drawback of performing simulations on finite size systems is an overestimation of the SF fraction and only a careful size-scaling analysis gives reliable quantitative information. On the other hand, the computation of the twisted problem turns out to be demanding in terms of computational resources: this limits the number of disorder realizations and results in a large uncertainty in the value of the SF fraction. The aim of the present section is to derive an algorithm to extract the superfluid fraction of a 1D Bose gas in the thermodynamic limit. Here it is shown that the correct procedure to compute this quantity involves the harmonic average of the SF fractions of small-size systems.

The first order contribution to the energy difference of Eq. (3.16) can be computed from the Gross-Pitaevskii energy functional

$$E_{GP} = \int -\frac{\hbar^2}{2m}N_0\phi_0^*\nabla^2\phi_0 + N_0|\phi_0|^2V + \frac{g_0}{2}N_0^2|\phi_0|^4. \tag{3.22}$$

Writing the field in the density-phase formalism $\sqrt{N_0}\phi_0 = \sqrt{\rho_0}e^{i\theta}$, the only term contributing to ΔE comes from the Laplacian and it reads

$$\begin{aligned}
\sqrt{N_0}\nabla^2\phi_0 = \nabla^2(\sqrt{\rho_0}e^{i\theta}) &= \nabla\left((\nabla\sqrt{\rho_0})e^{i\theta} + i(\nabla\theta)\sqrt{\rho_0}e^{i\theta}\right) \\
&= (\nabla^2\sqrt{\rho_0})e^{i\theta} + 2i(\nabla\sqrt{\rho_0})(\nabla\theta)e^{i\theta} + i(\nabla^2\theta)\sqrt{\rho_0}e^{i\theta} - (\nabla\theta)^2\sqrt{\rho_0}e^{i\theta},
\end{aligned} \tag{3.23}$$

where ρ_0 is the leading-order term of the density. Appling $\sqrt{\rho_0}e^{-i\theta}$ from the left and assuming small density fluctuations, the first real-valued correction to the energy is $\rho_0[\nabla\theta]^2$, and, at leading order in the phase twist, the energy difference is given by the kinetic term

$$\Delta E = E_\Theta - E_0 = \int \frac{[\nabla\theta(x)]^2}{2m}\rho_0(x)\mathrm{d}x, \tag{3.24}$$

where $\theta = \langle\hat\theta\rangle$ (in agreement with the correction at second order computed by Castin [Castin, 2004]). If one splits the system in $\mathcal{N}$ subsystems, this formalism can be extended to the single intervals and the total energy difference is the sum of the single contributions, i.e.

$$\Delta E = \sum_i^{\mathcal{N}} \frac{(\theta_i - \theta_{i-1})^2}{2m}\rho_{0i}, \tag{3.25}$$

where θ_i and θ_{i-1} are the phases at the boundaries of the ith subsystem. As far as the bin size is small enough to guarantee that each subsystem covers a zone with uniform potential, the densities ρ_{0i} coincide with the SF densities (this is exact in the infinitesimal version of the theory). Minimizing this energy functional (3.25) with the constraint $\sum_i \theta_i - \theta_{i-1} = \Theta$, via the Lagrange multipliers, shows that the total SF fraction is related to the harmonic average of the density[1] in the single bins [Fontanesi et al., 2010, Altman et al., 2010] as

$$\Delta E = \left(\frac{\Theta}{L}\right)^2 \left[\frac{1}{\rho_{0i}}\right]^{-1} \implies \rho_S = \left(\sum_i \frac{1}{\rho_{0i}}\right)^{-1}. \tag{3.26}$$

An analogous result has been recently obtained by Vosk and Altman [Vosk & Altman, 2011].

---

[1]This conclusion has a strong analogy with series of capacitors in electromagnetism. In fact, the electrostatic energy of a capacitor of capacity C at a voltage ΔV takes the form $U = C(\Delta V)^2/2$ (cfr. equation 3.24) and the total capacity of capacitors connected in series is the harmonic average of single capacities.

This criterion becomes evident if one thinks of a uniform potential with a single narrow but infinite barrier. Separating the system in $\mathcal{N}$ bins, $\mathcal{N}-1$ bins would be uniform and would have $\rho_{0i} = 1$, whereas the bin containing the peak would have $\rho_0 i = 0$. The total superfluid fraction would however be zero, because of the presence of the barrier through which the superfluid cannot flow. An harmonic average of the single superfluid fractions would give the correct vanishing result, unlike an arithmetic average.

3.3.3 NUMERICAL SIMULATIONS

In Fig. 3.8 the superfluid fraction is reported as a function of interaction energy for three different fixed values of disorder that are intended to explore different regimes of the gas. Each point shown in Fig. 3.8 is computed as a harmonic mean of the superfluid fraction of each realization and the error bars are computed accordingly. The shaded zones show the phase boundaries predicted by studying the long-range decay of the one-body density matrix: the prediction based on superfluidity are consistent with the previous results. In fact, a zero superfluid fraction is consistent with all the cases belonging to the insulating phase, whereas the points corresponding to the quasicondensed phase acquire a finite ρ_S. It is worth noticing that the average procedure is most demanding when close to the boundary and this is reflected in larger error bars in the proximity of the phase transition.

The SF fraction is computed from the Gross-Pitaevskii solution without excitations, this prediction can be directly compared to the one extracted via the $g_1(r)$, in fact they are both correct in the limit $\rho_0 \to \infty$. This analysis gives a rather smooth behaviour for ρ_S, and it does not allow to identify any jump in the superfluid fraction, that should be present because the quantum phase transition is of the BKT universality class (see Section 1.4 and [Nelson & Kosterlitz, 1977]).
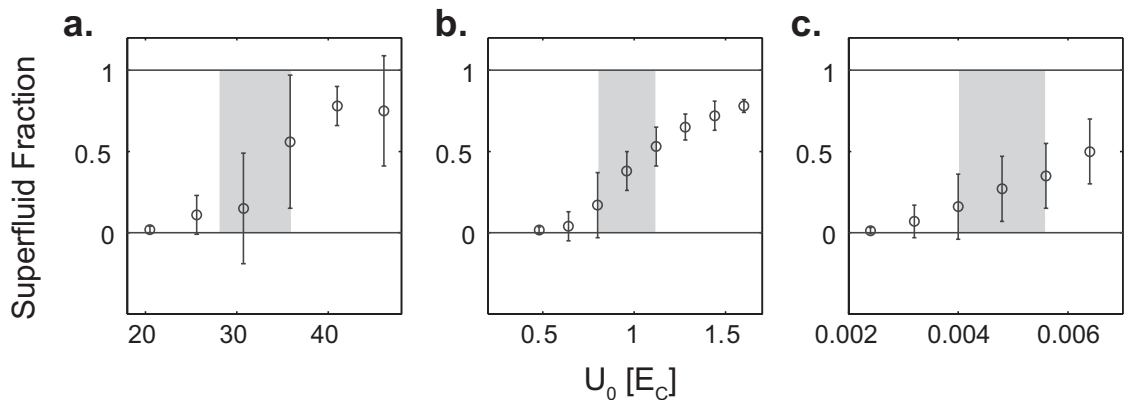

Figure 3.8: Superfluid fraction for three values of disorder: **a.** $\Delta = 12.8\,E_c$, **b.** $\Delta = 0.8\,E_c$, **c.** $\Delta = 0.016\,E_c$. The average superfluid fractions and their error bars are shown as a function of the interaction energy. The shaded zones mark the phase transition computed through the degree of coherence.

3.4 PHASE DIAGRAM

At this point, it's time to go back to the phase diagram obtained numerically for the quantum phase transition in the weakly interacting limit, reported again for convenience in Fig. 3.9. This phase diagram, drawn in the interaction-disorder plane, includes the
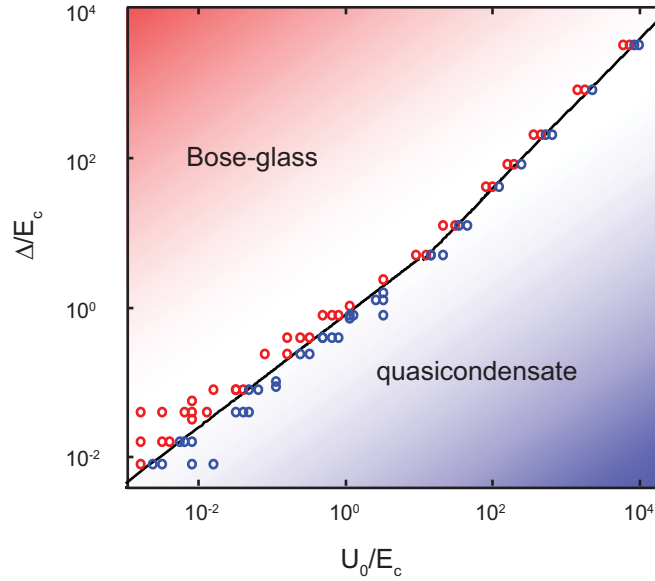

Figure 3.9: Quantum phase diagram of a disordered 1D weakly interacting Bose gas. The red circles mark insulating phases whereas the blue ones corresponds to states in the quasicondensed phase. The black line is a guide for the eye that roughly shows the phase boundary.

two phases that can be described within a Bogoliubov approach, i.e. the quasicondensate and the BG. The former occurs for dominating interaction, whereas the latter appears when disorder prevails. This trend is valid throughout the whole phase diagram with no evidence of a resurgence of the BG phase at large interaction and weak disorder (explanations and comments below).

A remarkable feature is that the phase boundary is characterized by two different power-laws relations depending on the interaction energy at which the transition occurs. In fact, the ratio $\kappa = U_0/E_c$ is a signature of the gas regime: in the uniform case ($U_0 = \mu$) it can be equivalently written in terms of the ratio between the healing length and the correlation length of the potential $\kappa = (\eta/\xi)^2$. The value of κ determines if the length-scale of the density modulation is given by the healing length ($\kappa \ll 1$) or by the correlation length of the potential ($\kappa \gg 1$). In the first case the underlying disorder potential varies on scales much smaller than the modulation of the density and the Bose gas perceives the disorder as a white noise (WN) potential. In the opposite limit, the gas responds on scales shorter than the correlation length, therefore the density is modulated on lengths of the order of η and the ground state wavefunction reflects the disorder profile: this is

the so-called Thomas-Fermi (TF) regime. A sketch of the different regimes together with the phase boundary is reported in Fig. 3.10.
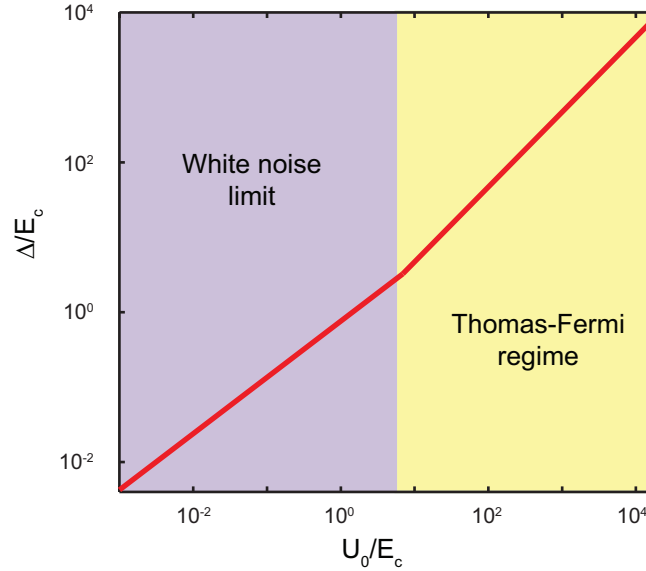

Figure 3.10: Sketch of the quantum phase diagram of a disordered 1D weakly interacting Bose gas. The vertical axis denotes the disorder strength Δ/E_c whereas the horizontal axis denotes the strength of the interaction. The value of the ratio $U_0/E_c = \kappa$ marks the regime of the gas: $\kappa \ll 1$ in the WN limit (shaded in blue) and $\kappa \gg 1$ in the TF regime (shaded in yellow). The phase boundary is shown by the red line.

The boundary follows two power-law relations of the form

$$\frac{\Delta}{E_c} = \left(\frac{U_0}{E_c}\right)^\varsigma, \tag{3.27}$$

where, upon numerical accuracy, $\varsigma = 3/4$ in the WN limit and $\varsigma = 1$ in the TF regime. Being the power law in the origin smaller than 1, the phase boundary has an infinite slope, in agreement with previous theoretical calculations [Falco et al., 2009b]. A natural outcome of this shape is that, starting from a BG situation, the phase transition can be triggered simply by tuning the correlation length of the disordered potential, leaving the properties of the gas unchanged. This condition implies that in an ideal experiment where the correlation length η is reduced at constant interaction and disorder amplitudes, one would always end up in the quasicondensed phase when approaching the WN limit.

The extent of the mean-field phase diagram presented in this work deserves a comment. The validity of the Bogoliubov model presented in Chapter 2 is restricted to the weakly interacting regime. Here, a phase diagram extending to large values of U_0/E_c is presented. This apparent paradox is easily explained by considering the conditions of validity listed in Section 2.3. The relevant constraint, that guarantees the interaction to be weak, is

$1/\sqrt{g_0\rho} \gg 1/\rho$ that is trivially satisfied for any fixed $U_0 = g_0 N_0 / L$ provided that $g_0 \to 0$ and $\rho \to \infty$. This guarantees that the coherence length spreads across a portion of the system containing many particles (infinitely many in this case), so that the system is far away from the strongly correlated regime where single particles – or islands of particles – are separated by strong interactions and the coherence is limited to a few bosons. As stated in Section 2.3, the mean-field description does not hold in the strongly interacting regime, that leads to an interaction dominated Bose glass phase. Consequently, the occurrence of the BG phase at strong interaction [Giamarchi & Schulz, 1988] cannot be reproduced by this model. Moreover, the model cannot be applied in the disorder-dominated case, where the coherence extends only within single maxima of the density and the system is in the so-called Lifshitz glass phase [Lugan et al., 2007a]. This phase would lay in a narrow region close to the vertical axis ($U_0/E_c \to 0$) in Fig. 3.9.

3.4.1 SCALING PROPERTIES

The functional dependencies of the phase boundary in Fig. 3.9 find an elegant explanation in a scaling analysis of the two regimes. In this section the numerical results are explained by two analytical arguments holding respectively in the WN and TF regimes.

$\kappa \ll 1$: THE WHITE NOISE LIMIT

In the part of the phase diagram where $\kappa \ll 1$, the phase boundary follows a power law

$$\frac{\Delta}{E_c} = C \left(\frac{U_0}{E_c} \right)^{3/4}, \tag{3.28}$$

where C is a proportionality constant. In this regime of very weak interaction the Bose gas is in the white-noise limit. In fact, the limiting case $\kappa \to 0$ corresponds to an uncorrelated disordered potential. Here, the healing length ξ is much larger than η and the modulation of ϕ_0 occurs on a length-scale comparable to ξ. In some works this is also referred to as *smoothed regime* [Sanchez-Palencia, 2006] with reference to the weak perturbation perceived by the density distribution. In experiments, this limit can be attained either by shortening the correlation length of the potential or by lowering the interaction between particles.

> In Fig. 3.11**a** the ground state is shown for a case close to the WN limit ($U_0 = \Delta = 1.6 \times 10^{-3} E_c$). ϕ_0 is spread over many correlation lengths and slowly modulated with respect to the length scale given by η. This example describes a gas in the superfluid phase, as also evident from the shape of the low-lying Bogoliubov excitations. In fact they are very close to plane waves with small disorder-induced modulations and a regular spacing between the nodes.

As seen in Chapter 1.3, the correlation of the disorder can be written as

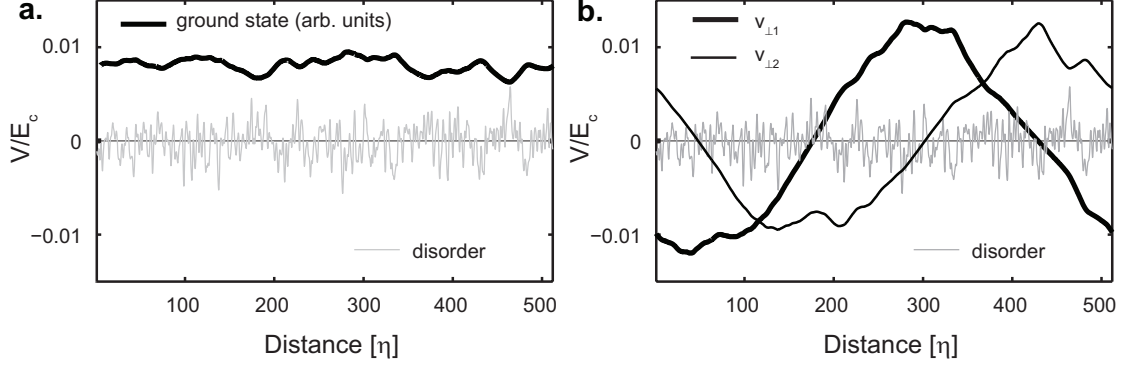$$\langle V(r)V(r') \rangle = \Delta^2 f_{r-r'}, \tag{3.29}$$

Figure 3.11: a. Ground state and **b.** first two excitations $v_\perp j(r)$ for $U_0 = \Delta = 1.6 \times 10^{-3}\, E_c$, where the system is in the superfluid phase and in the WN regime.

where for a gaussian correlated potential the correlation function takes the form

$$f_{r-r'} = e^{-(r-r')^2/2\eta^2}. \tag{3.30}$$

The peculiarity of the WN limit is the δ-correlation of the potential that can be expressed as

$$\langle V(r)V(r')\rangle = w\delta(r - r'), \tag{3.31}$$

where a single parameter w, with the dimensionality $[E^2 L]$, characterizes the disorder. The overall GP problem is now function of the three parameters w, m, the bosonic mass determining the kinetic component, and U_0. Neglecting the interaction and focusing on the 1D Schrödinger problem, we can combine the two other quantities to define units of length and energy as

$$l_0 = \left(\frac{\hbar^2}{2mw^{1/2}}\right)^{\frac{2}{3}}, \qquad E_0 = \left(\frac{2w^2 m}{\hbar^2}\right)^{\frac{1}{3}}. \tag{3.32}$$

These are the relevant scales entering the problem in the WN limit and any energy quantity has to be proportional to E_0 in the WN regime.

The limit for $\eta \to 0$ of the Gauss-correlated potential in Eq. (3.30) gives $f_{r-r'} = \sqrt{2\pi}\eta\delta(r-r')$ and a direct comparison of equations (3.29) and (3.31) implies $w = \sqrt{2\pi}\eta\Delta^2$. Recalling that $E_c = \hbar^2/(2m\eta^2)$, equations (3.32) can be rewritten as

$$l_0 = \frac{\eta}{(2\pi)^{1/6}}\left(\frac{E_c}{\Delta}\right)^{\frac{2}{3}}, \qquad E_0 = \Delta\left(2\pi\frac{\Delta}{E_c}\right)^{\frac{1}{3}}. \tag{3.33}$$

In the WN limit every length and energy have to scale proportionally to these two quantities, in particular, the critical interaction energy should be proportional to this unique

energy scale, $U_0 \propto E_0$. From this, it follows the scaling relation

$$\frac{\Delta}{E_c} \propto \left(\frac{U_0}{E_c}\right)^{\frac{3}{4}}, \tag{3.34}$$

that coincides with the numerical findings.

For what concerns the proportionality constant in the WN limit

$$\frac{U_0}{E_c} = \frac{1}{C^{4/3}} \left(\frac{\Delta}{E_c}\right)^{4/3}, \tag{3.35}$$

the numerics gives $C \sim 0.9$. If one defines $E_* = E_0/\sqrt[3]{2\pi}$, the proportionality between the critical interaction energy and the energy scale E_* is approximately 1.1, in good agreement with the theoretical prediction $U_0/E_* \simeq 1$ [Aleiner et al., 2010].

$\kappa \gg 1$: THE THOMAS-FERMI REGIME

In the opposite limit $\kappa \gg 1$ the healing length of the condensate is smaller than the correlation length of the potential. This implies that any modulation occurs on a length-scale comparable to η. The phase transition takes places at large values of U_0/E_c and Δ/E_c, so that the interaction and disordered terms are the relevant ones in equation (2.8) and the kinetic component becomes negligible. In this limit one can write the approximate expression

$$[V(r) + g\rho_0(r)] \sqrt{\rho_0(r)} = \mu\sqrt{\rho_0(r)}, \tag{3.36}$$

that has the solution

$$\begin{aligned}
\rho_0(r) &= [\mu - V(r)]/g && \text{if} \quad V(r) < \mu, \\
\rho_0(r) &= 0 && \text{if} \quad V(r) > \mu,
\end{aligned} \tag{3.37}$$

and the density modulation mirrors the distribution of the underlying potential where $V(r) < \mu$.

An example of a realization that lies towards the TF regime is shown in Fig. 3.12. The ground state wavefunction and the low-energy excitations are shown respectively in Figs. 3.12a and 3.12b for $U_0 = \Delta = 25.6\,E_c$. It is evident how, in this regime, the ground state wavefunction fills the potential minima and mirrors the distribution of the disorder. This example describes a situation in the BG phase, indeed the nodes of the excitations are pinned to the low-density regions (as discussed in Chapter 2) and, despite their phase character, their shapes are very different from plane waves. The profiles of the $v_{\perp j}$-modes follow closely the ground state amplitude. Although the ratio Δ/U_0 is the same as in the example presented in Fig. 3.11, the two situations describe the gases in different quantum phases: this is already a clue that the phase transition can be triggered by simply tuning the correlation energy E_c.
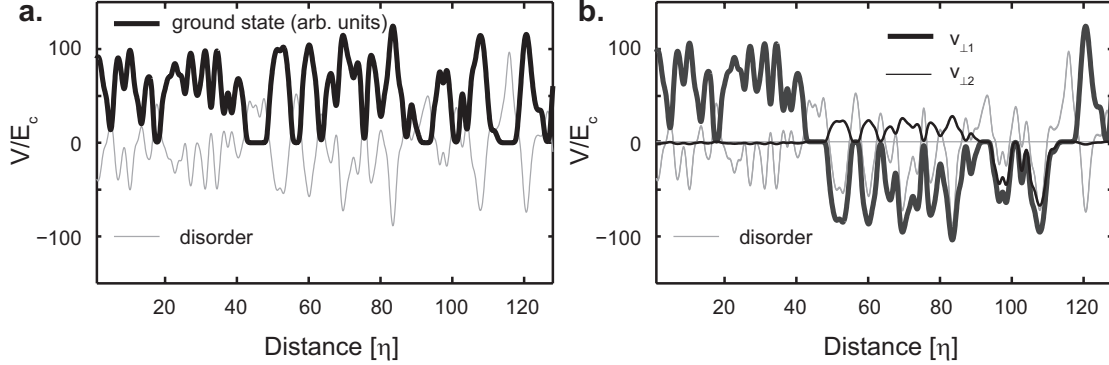
Figure 3.12: a. Ground state and **b.** first two excitations $v_\perp j(r)$ for $U_0 = \Delta = 25.6\,E_c$, where the system is in the Bose glass phase and in the TF regime.

A scaling argument can once again be used to determine the analytical dependence of the boundary in this regime. Being the correlation length much longer than the other length scales, the density is always modulated over distances of the order η, that becomes no longer relevant in determining the quantum phase. Indeed, in this limit E_c is negligible and the thermodynamic phase is only determined by a one-to-one competition between disorder and interaction energies. This finally explains the linear relation between the variables in Fig. 3.10 for large κ.

Neglecting the kinetic energy is in contradiction with the existence of a quasicondensed phase. Indeed, this term is the responsible for the build-up of quasi-long range order across the system. This apparent paradox arises because the kinetic energy corrections propagate the coherence even at large values of disorder and interaction. In fact, the TF approximation fails when the density is low because the damped interaction term becomes of the order of the kinetic energy and the latter is not negligible any longer. In other words, this limit reproduces faithfully the density distribution in case of large U_0/E_c, but it fails in reproducing low-density tails.

In both the examples shown in Fig. 3.11 and 3.12 the ratio between interaction and disorder amplitudes is $\Delta/U_0 = 1$. The transition between SF and BG can apparently be tuned by only varying the disorder correlation length η, as already remarked when the phase diagram was presented.

HIGHER DIMENSIONALITY

It is possible to generalize the previous scaling arguments to arbitrary dimensionality to infer the trend of the phase boundary in two and three dimensions.

For the TF case the argument about the competition between interaction and disorder amplitude holds, therefore the relation is again linear for large values of U_0/E_c.

In the WN limit, the proportionality of any energy to the energy E_0 is universal, but E_0 depends on the dimensionality. In fact, relations (3.29) and (3.31) are valid in

arbitrary dimensions and generalizing the previous argument, one obtains that w has the dimensionality $[E^2 L^D]$ (from the definition in Eq. (3.31)). Following the same approach shown for the 1D case, every quantity having the dimension of an energy must be proportional to

$$E_0 = w^{\frac{2}{4-D}} \left(\frac{2m}{\hbar^2} \right)^{\frac{D}{4-D}} . \tag{3.38}$$

The limit for $\eta \to 0$ of the Gauss-correlated potential gives $f_{\mathbf{r}-\mathbf{r}'} \propto \eta^D \delta(\mathbf{r} - \mathbf{r}')$. Comparison with Eq. (3.31) implies $w \sim \Delta^2 \eta^D$. Considering again that the critical interaction energy should be proportional to E_0 in the WN limit and using $\eta^D = [\hbar^2/(2mE_c)]^{D/2}$, one can conclude that

$$\frac{\Delta}{E_c} \propto \left(\frac{U}{E_c} \right)^{1-\frac{D}{4}} . \tag{3.39}$$

The prediction for the exponents in $2D$ and $3D$ are respectively $1/2$ and $1/4$. Thus the slope in the origin remains infinite and the difference with respect to the linear relation in the TF limit becomes more pronounced in higher dimensions. These results are the same that have been found by Falco and coworkers [Falco et al., 2009b].

3.4.2 Previous Results

The phase diagram computed here can be compared to the results obtained with other models. The first qualitative phase diagram of the disordered bosonic problem was obtained by Giamarchi & Schultz through a renormalization group analysis [Giamarchi & Schulz, 1987, Giamarchi & Schulz, 1988]. They focused mainly on the strongly interacting regime, reproducible within their formalism. Another very common approach is the study of the phase diagram of the disordered bosonic problem in the context of the Bose-Hubbard Hamiltonian [Fisher et al., 1989]

$$H_B = -J \sum_i \hat{a}_{i+1}^\dagger \hat{a}_i + \hat{a}_i^\dagger \hat{a}_{i+1} + \frac{1}{2} U \sum_i \hat{n}_i (\hat{n}_i - 1) + \sum_i \varepsilon_i \hat{n}_i, \tag{3.40}$$

where a_i and $a_i^\dagger$ are annihilation and creation operators, J is the hopping strength, U the repulsive on-site energy and ε_i are independent random variables accounting for the disorder.

The phase diagram in the $U - \Delta$ plane, with Δ marking the amplitude of the disorder through the distribution of the ε_i's, has been extracted using several approaches: Monte Carlo methods [Prokof'ev & Svistunov, 1998, Gurarie et al., 2009], density-matrix renormalization group [Pai et al., 1996, Rapsch et al., 1999], bosonization analysis [Deng et al., 2008], numerical inspection of the superfluid fraction [Roth & Burnett, 2003a]. Three examples of phase diagrams computed in the case of low filling factor are reported in Fig. 3.13. The common feature is the presence of a single superfluid lobe extending from the disorderless axis ($\Delta = 0$) to finite values of disorder. For integer filling factors, the under-
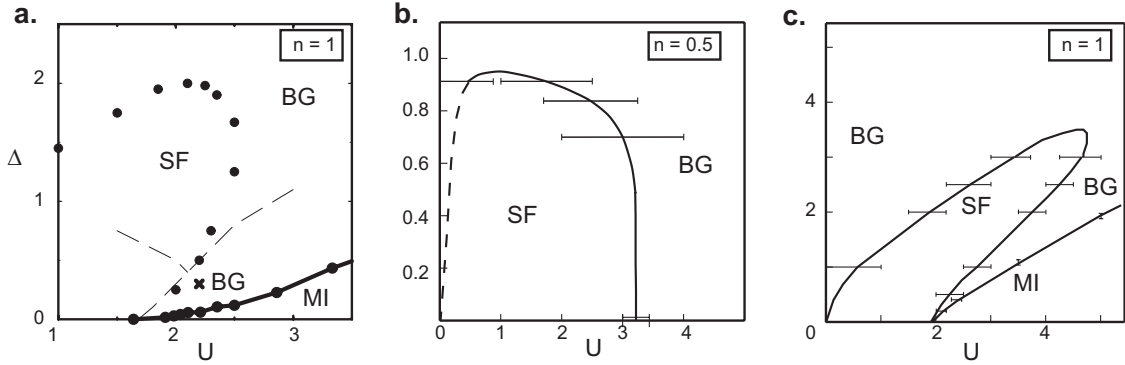
Figure 3.13: Phase diagram of disordered Bose-Hubbard model. n denotes the filling factor of each phase diagram. **a.** Monte Carlo calculation at unitary filling extracted from [Prokof'ev & Svistunov, 1998]. **b.** and **c.** Density-matrix renormalization group calculations, respectively for half and unitary filling, extracted from [Rapsch et al., 1999]. The Mott insulator is not present when the filling is not integer.

lying lattice structure entails the existence of the Mott-insulating phase for strong enough repulsive interaction. For non-integer filling there is no Mott phase and at large values of interaction a BG insulating phase is restored by the creation of islands of condensate disconnected by interaction [Rapsch et al., 1999]. The re-occurrence of an insulating phase at large interaction – due to the enhanced phase fluctuations – is a common feature of these studies [Scalettar et al., 1991] that is not present in the numerical results obtained here (cfr. Fig. 3.9). This discrepancy is a natural consequence of the Bogoliubov model assumed here. First of all, the hypothesis of weak interaction is in contradiction with the strong correlations that drive the system back in the insulating phase at large U_0. In the $\Delta - U_0$ plane the re-entrance shifts to the right when increasing the particle number, and eventually goes to $U_0 \to \infty$ when the mean-field approach is exact, hence, the strongly-interacting insulator disappears for $\rho \to \infty$ (similarly to the Mott lobes of Fig. 1.3 in the $\mu - J$ plane for large population).

The phase transitions occurring in the two regimes have a different nature [Giamarchi & Schulz, 1988]: on one side ($\Delta \sim U_0$) interaction and disorder compete in determining the quantum phase of the gas whereas in the strongly correlated phase ($U_0 \gg \Delta$) interaction has a detrimental effect on the coherence of the system. In addition, the distribution of the density in the strongly correlated phase is rather homogeneous as opposed to the case of very weak interaction, marked by a high inhomogeneity [Giamarchi & Schulz, 1988, Scalettar et al., 1991]. These two phases are sometimes differentiated as *Anderson-glass* and *Bose-glass*, but a universal consensus about the nature of the two phases is still lacking.

The diagram presented in this work shows some analogies with the weakly-interacting limit (close to the origin) of the phase diagrams in Fig. 3.13. In fact, the insulating phase appears for large values of disorder, whereas strong interactions drive the system in the SF

phase. In this regime the present analysis can be more detailed than the previous ones, mainly because it does not suffer any limitation when dealing with large populations. This allows to find good numerical accuracy to estimate quantitatively the boundary and its functional dependencies.

To our knowledge this is the first time the mean-field phase diagram for disordered bosons is quantitatively characterized. The results shown in Fig. 3.9 refer to a 1D Bose gas in presence of a gaussian disorder. A qualitative quantum-state diagram was recently computed in the case of weak repulsive interaction in presence of speckle potential [Lugan et al., 2007a] and it is reported in Fig. 3.14**a**. By studying the density profile of the gas, the authors found the coexistence of three quantum phases separated by crossovers as a function of chemical potential and disorder amplitude: namely a *Lifshitz glass*, a *fragmented condensate* and a *quasicondensed phase*. With "*fragmented condensate*" it is meant a system formed by disconnected islands of condensate, that can be identified with the insulating phase called in this work "*Bose glass*". The link between the fragmentation criterion, seen as a property of the density profile, and the quantum phase transition is the subject of Chapter 4. The "*Lifshitz glass*" is characterized by a coherence extending over single minima. No evidence has been found in the present simulations of two distinct insulating phase at vanishing interaction energy: this fact was expected because a phase made of localized single-particle islands, such as the Lifshitz glass, cannot be described by the present model (as explained in Section 2.3 and also found by equivalent approaches [Cetoli & Lundh, 2010]).
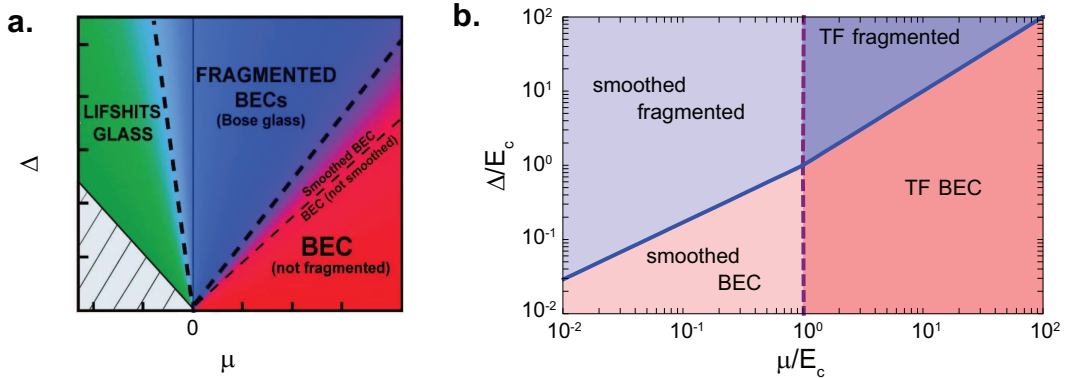
Figure 3.14: Schematic representation of the crossover form a quasicondensed state and a *fragmented* BEC characterized through the study of the density profile. **a.** Quantum phase diagram evaluated for fixed $\alpha_R = \hbar^2/2m\eta^2\Delta$ (extracted from [Lugan et al., 2007a]) **b.** Sketch of the phase diagram rescaled with respect to the correlation energy (extracted from [Lugan, 2010]). The vertical dashed line separate the regimes of the gas, namely smoothed and Thomas-Fermi. The blue solid line denotes the crossover between the two quantum phases.

Lugan *et. al.* found that linear relations separate these quantum phases in the $\mu - \Delta$ plane. This result is not in contradiction with the one presented in this thesis because the

quantities entering the problem are not rescaled: the correlation length of the potential does not appear explicitly in this plot, implying that their graph is evaluated for fixed Δ/E_c. As the phase boundary only depends on U_0/E_c and Δ/E_c, one obtain that the critical interaction is proportional to E_c (and therefore to Δ). An even more convincing argument is given by Lugan [Lugan, 2010], that, using the same method, computed the results rescaled to the correlation energy and found a strikingly similar schematic phase diagram (reported in Fig. 3.14**b**), characterized by the same functional dependencies as in the present work, in the two regimes called *smoothed* and *Thomas-Fermi*. These data are computed as a function of the chemical potential μ: the relation between the average interaction energy U_0 and the chemical potential μ is given by the equation of state. These two quantities display a monotonous relation [Lugan, 2010]. Hence, the quantum phase diagram as a function of μ might be slightly modified, but would be marked by the same functional behaviours, because the same scaling arguments, as for U_0, hold.
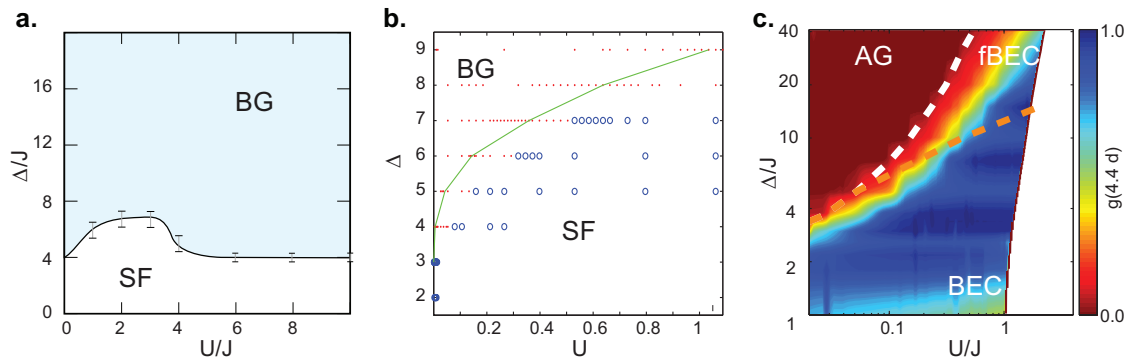

Figure 3.15: Different phase diagrams obtained in presence of a quasiperiodic potential, with J indicating the hopping energy in the Bose-Hubbard model. **a.** Theoretical phase diagram of the Bose Hubbard model for half-integer filling computed via density-matrix renormalization group in Ref. [Roux et al., 2008]. **b.** Theoretical phase diagram in the weakly interacting regime computed via a Bogoliubov-like approach in Ref. [Cetoli & Lundh, 2010]. The blue circles correspond to a non-vanishing superfluid fraction whereas the red dots denote cases where $\rho_S = 0$. On the left of the green line the one-body density matrix decays exponentially. **c.** Experimental phase diagram extracted by studying the coherence at 4.4 lattice sites of a ^{39}K gas in a 1D quasi-periodic potential as reported in Ref. [Deissler et al., 2010].

As illustrated in Chapter 1, quasiperiodic potentials are another common way of realizing optical disorder in current experiments [Fort et al., 2005]. Several theoretical studies have been performed on these systems and some of the phase diagrams obtained in the disorder-interaction plane are shown in Fig. 3.15. An analysis recently performed within a mean field model by Cetoli & Lundh [Cetoli & Lundh, 2010], was aimed at studying the same problem presented here in presence of a quasiperiodic potential: the phase diagram that they obtained is shown in Fig. 3.15**b** on a linear scale. The functional behaviour of the boundary is compatible with the results obtained in this thesis, in particular the boundary bends in the origin as an onset of an infinite slope that smooths

out for larger interaction. However, a substantial difference arises in the limit of very weak interaction: they do not find any evidence of an insulating phase below a certain value of disorder strength. This effect is due to the quasi-periodicity of the underlying potential. Indeed the non-interacting system, in presence of incommensurate bichromatic potential, is localized only if the external potential exceeds a critical value (see Section 1.3.3) and this feature seems to survive in the regime of weak-interaction of the interacting bosonic model [Roth & Burnett, 2003a, Deng et al., 2008, Bar-Gill et al., 2006, Roux et al., 2008]. This is also evident in the phase diagram shown in Fig. 3.15**a** obtained by means of the density-matrix renormalization group technique for the Bose-Hubbard model at half-integer filling. The underlying periodicity of the two lattices makes the system different from a truly random disorder where any finite amount of disorder localize the single-particle problem [Anderson, 1958, Kramer & MacKinnon, 1993]. The experimental evidence [Deissler et al., 2010], obtained by studying the first order correlation function of a weakly interacting ^{39}K gas, seem to confirm the survival of the superfluid phase at vanishing interaction (Fig. 3.15**c**).

THE FRAGMENTATION CRITERION

Contents

In the previous chapter, the quantum phase transition occurring in a 1D Bose gas in presence of disorder has been investigated. It has been stressed that the onset of the BG phase comes along with the formation of coherent islands joined by weak links: these entities lose their reciprocal coherence because of large barriers in the disordered potential. This intuitive picture reminds of a separation of the gas in uncorrelated *fragments*: for this reason the crossover from a delocalized state to a localized one is often referred to as *fragmentation* [Sanchez-Palencia, 2006, Lugan et al., 2007a, Falco et al., 2009a]. Although this is often evoked as a criterion for the transition from a SF phase to a BG, to our knowledge a rigorous definition of fragmentation of the density profile and a proof of its relation to the quantum phase of the gas, are still lacking.

In this thesis we propose an analytical argument –supported by numerical simulations– that relates the onset of the quantum phase transition to the probability distribution of the density of the gas. This argument links the occurrence of minima in the density to the superfluid fraction of the gas itself and it relies on the validity of the mean-field approach, therefore it is strictly valid for infinite density and vanishing interaction constant. The purpose of this chapter is twofold: it aims at giving a rigorous definition of fragmentation in the framework of 1D Bose gas and understanding the relation between the fragmentation threshold and the occurrence of the quantum phase transition. The traditional idea of fragmentation is linked to the macroscopic occupation of multiple states, as opposed

to a single condensate, as it is described in Ref. [Nozières, 1995] and illustrated in Section 4.1. The notion of density fragmentation and its link to the superfluid-insulator transition is presented in Section 4.2 together with the support of numerical simulations. Section 4.3 is devoted to the analysis of the effect of realistic conditions on the fragmentation analysis. In particular, the effect of a harmonic trap and of a finite spatial resolution, on ideal experiments, are investigated.

In this chapter a method to identify the phase transition through the study of the density distribution is proposed. This result bears a clear experimental advantage, as the density profile of a Bose gas is a quantity that can be easily investigated with the current in-situ imaging techniques. The transition between a quasi-condensate and an insulator – and a possible spatial crossover between the two phases – could be unveiled through a local investigation of the statistical distribution of the density profile. This is very promising because it exploits a local property, namely the value of the density and its statistical distribution over the disorder ensemble. The approach we propose does not need to measure large systems but rather the collection of data for several disorder realizations, so as to obtain a significant statistical analysis.

4.1   TRADITIONAL NOTION OF FRAGMENTATION

Fragmentation is traditionally defined as the macroscopic occupation of two or more single-particle states [Nozières, P. & Saint James, D., 1982, Nozières, 1995, Mueller et al., 2006], in contrast with conventional condensation characterized by the macroscopic occupation of a single quantum state. To illustrate this phenomenology let's consider a uniform system with two degenerate (or quasi-degenerate) quantum states, namely 1 and 2, with the corresponding creation and annihilation operators $\hat{a}_i^\dagger$ and $\hat{a}_i$ ($i = 1, 2$) and the orthogonal single-particle wavefunctions $\psi_i(r)$. The Bose condensed state of a N-particle system in the state 1 is

$$|BEC\rangle = |N, \psi_1\rangle = \frac{1}{\sqrt{N!}}(\hat{a}_1^\dagger)^N|0\rangle. \tag{4.1}$$

On the contrary, a fragmented state is characterized by (at least) two macroscopic eigenvalues of the one-body density matrix: let's assume that N_1 are particles in the state 1 and $N_2 = N - N_1$ are in the state 2. The fragmented wavefunction, in second quantization, reads

$$|FR\rangle = |N_1, \psi_1; N_2, \psi_2\rangle = \frac{1}{\sqrt{N_1!N_2!}}(\hat{a}_1^\dagger)^{N_1}(a_2^\dagger)^{N_2}|0\rangle. \tag{4.2}$$

As condensation typically occurs in low-momentum states, the energy difference between the two states only comes from the interaction Hamiltonian, neglecting the kinetic component,

$$H_{int} = \frac{g}{2}\int \hat{\Psi}^\dagger(r)\hat{\Psi}^\dagger(r)\hat{\Psi}(r)\hat{\Psi}(r), \tag{4.3}$$

where the field operator, in terms of the single-particle operators, reads $\hat{\Psi}(r) = \psi_1(r)\hat{a}_1 + \psi_2(r)\hat{a}_2$. The contribution of the interaction term to the energy in the two cases reads

$$E_{BEC} = \frac{g}{2}N(N-1)\int |\psi_1(r)|^4 \mathrm{d}r \tag{4.4}$$

$$E_{FR} = \frac{g}{2}\left[\sum_{i=1,2}\left(N_i(N_i-1)\int |\psi_i(r)|^4 \mathrm{d}r\right) + 4N_1 N_2 \int |\psi_1(r)|^2|\psi_2(r)|^2 \mathrm{d}r\right].$$

In the limit of macroscopic population $N_1, N_2 \gg 1$ one can consider only the leading order that results in

$$E_{BEC} \simeq \frac{g}{2}(N_1 + N_2)^2 \int |\psi_1(r)|^4 \mathrm{d}r \tag{4.5}$$

$$E_{FR} \simeq \frac{g}{2}\left[N_1^2 \int |\psi_1(r)|^4 \mathrm{d}r + N_2^2 \int |\psi_2(r)|^4 \mathrm{d}r + 4N_1 N_2 \int |\psi_1(r)|^2|\psi_2(r)|^2 \mathrm{d}r\right].$$

The integrals $\int |\psi_i(r)|^4 \mathrm{d}r$ give the spatial extent of $\psi_i(r)$. In absence of external potential it is reasonable to assume that there is a large density overlap between the single-particle wavefunction $|\psi_1(r)|^2 \simeq |\psi_2(r)|^2$ that entails similar spatial extents. If the integrals in Eq. (4.4) take the same value, the energy difference between fragmented case and condensed one results in

$$E_{FR} - E_{BEC} = gN_1 N_2 \int |\psi_1(r)|^4. \tag{4.6}$$

This quantity is positive and we can conclude that repulsive interaction inhibits fragmentation in the uniform case through the exchange term appearing in Eq. (4.4). This argument relies of the assumption of large density overlap between the wavefunctions, but this can be invalidated by the presence of a non-uniform external potential. In fact, single-particle states can have different localization lengths and a negligible overlap in presence of large barriers.

To illustrate this point we study the case of a symmetric double-well potential separated by an infinite barrier: the two-mode formalism adopted above is well suited to describe this scenario [Mueller et al., 2006]. Condensation would occur in the symmetric single particle state $\psi_S(r)$ that is degenerate with the antisymmetric solution $\psi_A(r)$. The combination of this two states gives the two wavefunctions confined in the single wells, namely

$$\psi_L(r) = \frac{\psi_S(r) + \psi_A(r)}{\sqrt{2}}, \qquad \psi_R(r) = \frac{\psi_S(r) - \psi_A(r)}{\sqrt{2}}, \tag{4.7}$$

with the same single-particle energy. The energy of N-particles occupying the state ψ_S can be compared to the energy of $N/2$-particles occupying each single-particle state localized on the wells, namely $|BEC\rangle = |N, \psi_S\rangle$ and $|FR\rangle = |N/2, \psi_L; N/2, \psi_R\rangle$. In the case of a single condensate one obtains

$$E_{BEC} = \frac{g}{2}N(N-1)\int \psi_S^4 \, \mathrm{d}r, \tag{4.8}$$

where each particle interact with the remaining $N-1$ and the factor $1/2$ avoids double counting. In the case of a fragmented condensate, the $N/2$ particles in each well interacts with $N/2 - 1$ particles and the total interaction energy is

$$E_{FR} = 2\,\frac{g}{2}\frac{N}{2}\left(\frac{N}{2}-1\right)\int \psi_L^4 \ \mathrm{d}r. \tag{4.9}$$

The spatial extent of ψ_L and ψ_R is half the size of ψ_S, therefore $\int \psi_L^4 \ \mathrm{d}r = 2\int \psi_S^4 \ \mathrm{d}r$ and the previous expression becomes

$$E_{FR} = \frac{g}{2}N(N-2)\int \psi_S^4 \ \mathrm{d}r, \tag{4.10}$$

that is lower than the energy of the single condensate. The presence of a barrier can induce the fragmentation of the condensate [Spekkens & Sipe, 1999, Streltsov et al., 2004, Spekkens & Sipe, 1998].

The parallel drawn with the double well potential highlights the link of this model with the case of disordered bosons. This last intuitive picture describes rather a transition from a condensed state to two fragmented single-particle states: a state that looks like the Lifshitz-glass phase, where disorder (in this case the central barrier) is much stronger than interaction. However, the main message is that the traditional notion of fragmentation and the density fragmentation, under investigation in this chapter, are indeed closely related.

In this chapter fragmentation is analyzed under a different point of view, i.e. by considering the behaviour of the density in presence of barriers in the underlying potential. The model presented here sheds light on the analogies between the traditional notion of fragmentation and the occurrence of the phase transition. The aim of the next section is to extend the concept of fragmentation to the fragmentation of the density distribution seen as a marker of the quantum phase transition.

4.2 DENSITY FRAGMENTATION CRITERION

As emerged from the analysis carried out in the previous chapter, the quantum phase transition occurs with the formation of islands (fragments) separated by weak links. Weak links arise in correspondence to low-density zones where the phase fluctuations are more likely to change sign reducing the coherence between the two neighbouring islands. The proliferation of these weak links, given by strong disorder, destroy the quasi-long-range order. It is evident that a study of the density fragmentation must contain information about the statistics of occurrence of low-density areas and their influence on the phase coherence.

A quantity that naturally characterizes the statistics of the density is its probability distribution (PDD), in particular, the PDD in the small-density limit turns out to have a crucial role in determining the quantum phase of the gas. In this section it is proven and checked numerically that a 1D weakly interacting Bose gas is fragmented when the PDD is non-zero in the limit of vanishing density and that this threshold coincides with the onset of the quantum phase transition.

4.2.1 Analytical argument

The analytical argument presented here is based on the averaging procedure of the superfluid fraction derived in Section 3.3.2. The goal of the present analysis is to establish a link between the PDD and the quantum phase transition. The discrimination between the quantum phases of the gas has been made in the previous chapter via the build-up of quasi-long range order and by the value of the SF fraction. This latter can be characterized by evaluating the response of the system to a velocity field, that is equivalent to imposing twisted boundary conditions (see Section 3.3). The expression for the superfluid fraction f_S – recalled here for convenience – is proportional to the difference of the energies in the moving frame, E_Θ, and in the rest frame, E_0, as [Fisher et al., 1973]

$$f_S = \frac{2mL^2}{\hbar^2 N} \lim_{\Theta \to 0} \frac{E_\Theta - E_0}{\Theta^2}. \tag{4.11}$$

Within the density-phase formalism ($\hat{\Psi} = \hat{\rho} e^{i\hat{\theta}} = (\rho_0 + \delta\hat{\rho}) e^{i\hat{\theta}}$), the energy difference can be computed from the Gross-Pitaevskii energy functional, and, at leading order in the phase twist, is given by the kinetic term (cfr. Eq (3.24))

$$E_\Theta - E_0 = \int \frac{(\nabla\theta(x))^2}{2m} \rho_0(x) \mathrm{d}x, \tag{4.12}$$

where $\theta = \langle\hat{\theta}\rangle$. The main result obtained in Section 3.3.2 is that the total superfluid fraction is related to the harmonic average of the density [Fontanesi et al., 2010, Altman et al., 2010] as

$$\frac{1}{\rho_S} = \int \frac{1}{\rho_0(x)} \mathrm{d}x. \tag{4.13}$$

The validity of the Bogoliubov prescription, $\langle\delta\hat{\rho}\rangle/\rho_0 \ll 1$, ensures that ρ_0 contains the relevant information about the density distribution. In fact, the Bogoliubov approximation becomes more and more accurate for increasing average density, N_0/L, at constant interaction $g_0 N_0/L$, with N_0 the number of bosons in the ground state. Deep in the mean-field limit $N_0/L \to \infty$, the relative contribution of the fluctuations $\langle\delta\hat{\rho}\rangle/\rho_0$ vanishes (see Chapter 2.3) and the density profile is well described by $\rho_0(x)$ [Castin, 2004].

A convergent integral in Eq. (4.13) would imply a finite SF fraction, whereas if it diverges $\rho_S = 0$ and the gas would be in the normal phase. Considering that the system under investigation has homogeneous disorder, one can write the equality $P(\rho_0)\mathrm{d}\rho_0 = P(x)\mathrm{d}x$, where the spatial probability distribution, $P(x)$, is constant. This allows to perform a change of variable in the integral and it gives

$$\frac{1}{\rho_S} = \int \frac{1}{\rho_0(x)} P(x) \mathrm{d}x = \int \frac{1}{\rho_0} P(\rho_0) \mathrm{d}\rho_0. \tag{4.14}$$

The convergence of the integral in Eq. (4.14) is determined by the behavior of $P(\rho_0)$ in the limit $\rho_0 \to 0$. If one writes $P(\rho_0 \to 0) = \rho_0^\beta$, the condition to be in the superfluid

phase is $\beta > 0$, whereas a nonzero value of $P(\rho_0 \to 0)$, i.e. $\beta \leq 0$, results in a glassy phase.

This argument concerning the density fragmentation can be easily switched to the distribution of the ground-state wavefunction, $P(\phi_0)$. Keeping in mind that this quantity has to satisfy

$$P(\phi_0)\mathrm{d}\phi_0 = P(\rho_0)\mathrm{d}\rho_0, \tag{4.15}$$

expression (4.14) can be rewritten as

$$\frac{1}{\rho_S} = \int \frac{1}{|\phi_0|^2} P(\phi_0)\mathrm{d}\phi_0. \tag{4.16}$$

Given that $P(\phi_0 \to 0) = \phi_0^\zeta$, this integral is convergent if and only if $\zeta > 1$, thus $P(\phi_0 \to 0)$ is super-linear in the SF phase. This relation is less useful both because of the lower relevance to experimental data and because of the difficulty of identifying a linear relation.

4.2.2 NUMERICAL SIMULATIONS

The PDD can be computed numerically, by solving the GPE (2.8) on finite size systems and performing a configuration average to increase the accuracy of the statistical sampling. The phase boundary, for such a system, has been characterized in Chapter 3 in independent ways, through the study of the superfluid fraction and of the one-body density matrix.

> Fig. 4.1.**a** shows the PDD computed in presence of Gaussian disorder for fixed disorder amplitude $\Delta_g = 12.8\ E_c$ and different values of interaction $U_0 = 25.6\ E_c$, $38.4\ E_c$, $46.08\ E_c$ (all in the TF regime). These three values correspond to cases in the BG, phase boundary and SF phases respectively. In the homogeneous case $P(\rho_0)$ is expected to have a single peak at the value $\rho_0/\rho_H = 1$, where ρ_H is the constant solution of the homogeneous problem. The inclusion of a small disorder [Sanchez-Palencia, 2006] broadens this peak, but $P(\rho_0)$ preserves a vanishing tail for $\rho_0 \to 0$ in the superfluid phase (solid curve in Fig. 4.1**a**). For decreasing interaction the weight of the low-density part becomes more important (dashed curve in Fig. 4.1**a**) until the phase boundary is eventually crossed and the PDD develops a finite component in the limit $\rho_0 \to 0$ (dot-dashed lines in Fig. 4.1**a**). Fig. 4.1**b** shows a similar analysis carried out for the WN regime, for $\Delta_g = 0.016\ E_c$ and $U_0 = 0.0032\ E_c$, $0.0048\ E_c$, $0.0064\ E_c$. As for the TF case, these three cases lie in the BG, phase boundary and SF phases respectively.

> Comparing panels **a.** and **b.** in Fig. 4.1, it is clear that the PDD has different shapes in the TF and WN regimes. However, in both cases, the fragmentation allows to differentiate between SF and BG phases. The numerical analysis summarized in Fig. 4.1 confirms the criterion stemming from Eq. (4.14), namely that the SF fraction is nonzero if and only if $P(\rho_0 \to 0) = 0$.
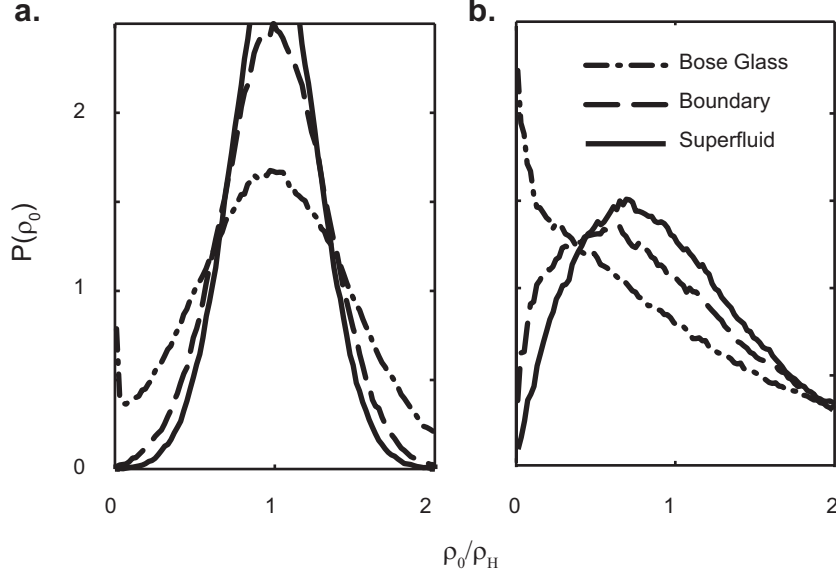
Figure 4.1: Probability distribution of the density in two different regimes in presence of Gaussian disordered potential. **a.** Towards the TF regime, $\Delta_g = 12.8\ E_c$ for $U_0 = 25.6\ E_c$ (dot-dashed), $38.4\ E_c$ (dashed), $46\ E_c$ (solid). **b.** Towards the WN limit, $\Delta_g = 0.016\ E_c$ for $U_0 = 0.0032\ E_c$ (dot-dashed), $0.0048\ E_c$ (dashed), $0.0064\ E_c$ (solid). ρ_H is the density in the homogeneous case.

$P(\rho_0)$ can be evaluated analytically in certain regimes. In the TF regime, when the kinetic term is negligible, the density follows the external potential according to the TF approximation as

$$\rho_0(x) = [\mu - V(x)]/g \qquad \text{if} \quad V(x) < \mu,$$
$$\rho_0(x) = 0 \qquad \text{if} \quad V(x) > \mu. \qquad (4.17)$$

In this regime the distribution of $\rho_0(x)$ reproduces the distribution of the potential at any finite value, with an additional finite contribution in zero, given by the sum of the regions where $V(x) > \mu$. A very similar feature can be indeed noticed in the insulating case of Fig. 4.1**a** (dot-dashed line) where the PPD has a Gaussian-like shape with a peaked contribution in 0. Following the fragmentation argument, this case is always insulating as it can be expected, since the absence of a kinetic component prevents the formation of any quasi-long range order or superfluid flow. This is not in contradiction with the phase transition occurring at large values of U_0/E_c, because the kinetic energy corrections to (4.17) are responsible for the build-up of the quasi-long-range order, while if the description (4.17) holds strictly the state is insulating.

To make a link with current experiments, the same analysis in presence of attractive speckle pattern (presented in Chapter 1.3.2) has been performed. The
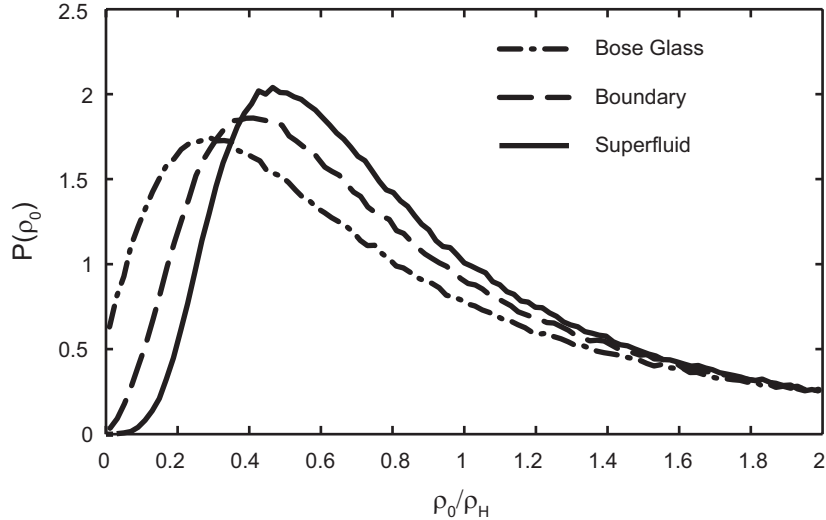
Figure 4.2: Probability distribution of the density in presence of attractive speckle potential, obtained from an average on disorder configurations. Three value of interaction across the phase boundary are shown, $U = 2.6\ E_c$ (dot-dashed), $3.1\ E_c$ (dashed), $3.5\ E_c$ (solid), for fixed disorder strength $\Delta_s = 3.2\ E_c$. ρ_H is the density in the homogeneous case.

fragmentation study, shown in Fig. 4.2, is performed for fixed disorder amplitude, $\Delta_s = 3.2\ E_c$, for different interaction energies, $U_0 = 2.6,\ 3.1,\ 3.5\ E_c$. Being the attractive speckle potential bound from above, the distribution is not centered around its mean value. The choice of the potential strongly affects the shape of the PDD, but the limiting behavior $P(\rho_0 \to 0)$ is only determined by the phase of the gas, consistently with the conclusions drawn for Gaussian disorder. From this inspection we extract the critical value of the interaction energy $U_0 \simeq 3.1\ E_c$ that will be important in the analysis that follows.

4.3   REALISTIC CONDITIONS

The experimental study of ultracold atomic gases in real systems shows many complications that one has to deal with, as, among others, the presence of a trap, the finite number of particles, the fact that the system is not strictly one-dimensional. As this chapter is intended to give a new viable route to determine the phase transition in current experiments, the effect of some real-life factors on the fragmentation analysis will be discussed.

In particular, the quantum degenerate Bose gas is experimentally realized as a cloud trapped by a harmonic potential that gives a parabolic shape to the density profile. In Section 4.3.1 the effect of the trapping potential is analyzed and a way to include its presence in the fragmentation analysis through a local investigation is suggested. Another

crucial experimental limitation [Hulet, 2011] comes from the finite spatial resolution of the in-situ imaging apparatus. This limits the capability of describing correctly the density profile and it can, therefore, invalidate the study of the PDD. The effect of a finite spatial resolution is investigated in Section 4.3.2. The aim of this analysis is to give an idea of the effect of these elements on the density distribution and to understand which conclusions can be extracted from the experimental data.

4.3.1 TRAPPED CASE

Homogeneous systems are useful theoretical tools to inspect the phase transition, but current experiments [Chen et al., 2008, Deissler et al., 2010] are performed on trapped systems. The harmonic trap introduces a spatial inhomogeneity in the density profile, and thereby in the interaction energy $U(x) = g\rho_0(x)$. To deal with a realistic situation we consider a speckle disorder on the top of a harmonic trapping potential, as it has been investigated in recent experiments [Chen et al., 2008, Clément et al., 2008], and we perform the simulations on a system of experimentally achievable size $(200\eta_s)$ [Dries et al., 2010].

The harmonic trap is implemented by adding to the external potential a quadratic term of the form $V_{trap} = m\omega_r^2 r^2/2$. The inclusion of a harmonic potential requires to convert the expression of the quadratic potential in units of E_c, $\tilde{V}_{trap}$. Some straightforward calculations give

$$\frac{m\omega_r^2 r^2}{2E_c} = \frac{m\omega_r^2\eta^2}{2E_c}\left(\frac{r}{\eta}\right)^2 = \frac{1}{4}\frac{\hbar^2\omega_r^2}{E_c}\frac{2m\eta^2}{\hbar^2}\left(\frac{r}{\eta}\right)^2 = \left(\frac{\hbar\omega_r}{2E_c}\right)^2\left(\frac{r}{\eta}\right)^2. \quad (4.18)$$

Typically the frequency of the trap is given in Hz and it is sufficient to know its relation with the correlation energy to describe a realistic system via Eq. (4.18).

The local density approximation is valid as long as the trapping potential is shallow with respect to the interaction energy, i.e. $U \gg V_{trap}$. The gas has to be in the TF regime with respect to the trap frequency: this means that $\xi \ll R_{TF}$ where R_{TF} is the Thomas-Fermi radius, i.e. the semi-extension of the cloud computed neglecting the kinetic term. In this way, the density profile in presence of the disorderless trap is approximately parabolic and can be extracted from the GP equation. In fact,

$$\rho_0(r) = [\mu - m\omega_r^2 r^2/2]/g \qquad \text{if} \qquad V_{trap}(r) < \mu,$$
$$\rho_0(r) = 0 \qquad\qquad\qquad \text{if} \qquad V_{trap}(r) > \mu. \qquad (4.19)$$

Here μ takes the value of the interaction energy at the center of the trap, where $V_{trap} = 0$.

On the contrary, if the condition is not fulfilled, the profile is Gaussian and the quasi-1D Thomas-Fermi approximation starts to break down. For clarity,
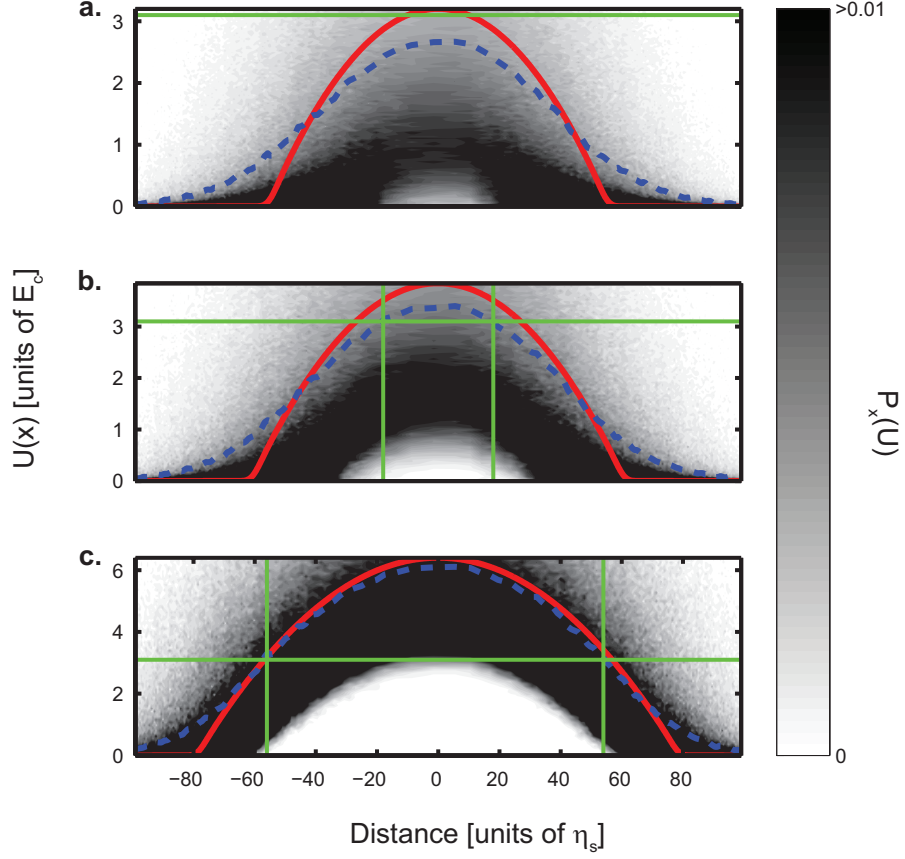
Figure 4.3: Local probability distribution of the interaction energy (proportional to the density) in a harmonic trap ($\hbar\omega_t = 0.064\ E_c$) for three different values of the interaction energy $U_C(0)$: **a.** $3.2\ E_c$, **b.** $3.84\ E_c$, **c.** $6.4\ E_c$ and for fixed speckle disorder intensity ($\Delta_s = 3.2\ E_c$). The distributions are obtained by averaging over 2000 configurations of disorder. The red solid lines are the interaction energy profiles in the disorderless cases. Blue dashed lines represent the spatial distribution of the average interaction energies. The green thin lines indicate the boundary in the thermodynamic limit extracted analyzing the untrapped case.

> this condition does not imply that the gas is in the TF regime with respect
> to the underlying disorder, in fact $\eta \ll R_{TF}$.

The PDD can be obtained by evaluating the histogram of the density at a fixed position for several disorder realizations. In what follows, we represent these histograms as $P_x(U)$, namely as a function of the interaction energy, $U(x) = g\rho_0(x)$, rather than as a function of the density ρ_0. In this way the average of $P_x(U)$ is the average interaction energy and can be directly associated to a point on the phase diagram.

The presence of a trap allows to vary spatially the interaction energy, so that, for a fixed value of disorder the two phases can coexist in the trap: the superfluid phase close

to the center of the trap, where interaction is stronger, and the insulator in the regions closer to the edges. This can be depicted as a situation of spatial phase separation, where a critical spatial point r_c separating the two coexisting phases, can be identified. One can wonder whether the critical interaction U_C, extracted from the critical spatial point r_C, is compatible with the result in the thermodynamic limit where the trap is absent.

The density plots in Fig. 4.3 show the spatially resolved probability distributions, $P_x(U)$, as a function of position and interaction energy for fixed disorder amplitude, $\Delta_s = 3.2\ E_c$. The blue dashed line is the average interaction energy $\overline{U}(x) = \int g\rho_0(x)P_x(\rho_0)\mathrm{d}\rho_0$, and the red solid line represents the interaction profile in absence of disorder $U_C(x)$, i.e. the solution of the GPE with $V(x) = m\omega_t^2 x^2/2$, where ω_t is the trapping frequency. Note that the disorder combined with a shallow trapping potential makes the average density profile different from the disorderless one. In fact, it extends beyond the disorderless TF radius and reaches a lower value in the center of the trap. This fact is relevant when comparing the critical values of interaction at the transition between the trapped and untrapped cases.

It is important to understand whether the fragmentation threshold, in the trapped case, coincides with the one extracted in the thermodynamic limit. For the chosen value of the disorder amplitude, the fragmentation analysis in the untrapped case gives a transition at an interaction strength $U_H \simeq 3.1\ E_c$ (cfr. Fig. 4.2). In Fig. 4.3**a** the gas is fragmented at all positions, consistent with the homogeneous boundary, as the maximal interaction energy $\overline{U}(0) \simeq 2.7\ E_c < U_H$. When the interaction energy is increased, SF and BG phases coexist (see panels **b.** and **c.**). The fragmentation threshold of the interaction energy can be extracted directly from the spatially resolved PDDs. The values of the average interaction at the threshold is in good agreement with U_H (cfr. Fig. 4.3**b** and **c**) even if one can already notice a signature of a small penetration of the superfluid phase into the insulator. The good agreement of the trapped case with the untrapped one occurs as long as the local density approximation is valid ($\hbar\omega_t \ll U$). For tighter traps (simulations not shown), the fragmentation line moves to lower values of the average interaction energy and the effect of the quasicondensate that penetrates the BG is more pronounced. This effect, that in fluid dynamics can be seen as the superfluid propagating into the insulating phase (cfr. Fig. 4.5), becomes obvious when considering the limit $\hbar\omega_t \gg U, \Delta$, where the density profile is the non-fragmented harmonic oscillator ground state. The penetration effect is more pronounced when the transition occurs at the edges of the trap where the density gradient is steeper. Therefore, the best agreement between the phase transition of the trapped and homogeneous gases is obtained when the transition occurs close to the center of the trap.

4.3.2 Finite Resolution

In current experiments the resolution of the apparatus represents one of the main limitations to the correct interpretation of the experimental data. For this purpose, here, we study the role of a finite spatial resolution on the statistical analysis proposed in this chapter. The resolution is included in the simulation via a convolution of the ground state
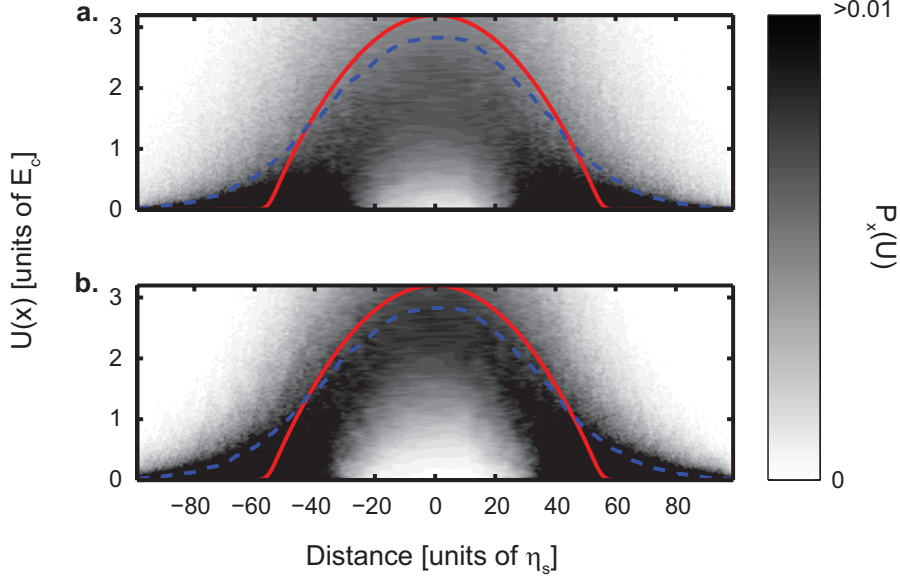
Figure 4.4: Effect of a finite resolution on the local probability distribution of the interaction energy in a harmonic trap ($\hbar\omega_t = 0.064\ E_c$) for the insulating state of Fig. 4.3a: $U_C(0) = 3.2\ E_c$ and $\Delta_s = 3.2\ E_c$. Panel **a.** shows a resolution $R = \eta$, whereas in panel **b.** $R = 2\eta$.

wavefunction with a Gaussian of standard deviation R. The finite resolution makes it harder to identify the insulating phase through a statistical study of the density because it smooths out the profile, cutting narrow minima from the statistics. This limitation acts differently in different regimes: supposing the ratio η/R fixed, the finite resolution would not affect the statistics in the WN limit, where modulations of the density occur on the scale of the healing length, much longer than η and thus than R. In other words, independently on the value of η/R, going towards the WN limit one can reach a regime where $R \ll \xi$, where the density profile is correctly described. On the contrary, the condition $\eta/R \lesssim 1$, would strongly affect the statistics in the TF regime, where the length scale of the modulation is the correlation length of the potential. Fig. 4.4 shows the effect of finite resolution on the probability distribution of a trapped Bose gas for $U_C(0) = 3.2\ E_c$ and $\Delta_s = 3.2\ E_c$. The statistical analysis of the distribution (Fig. 4.3**a**) identifies a completely fragmented state. The introduction of a finite resolution ($R = \eta$) in Fig. 4.4**a** opens a window in the center of the trap as if the Bose gas was partially superfluid. This effect become even more significant for a worse resolution ($R = 2\eta$), as shown in Fig. 4.4**b**, where the gas appears to be predominantly superfluid. For this set of parameters, the transition would be placed at $U \sim 3$, $2.9\ E_c$ respectively. Therefore, a reasonable criterion to correctly estimate the fragmentation threshold is $R \lesssim \sqrt{\eta^2(1 + E_c^2/\Delta^2) + \xi^2}$, where the resolution is smaller with respect to all the other relevant length-scales, namely the single particle localization, the correlation length and the healing length.

Both the finite resolution and the harmonic trap tend to displace the apparent frag-
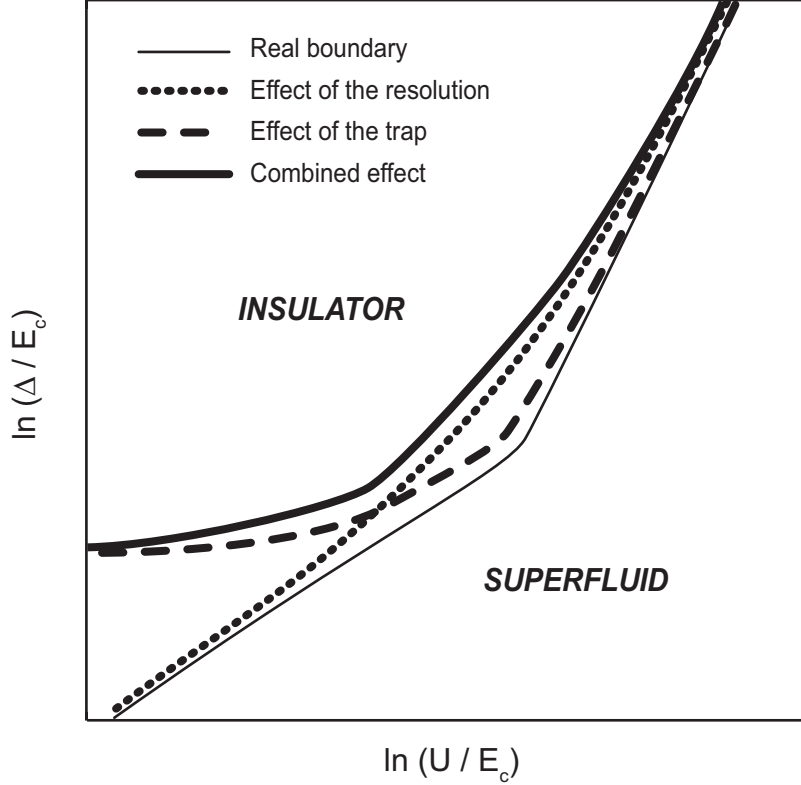
Figure 4.5: Sketch of the phase diagram of the 1D Bose gas in presence of disorder. The effect of realistic limitations in experiments are qualitatively shown. The solid thin line represents the actual phase boundary, the dotted line is the phase boundary extracted with a finite resolution of the experimental setup, for a fixed ratio η/R (see text). The dashed line is the fragmentation boundary considering a harmonic potential of fixed trapping frequency. The trap tends to displace the boundary towards the insulating phase. For $\hbar\omega_t \gtrsim U$ the local density approximation breaks down and the profile is never fragmented. The combined effect is shown by the thick solid line.

mentation threshold towards the insulator phase with respect to the actual boundary. Therefore, in experiments, the superfluid fraction is overestimated, but a quantitative correction to the boundary can be computed knowing the value of the resolution and the trapping frequency. A qualitative sketch of the effect of real conditions on the actual phase diagram is shown in Fig. 4.5. From this sketch it appears that the trapped system does no longer reflect the properties of the thermodynamic limit deep in the WN regime. Indeed, fragmentation would occur on a scale much longer than the ground state of the trap.

4.3.3 CURRENT EXPERIMENTS

These predictions have been tested for realistic data referring to an experiment carried out at Rice University (Texas, USA) [Dries et al., 2010, Hulet, 2011]. The motivation of simulating a real system was to identify the best regime to spot the phase transition and to estimate the error due to the presence of the trap and to the finite resolution of the imaging apparatus.

The experiment is performed with ^7Li, a bosonic alkali gas with a very wide Feshbach resonance [Pollack et al., 2009] that allows to explore a large range of interaction strength. Disorder is created by scattering light through a diffusive plate, resulting in a repulsive speckle potential. Among the relevant data to inspect the phase transition there are the mass of the Lithium atoms ($m_{7Li} \simeq 7u$) and the correlation length of the speckle potential, $\eta_s = 3.4\mu m$. The value of the correlation energy comes from the combination of these two: $E_c \sim 62 \times \hbar$ Hz. A crucial parameter for the creation of the cloud is the trapping frequency $\omega_r = 4.5$ Hz. Exploiting the Feshbach resonance they realized atomic clouds for different values of the chemical potential ($\mu_{1,2,3,4} = 220, 105, 50, 23$ Hz$\times\hbar$): in the present scheme this quantity coincides with the interaction energy in the center of the trap in absence of disorder. In the table shown below the experimental data for the chemical potential and the TF radius are listed together with the conversions in the units used for the numerical simulations (η_s and E_c).

$\mu/\hbar$	R_z	$\mu[E_c]$	$R_z[\eta_s]$
220 Hz	178 μm	3.5	50
105 Hz	123 μm	1.7	36
50 Hz	85 μm	0.8	25
23 Hz	58 μm	0.37	17

The lowest value of the interaction will not be considered in the analysis that follows because the TF approximation with respect to the trapping frequency starts to break down at such low values of interaction ($\mu \sim 5\hbar\omega_r$). Disorder amplitude Δ_s is considered tunable at will, as it depends on the intensity of the laser field.

The effect of changing the chemical potential is twofold: first of all a larger μ increases the size of the cloud by increasing the TF radius. The three density profiles (or rather the interaction profiles $U(x)$) are shown in Fig. 4.6, as computed in absence of disorder. The cloud sizes are consistent with the ones listed above. In second place, in presence of disorder, as the correlation length is kept fixed, an increase of μ corresponds to a reduction of the healing length. A decrease of the ratio ξ/η_s drives the system toward the TF regime with respect to the underlying disorder.

The phase boundary has been determined by studying the fragmentation threshold at fixed chemical potentials ($\mu_{1,2,3}$) in absence of the trap. This allowed to detect three values of critical disorder. In Fig. 4.7 it is shown an example of probability distribution of the density for $\mu = 3.5$ E_c. The distribution is strongly asymmetric and, being the speckle potential repulsive, it shows a slow decaying tail at low densities, the crucial zone for detecting the phase transition. An attractive speckle potential would be peaked closer to the origin, with a slow tail at large densities (cfr. Fig. 4.2). Instead, a Gaussian
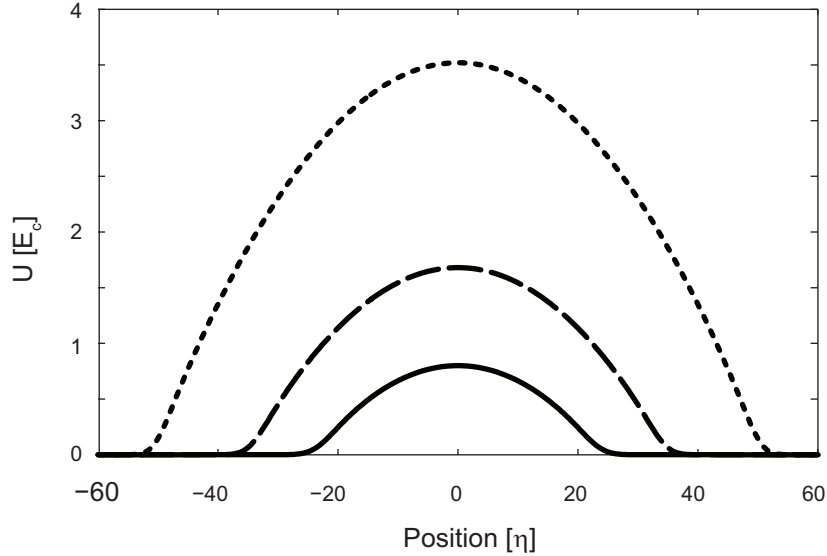
Figure 4.6: Interaction energy profiles in absence of disorder for three value of the chemical potential $\mu = 3.5$, 1.7, 0.8 E_c. the size of the atomic cloud increases for larger μ and it extends from $-R_{TF}$ to R_{TF}. The profiles are approximately parabolic, except for the tails where the TF approximation fails because the kinetic component becomes significant.

potential would have a more symmetric distribution, as shown in Section 4.2. In this sense, this feature is disadvantageous for spotting the transition and it translates into the requirement of a larger number of disorder realization to obtain a smooth and reliable configuration average for the PDD. The repulsive speckle potential is probably the less advisable disorder type to investigate the fragmentation of the gas because its large-amplitude fluctuations decay only exponentially.

Considering the presence of a trapping potential, a fragmentation analysis, as the one performed in Section 4.3.1, can be carried out by tuning the disorder strength. Since the chemical potential is spatially dependent, for each value of disorder a critical interaction energy can be found at the fragmentation threshold. Each pair of values for disorder and interaction represents a point on the phase boundary: this result is reliable provided that the trap is not too steep in the point where the spatial phase transition occurs and that the local density approximation holds. These simulations give the points of the phase boundary via the critical interaction strength extracted from the fragmentation threshold for different values of disorder. The sketch of phase diagram in Fig. 4.8 (dashed curve) shows some points ($\square$) extracted from this fragmentation analysis. This is the phase diagram in presence of repulsive speckles: despite the few available points and the small interval under investigation, it is possible to identify a trend analogous to the one appearing in the phase diagram obtained in presence of Gaussian disorder (Fig. 3.4).

The main limitation of their experimental apparatus is the spatial resolution of the imaging system. The spatial resolution correspond to a Gaussian of width $\sim 3\mu m$, thus
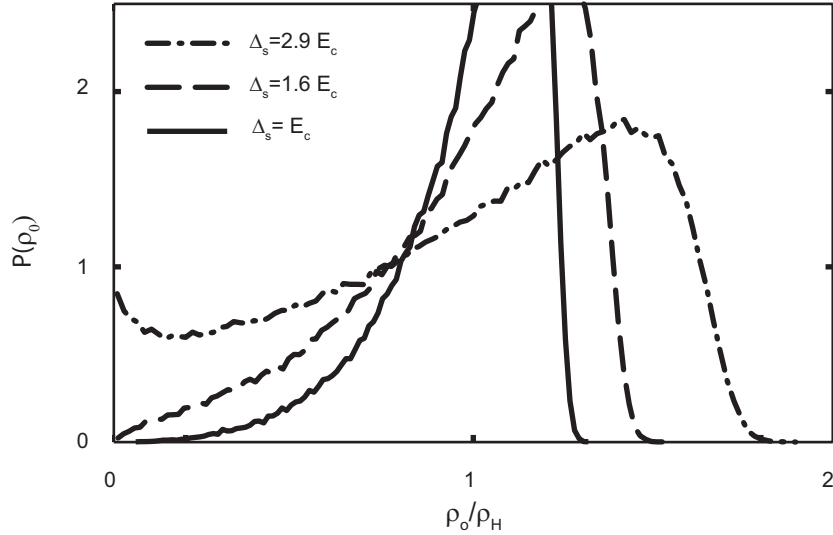
Figure 4.7: Probability distribution of the density in presence of repulsive speckle potential, obtained from an average on disorder configurations. Three value of disorder across the phase boundary are shown, $\Delta_s = 2.9\ E_c$, $1.6\ E_c$, E_c, for fixed interaction strength $\mu = 3.5\ E_c$. ρ_H is a constant value, the density in the homogeneous case.

comparable to the correlation length of the potential[1]. It is important to quantitatively estimate the shift of the phase boundary given by the finite spatial resolution of the apparatus. To do so, the investigation carried out in the previous section is repeated by taking into account the spatial resolution as explained in Chapter 4.3.2. In Fig. 4.8 the true phase boundary is plotted together with the apparent phase boundary estimated in presence of a finite resolution. As expected the shift due to the finite resolution is larger for larger values of the interaction energy, i.e. for smaller healing length. In fact, a small healing length is hardly sampled with a poor resolution. This confirms that the effect of a finite resolution on the fragmentation analysis is to overestimate the superfluidity of the gas.

In which regime is it more convenient to investigate the phase transition? Moving to small values of the chemical potential presents some advantages because the density distribution can be sampled correctly (the resolution does not play a relevant role any longer), and, in addition, this regime is closer to the "smoothing regime" where the dynamics of the system occur on length-scales larger than the scale given by the disorder: the Bose gas distribution is not simply the replica of the disorder distribution. This regime is further from the regime of classical localization [Aspect & Inguscio, 2009] and it highlights the quantum nature of the phase transition. On the other hand the system turns out to be smaller, therefore, the statistics and the accuracy of a spatial analysis would be poorer.

---

[1]This is not a coincidence, the imaging system that creates the speckle potential is the same used for the in-situ imaging.
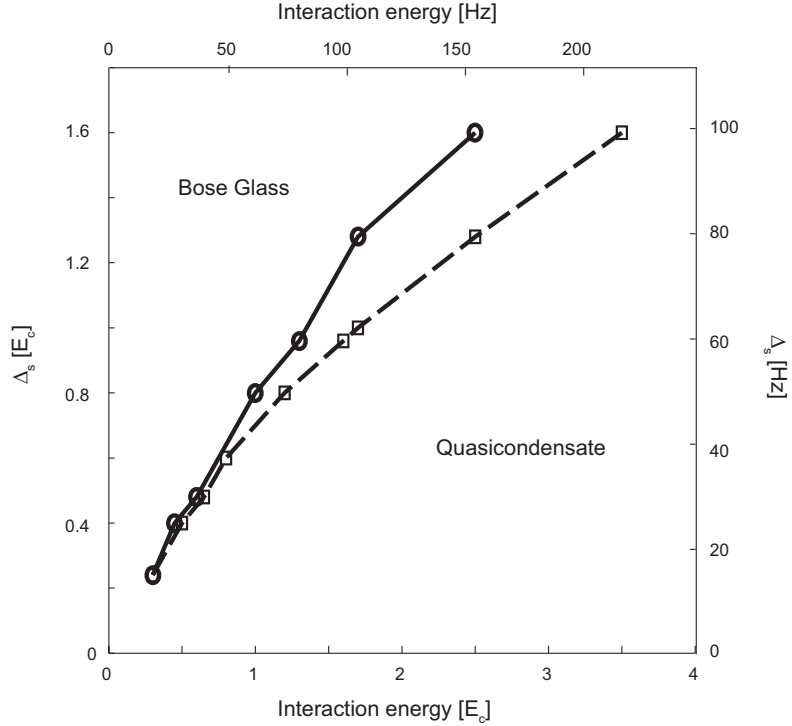
Figure 4.8: The actual phase diagram in the interaction-disorder plane in presence of repulsive speckles (marked by □ and with a dashed guide for the eye) is compared to the apparent phase boundary computed in presence of a finite spatial resolution of about 0.9η (marked by ○ and with a solid line as a guideline). Both these phase boundaries are extracted from a fragmentation analysis.

In the other direction (large chemical potential) the cloud (and so the statistics) would be more extended, but the error due to the resolution would be non-negligible. In some sense a perfect trade-off has to be found. An alternative way to move towards the WN limit would be by reducing the correlation length of the potential. This length scale does not have to be sampled by the imaging apparatus and can be tuned via the numerical aperture of the focusing lens.

BEYOND THE 1D BOSE GAS
AT ZERO TEMPERATURE

Contents

The study presented so far concerned the 1D Bose gas at zero temperature, where a quantum phase transition takes place. In one dimension there is no phase transition occurring at any finite temperature because the thermal fluctuations destroy quasi-long range order. On the other hand, the experiments deal with finite ultracold temperatures and finite trapped system, not the ideal configuration to inspect the quantum phase transition. In section 5.1 the finite temperature case is briefly discussed, within the limits of validity of the extended Bogoliubov model (see Section 2.3).

Another natural development of the previous analysis consists in studying the two-dimensional case. The physics of the 2D Bose gas is very rich and a brief review is given in section 5.2 together with some results obtained within the extended Bogoliubov method.

5.1 THE 1D BOSE GAS AT FINITE TEMPERATURE

No condensation or quasi-condensation occurs in 1D at finite temperature. The inclusion of thermal fluctuations entails an exponentially decaying one-body density matrix at any finite temperature. On the other hand, as shown in Section 1.2.3, the presence of a harmonic trap can restore quasi-condensation and even true condensation for sufficiently low temperatures, thanks to a cutoff in the long distance phase fluctuations [Petrov et al., 2000].

Here we present a simple study of the effect of thermal fluctuation on a 1D Bose gas in the thermodynamic limit in the regime where the extended Bogoliubov theory is still valid. In Fig. 5.1 the degree of coherence of a uniform gas at finite temperature is shown. Temperature is included via the thermal energy $E_T = 1/(k_B T)$ in units of the correlation

energy E_c. A finite temperature produces thermal fluctuations, namely occupation of the Bogoliubov modes that contribute in decreasing the coherence according to Eq. (2.27).
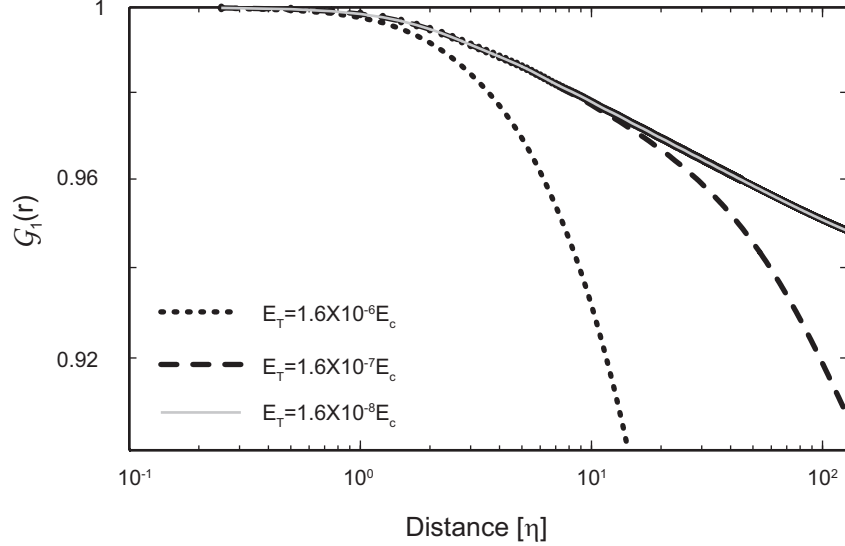

Figure 5.1: Degree of coherence $\mathcal{G}_1(r)$ for a unidimensional uniform Bose gas at fixed interaction energy $U_0 = 0.8\,E_c$ and finite temperature. The thick solid line marks the degree of coherence in the zero-temperature case and it overlaps – in this finite size system – with the lowest temperature case analyzed here and marked by the thin gray line. Increasing the temperature, a discrepancy in the long-range behaviour arises at long distance (dashed line), even if an overlapping region can still be identified. A further increase in temperature makes the difference between the two degrees of coherence substantial, and the exponential decay does not overlap at all with the zero-temperature algebraic decay. The effect of a finite temperature on the coherence is not substantially different from the one played by disorder (cfr. Fig. 3.2))

The case shown here is superfluid at $T = 0$ and the finite temperature here has a very similar effect to the presence of disorder. As far as the temperature is very low, the discrepancy with respect to the zero-temperature case occurs at very large distances, where the coherence develops an exponential tail and the difference with the algebraic decay at $T = 0$ becomes evident. This somehow justifies the experimental studies performed on atomic gases at very low temperature and inspecting the quantum phase transition that in principle only occurs at $T = 0$. A finite temperature is expected to have an analogous effect in presence of disorder, indeed both temperature and disorder are detrimental to long-range coherence.

The spectrum of excitations at finite temperature is not modified with respect to the one at $T = 0$ because there is no dependence on temperature in the BdGE. According to the study performed in this thesis, the nature of the insulating phase originating from disorder, that is marked by a diverging DoS, is substantially different to the one coming from thermal fluctuations, because of a different nature of the decoherence mechanism. However, being the spectrum identical, also the thermal Bose gas should show a diverging

DoS at a certain value of disorder. This change could be inspected by looking at the specific heat of the Bose gas, indeed, this quantity can be expressed as

$$c \propto \frac{\mathrm{d}E}{\mathrm{d}T},$$

(5.1)

i.e. as the derivative of the energy with respect to the temperature. The total energy can be expressed as a component coming from the ground state and a contribution of the excited states that follows a Bose distribution

$$E = E_0 + \int \frac{\varepsilon}{e^{\varepsilon/(k_B T)} - 1} D(\varepsilon) \mathrm{d}\varepsilon,$$

(5.2)

where the DoS $D(\varepsilon)$ appears. Hence, a change in the functional behaviour of the DoS should have measurable consequences on the specific heat of the gas that is experimentally accessible at ultra-low temperatures.

In addition, this model could be employed to inspect transport properties. This would be a way to test a phase transition that has been recently predicted for the 1D Bose gas at finite temperature [Aleiner et al., 2010]. This prediction would seem to contradict the common belief that no phase transition occurs in 1D at finite temperature. On the contrary, according to the authors, the thermodynamic functions are not singular at the transition and this unconventional phase transition – between an insulating and a fluid phase – occurs in the transport and energy-dissipation properties, although both phases are marked by exponentially decaying correlations.

5.2   The 2D Bose gas

The formalism presented in Chapter 2, valid for low-dimensional Bose gases, can describe the two-dimensional situation. Some preliminary numerical results are presented here.

The uniform 2D Bose gas at zero temperature is supposed to form a real condensate. The ground state solution would be a flat surface and its one-body density matrix decays to a constant finite value at infinite distance.

An investigation performed with the extended Bogoliubov method in presence of gaussian disorder is shown in Fig. 5.2. In Fig. 5.2**a** the density profile of the ground state wavefunction $\phi_0(x, y)$ is shown together with the underlying disorder potential profile (5.2**b**). The excitation spectrum can be computed diagonalizing the Bogoliubov-de Gennes matrix and two sample solution, at low and high energy, are shown in Figs. 5.3**a** ($v_{\perp 1}(x, y)$) and 5.3**b** ($v_{\perp 60}(x, y)$) respectively. From the excitation spectrum and the solution of the BdG problem the one-body density matrix and the degree of coherence can be extracted, as it has been done in Chapter 3 for the 1D case. Being the numerical problem more demanding than in the 1D case, thermodynamic properties cannot be easily inferred. In fact, given our computing facilities and the short time devoted to the 2D case, the numerical complexity limits the achievable size to arrays of the order of 200×200. Sampling the disordered potential with four points per correlation length means that the system is limited to about $50\eta \times 50\eta$: this turns out to be not sufficient to infer properties of

the gas in the thermodynamic limit. Even the constant value attained by $g_1(r - r')$ for $|r - r'| \to \infty$ cannot be reproduced by these finite size simulations. The simulations shown here are performed on a two dimensional grid $(20\eta \times 20\eta)$ with periodic boundary conditions, that makes it topologically equivalent to a torus.
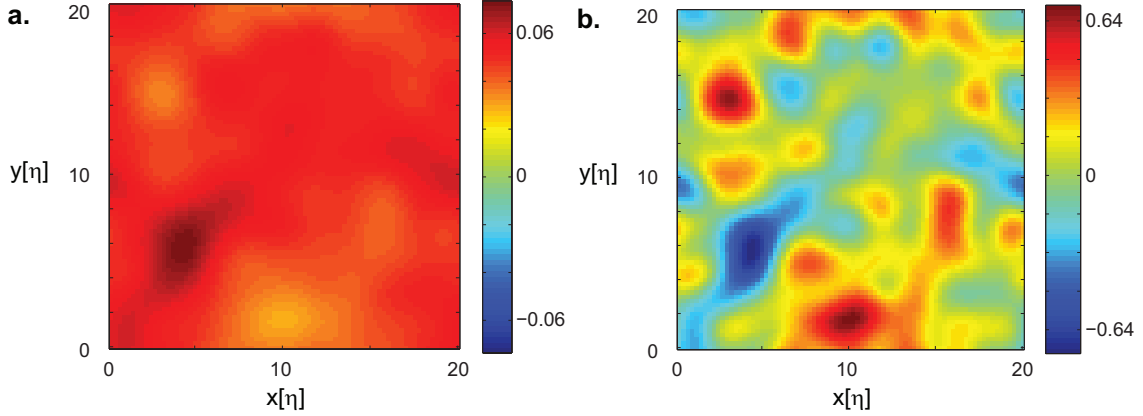
Figure 5.2: a. Ground state normalized wavefunction $\phi_0(x, y)$, solution of the GPE. **b**. Disorder profile $V(x, y)$ in units of the correlation energy E_c.
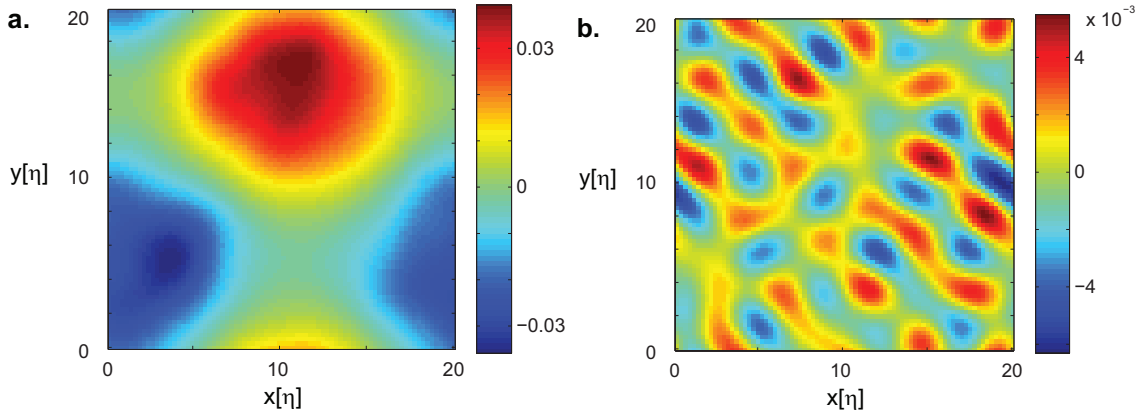
Figure 5.3: a. First $v_\perp(x, y)$-mode solution of the BdGE: this excitation has a phase character. **b**. Profile of $v_{\perp 60}(x, y)$: this excitation start to develop a fast-oscillating behaviour, typical of density fluctuations. The intensity of the modes deceases by increasing the excitation energy (cfr. the scale of the color bars).

Beyond the numerical issues, there are some conceptual complications that one has to take into account when moving to 2D at finite temperature. First of all, the occurrence of the phase transition comes along with the creation of vortex-antivortex pairs that

destroy superfluidity. This phenomenology is not contained in a Bogoliubov-like theory and derives from entropic arguments [Berezinskiĭ, 1972, Kosterlitz & Thouless, 1973]. For this reason a standard mean-field analysis would overestimate the critical temperature of the transition. To overcome this issue, the most viable way would be to supply the Bogoliubov method with an entropic analysis. Symmetry breaking approaches cannot describe the onset of topological excitations because the topology of the quasicondensate is fixed. However, in the past, perturbative field approaches have been combined with thermodynamic arguments to infer an estimate of the universal jump in the SF fraction of the uniform 2D Bose gas [Stoof & Bijlsma, 1993, Andersen et al., 2002, Lim et al., 2008]. Similar methods were also employed by Monte Carlo studies [Kagan et al., 2000, Pilati et al., 2008] and we argue that an analogous technique could be used within this extended Bogoliubov method.

In second place, the study of the quasicondensate-BG transition in 2D is obviously more difficult than in one dimension, because of the presence of a temperature component that competes with interaction and disorder in the determination of the quantum phase of the gas. Even the generalization of the fragmentation criterion would not be trivial. The fragmentation criterion holds in 1D because of the disconnected topology of two fragments separated by a large barrier. This argument does not hold in 2D because of the possibility to percolate around large bumps of the potential, therefore, if a similar criterion exists it has to be related to topological arguments.

CONCLUSIONS

In this thesis the phase diagram of a 1D Bose-gas at zero temperature in presence of spatially correlated disorder has been investigated. Using an extended Bogoliubov method, the superfluid-insulator quantum phase transition has been characterized by inspecting the long-range decay of the one-body density matrix, that discriminates two quantum phases: a quasicondensate and a Bose-glass phase. This analysis led to the identification of two regimes in which the boundary follows a power-law relation between disorder and interaction: a white noise limit, where a 3/4 power-law relation holds, and a Thomas-Fermi regime, where this relation becomes linear. This phase diagram has been confirmed by inspecting the superfluid fraction of the system. The phase fluctuations that trigger the phase transition by destroying the quasi-long-range coherence have been identified with the low-energy Bogoliubov modes. Their density of states diverges at low energy in the Bose-Glass phase while it approaches a constant value in the quasicondensed case. Moreover, the localization of the excitations always shows an $E^{-\alpha}$ divergence with $\alpha = 1$ marking the phase transition. Finally, we have demonstrated a relation between the quantum phase transition of the 1D Bose gas and the probability distribution of the density in the mean field limit. We found that the superfluid phase is marked by a vanishing probability at zero density, whereas in the insulating phase it develops a non-zero component.

From the theoretical point of view, the phenomenology behind the role of the phase fluctuations has been elucidated. The proliferation of the low-energy modes, due to the presence of weak-links in the system, explains the loss of long-range coherence. In addition, the phase diagram in the limit of vanishing interaction (infinite density) has been quantitatively determined and explained in the light of the existing results. An interesting point to clarify is the role of the finite density corrections on this mean-field prediction. In other words, it would be useful to quantify the link between the analysis at low-filling, e.g. obtained from discrete models, and the present investigation.

This theoretical analysis is crucial for future experiments aimed at the determination of the superfluid to Bose-glass phase transition. The weakly interacting regime analyzed in this thesis is indeed the closest to actual experimental setups that achieved Anderson localization in 1D bosonic systems with vanishing interaction. Current techniques allow to realize large atomic clouds with tunable interaction and disorder configurations with highly controllable features. The present analysis provides different ways to characterize the phase transition and it is precious in determining the most proper regime of the gas

to spot the transition. The criterion obtained for the fragmentation threshold gives an innovative way of characterizing the quantum phase of the gas, based on a local property of the gas that can be extracted from simple statistical averages and does not require large system sizes. This gives a viable route to the determination of the phase transition through a statistical analysis of the density profile.

The natural outlook of this work is an extension to two dimensional systems. However, this entails some difficulties that have to be taken into account. In two dimensions vortices, of entropic origin, are not considered in a Bogoliubov-like model, and have to be included to correctly describe the phenomenology leading to the BKT phase transition. In addition, the extension of the fragmentation argument cannot be trivially generalized because of the possibility of the gas to percolate around potential barriers. In addition, the problem would be numerically more demanding and the deduction of thermodynamic properties is not trivial. Finally, at zero temperature in 2D real condensation occurs, whereas quasicondensation arises at low temperature as a consequence of thermal fluctuations: this interplay with temperature bears an even richer phenomenology.

ONE-BODY DENSITY MATRIX

In this appendix, the expression of Eq. (2.28) is derived starting from the results of the extended Bogoliubov theory presented in Ref. [Mora & Castin, 2003].

The one-body density matrix in the density phase formalism is defined as

$$G_1(r, r') = \langle \hat{\Psi}^\dagger(r) \hat{\Psi}(r') \rangle = \langle \sqrt{\hat{\rho}(r)} e^{i[\hat{\theta}(r') - \hat{\theta}(r)]} \sqrt{\hat{\rho}(r')} \rangle. \tag{A.1}$$

Expanding this expression to the second order, Mora & Castin obtained for the reduced one-body density matrix

$$g_1(r', r) = \exp\left[-\frac{1}{2} \langle : (\Delta\theta)^2 : \rangle_2 - \frac{1}{8} \langle : (\Delta\delta\tilde{\rho})^2 \rangle_2 \right], \tag{A.2}$$

where the normal ordering is taken with respect to the $\hat{\Lambda}$-operators defined as the projection of the $\hat{B}$ operator, rid of the $\hat{P}$ and $\hat{Q}$ operators, orthogonal to ϕ_0

$$\hat{\Lambda}(r) = \sum_j u_{\perp j}(r) \hat{b}_j + v_{\perp j}(r) \hat{b}_j^\dagger, \tag{A.3}$$

the subscript $\perp$ denotes the projection orthogonal to ϕ_0. The $\hat{\Lambda}$ operators describe the excitations orthogonal to the quasicondensate [Castin & Dum, 1998] and they obey the commutation rules $[\hat{\Lambda}(r), \hat{\Lambda}^\dagger(r')] = \delta_{r,r'}/\ell - \phi_0(r)\phi_0(r')$. The expectation value $\langle \hat{\Lambda}^\dagger(r) \hat{\Lambda}(r) \rangle$ gives the density of non-condensed atoms at the position r.

The expressions for $\Delta\theta$ and $\Delta\delta\tilde{\rho}$ read

$$\Delta\theta = \hat{\theta}(r') - \hat{\theta}(r) = \frac{1}{2i}(\Delta\tilde{\Lambda} - \Delta\tilde{\Lambda}^\dagger) \tag{A.4}$$

$$\Delta\delta\tilde{\rho} = \delta\tilde{\rho}(r') - \delta\tilde{\rho}(r) = \frac{\delta\hat{\rho}(r')}{\rho_0(r')} - \frac{\delta\hat{\rho}(r)}{\rho_0(r)}, \tag{A.5}$$

where

$$\Delta\tilde{\Lambda} = \tilde{\Lambda}(r') - \tilde{\Lambda}(r), \qquad \tilde{\Lambda}(r) = \frac{\hat{\Lambda}(r)}{\sqrt{\rho_0(r)}} \tag{A.6}$$

$$\delta\hat{\rho}(r) = \sqrt{\rho_0(r)}[\hat{\Lambda}(r) + \hat{\Lambda}^\dagger(r)]. \tag{A.7}$$

With these definitions the exponent of Eq. (A.2) can be expressed in terms of the $\hat{\Lambda}$-operators by carefully inserting the expression for $(\Delta\theta)^2$ and $(\Delta\delta\tilde{\rho})^2$. Taking the normal ordering of the $\hat{\Lambda}$-operators and substituting their expressions in terms of the Bogoliubov modes in Eq. (A.3), one obtains

$$
g_1(r', r) =
$$
$$
\exp\Bigg[\sum_j \Big(2v_{\perp j}^*(r')v_{\perp j}(r') + 2v_{\perp j}^*(r)v_{\perp j}(r) - 2v_{\perp j}^*(r)v_{\perp j}(r') - 2v_{\perp j}^*(r')v_{\perp j}(r) \Big) \times (1 + p_j)
$$
$$
+ (2u_{\perp j}^*(r')u_{\perp j}(r') + 2u_{\perp j}^*(r)u_{\perp j}(r) - 2u_{\perp j}^*(r)u_{\perp j}(r') - 2u_{\perp j}^*(r')u_{\perp j}(r))p_j \Bigg], \quad (A.8)
$$

where $p_j = (e^{\varepsilon_j/(k_B T)} - 1)^{-1}$ comes from the term $\hat{b}_j^\dagger \hat{b}_j$, whereas the quantum fluctuations come from $\hat{b}_j \hat{b}_j^\dagger$. The last expression can be rewritten as

$$
g_1(r, r') = \exp\left[-\frac{1}{2} \sum_j (1 + p_j) \left| \frac{v_{\perp j}(r)}{\sqrt{\rho_0(r)}} - \frac{v_{\perp j}(r')}{\sqrt{\rho_0(r')}} \right|^2 + p_j \left| \frac{u_{\perp j}(r)}{\sqrt{\rho_0(r)}} - \frac{u_{\perp j}(r')}{\sqrt{\rho_0(r')}} \right|^2 \right],
$$
$$
(A.9)
$$

that coincides with the expression for the one-body density matrix in Eq. (2.27). The zero temperature case is recovered by imposing $p_j = 0$, so that the only contribution left comes from the Bogoliubov $v_\perp$-modes.

Crank-Nicholson algorithm

This appendix is devoted to the description of the semi-implicit Crank-Nicholson algorithm [Ames, 1992]. This finite difference method is typically used for the solution of partial differential equation and in particular has found a large popularity in the ultracold-quantum gases community for its efficiency in the solution of the GP equation (see among others [Chiofalo et al., 2000, Cerimele et al., 2000, Muruganandam & Adhikari, 2009]).

The time-independent GPE, reported here for convenience

$$\left[-\frac{\hbar^2}{2m}\Delta_r + V(r) + g_0 N_0 |\phi_0(r)|^2 \right] \phi_0(r) = \mu \phi_0(r), \tag{B.1}$$

is a partial differential equation in the spatial variable. Its peculiarity is the non-linear term entering the effective potential that makes it a non-linear Schrödinger equation. The numerical procedure to compute the solution ϕ_0 is achieved by discretizing the space in unphysical segments of length ℓ much smaller than the other length-scales coming into play, as discussed in Section 2.3. In this manner both the wavefunction and its derivatives are defined on a spatial grid and the solving procedure becomes a finite difference method.

The solution of the problem is achieved by introducing a fictitious imaginary time variable $t \to \tau = it$ and evolving an initial trial wavefunction. The introduction of an imaginary time component modifies the partial differential equation into

$$\hbar \frac{\partial}{\partial \tau} \psi_r^\tau = -H \psi_r^\tau, \tag{B.2}$$

where ψ_r^τ denotes $\psi(r, \tau)$, i.e. the wavefunction at the spatial point r at the imaginary time τ. Eq. (B.2) reads as a diffusion equation with an absorption term. If the solving algorithm is stable, the trial wave function, when propagated in imaginary time, converges to the ground state solution. In fact, the trial wavefunction can be decomposed on the basis of the eigenvectors of H as

$$\psi(r, \tau) = \sum_i \phi_i(r, \tau), \qquad \text{where} \qquad \hat{H}\phi_i(r) = \varepsilon_i \phi_i(r). \tag{B.3}$$

Applying the time-evolution operator to the trial wavefunction one obtains

$$\psi(r, \tau_2) = e^{-\hat{H}(\tau_2 - \tau_1)}\psi(r, \tau_1) = \sum_i e^{-\varepsilon_i(\tau_2 - \tau_1)}\phi(r), \tag{B.4}$$

and considering that the ground state energy ε_0 is the lowest eigenvalue

$$\lim_{\tau \to \infty} \psi(r, \tau) = Ce^{-\varepsilon_0(\tau)}\phi_0(r), \tag{B.5}$$

where $\tau = \tau_2 - \tau_1$. The trial wavefunction evolved in imaginary time converges to the ground state solution. The evolution in real time is a unitary transformation and as such conserves the norm of the wavefunction. On the contrary, imaginary-time evolution reduces the norm of the vector, therefore after each time-step the normalization of the wavefunction has to be restored.

Being the space-time discrete, the wavefunction is defined on a two-dimensional grid (x, τ) where the space and time steps are respectively Δx and $\Delta \tau$. The standard explicit method to solve partial differential equations approximates the function and its derivatives as

$$\psi = \psi_j^k, \tag{B.6}$$

$$\Delta \psi = \frac{-2\psi_j^k + \psi_{j+1}^k + \psi_{j-1}^k}{\Delta x^2}, \tag{B.7}$$

$$\frac{\partial}{\partial \tau}\psi = \frac{\psi_j^{k+1} - \psi_j^k}{\Delta \tau}, \tag{B.8}$$

where the differences in space are centered at the point $j - k$ of the grid. Inserting these expressions in Eq. (B.2) one obtains an explicit expression for the wavefunction at time $k + 1$ (ψ_j^{k+1}) as a function of the wavefunction at the time k. However, this numerical procedure is unstable, in the sense that small errors may grow with time instead of being damped, and it converges only for small values of $\Delta \tau / \Delta x^2$. This algorithm is second order accurate in the spatial coordinate, but only first-order accurate in time.

This instability is cured by using implicit algorithms. The Crank-Nicholson scheme described here is a semi-implicit algorithm that has the advantage of being unconditionally stable, i.e. any trial wavefunction would converge to the solution of the GP problem. In this scheme the field operator and its spatial and time derivatives are centered at the time $k + \Delta \tau / 2$ and can be expressed as

$$\psi = \frac{\psi_j^k + \psi_j^{k+1}}{2}, \tag{B.9}$$

$$\Delta \psi = \frac{-2\psi_j^k + \psi_{j+1}^k + \psi_{j-1}^k - 2\psi_j^{k+1} + \psi_{j+1}^{k+1} + \psi_{j-1}^{k+1}}{2\Delta x^2}, \tag{B.10}$$

$$\frac{\partial}{\partial \tau}\psi = \frac{\psi_j^{k+1} - \psi_j^k}{\Delta \tau}, \tag{B.11}$$

where the wavefunction is expressed as its average at the time k and $k + 1$.

Inserting these definitions, the time-dependent GPE reads

$$
\hbar \frac{\psi_j^{k+1} - \psi_j^k}{\Delta \tau} = \frac{\hbar^2}{2m} \left(\frac{-2\psi_j^k + \psi_{j+1}^k + \psi_{j-1}^k - 2\psi_j^{k+1} + \psi_{j+1}^{k+1} + \psi_{j-1}^{k+1}}{2\Delta x^2} \right)
$$
$$
- (V_j + U|\psi_j^k|^2) \frac{\psi_j^k + \psi_j^{k+1}}{2}.
$$

(B.12)

The effective potential at time k is renamed for simplicity $\tilde{V}_j^k = V_j + U|\psi_j^k|^2$. One can split the components at different times (k and $k+1$) as

$$
\psi_j^{k+1} \left(\frac{\hbar}{\Delta \tau} + \frac{\hbar^2}{2m\Delta x^2} + \frac{\tilde{V}_j^k}{2} \right) - \frac{\hbar^2}{4m\Delta x^2} \left(\psi_{j+1}^{k+1} + \psi_{j-1}^{k+1} \right) =
$$
$$
= \psi_j^k \left(\frac{\hbar}{\Delta \tau} - \frac{\hbar^2}{2m\Delta x^2} - \frac{\tilde{V}_j^k}{2} \right) + \frac{\hbar^2}{4m\Delta x^2} \left(\psi_{j+1}^k + \psi_{j-1}^k \right).
$$

(B.13)

Dividing by $\hbar^2/(4m\Delta x^2)$ one obtains

$$
\psi_j^{k+1} \underbrace{\left(\frac{2}{\Delta y} + 2 + \tilde{V}_j^k \right)}_{A_j} - \left(\psi_{j+1}^{k+1} + \psi_{j-1}^{k+1} \right) = \psi_j^k \underbrace{\left(\frac{2}{\Delta y} - 2 - \tilde{V}_j^k \right) + \left(\psi_{j+1}^k + \psi_{j-1}^k \right)}_{B_j},
$$

(B.14)

where $\Delta y = \hbar \Delta \tau/(2m\Delta x^2)$. This can be conveniently written in matrix form taking into account the periodic boundary conditions as

$$
M\psi^{k+1} = \begin{pmatrix} A_1 & -1 & 0 & \dots & -1 \\ -1 & A_2 & -1 & \dots & 0 \\ 0 & -1 & A_3 & \dots & 0 \\ \vdots & \vdots & \vdots & \ddots & \vdots \\ -1 & 0 & 0 & \dots & A_N \end{pmatrix} \begin{pmatrix} \psi_1^{k+1} \\ \psi_2^{k+1} \\ \psi_3^{k+1} \\ \vdots \\ \psi_N^{k+1} \end{pmatrix} = \begin{pmatrix} B_1 \\ B_2 \\ B_3 \\ \vdots \\ B_N \end{pmatrix},
$$

(B.15)

where the wavefunction at time $k+1$ appears in the first term, whereas the wavefunction at time k appears in the last one. The only assumption hidden in this procedure consists in taking $\tilde{V}_j^{k+1}$, contained in the M matrix of Eq. (B.15), as $\tilde{V}_j^k$., i.e. the effective potential at the time k. Being the wavefunction at time k (ψ^k) known, the wavefunction at the following time step ψ^{k+1} results from the inverted matrix: $\psi^{k+1} = M^{-1}B$.

This algorithm is unconditionally stable, disregarding conditions on the values of the parameters Δx and $\Delta \tau$ and it is second-order accurate both in space and time. Despite this, the choice of the time step affects the precision of the results, therefore, the best value has to be found as a trade-off between simulation time and precision. The price to pay for choosing an implicit algorithm that does not have convergence issues is the inversion of a matrix and the solution of a linear problem at each step. However, in the simulations shown here, the CPU and memory usage for solving the GPE are less demanding than the requirements for the diagonalization of the BdG matrix that represents the main numerical limitation in our scheme.

BIBLIOGRAPHY

[Abrahams et al., 1979] Abrahams, E., Anderson, P. W., Licciardello, D. C., & Ramakrishnan, T. V. (1979). Scaling Theory of Localization: Absence of Quantum Diffusion in Two Dimensions. *Phys. Rev. Lett.*, 42(10), 673–676. 2, 13

[Al Khawaja et al., 2002] Al Khawaja, U., Andersen, J. O., Proukakis, N. P., & Stoof, H. T. C. (2002). Low dimensional Bose gases. *Phys. Rev. A*, 66(1), 013615. 10

[Aleiner et al., 2010] Aleiner, I. L., Altshuler, B. L., & Shlyapnikov, G. V. (2010). A finite-temperature phase transition for disordered weakly interacting bosons in one dimension. *Nature Physics*, 6, 900–904. 46, 69, 97

[Altman et al., 2004] Altman, E., Kafri, Y., Polkovnikov, A., & Refael, G. (2004). Phase Transition in a System of One-Dimensional Bosons with Strong Disorder. *Phys. Rev. Lett.*, 93(15), 150402. iii, 25, 26

[Altman et al., 2008] Altman, E., Kafri, Y., Polkovnikov, A., & Refael, G. (2008). Insulating Phases and Superfluid-Insulator Transition of Disordered Boson Chains. *Phys. Rev. Lett.*, 100(17), 170402. 26, 55

[Altman et al., 2010] Altman, E., Kafri, Y., Polkovnikov, A., & Refael, G. (2010). Superfluid-insulator transition of disordered bosons in one dimension. *Phys. Rev. B*, 81(17), 174528. 25, 26, 55, 56, 63, 81

[Ames, 1992] Ames, W. F. (1992). *Numerical Methods for Partial Differential Equations.* Academic Press, New York. 105

[Andersen et al., 2002] Andersen, J. O., Al Khawaja, U., & Stoof, H. T. C. (2002). Phase Fluctuations in Atomic Bose Gases. *Phys. Rev. Lett.*, 88(7), 070407. 10, 99

[Anderson et al., 1995] Anderson, M. H., Ensher, J. R., Matthews, M. R., Wieman, C. E., & Cornell, E. A. (1995). Observation of Bose-Einstein Condensation in a Dilute Atomic Vapor. *Science*, 269, 198–201. i, 1

[Anderson, 1958] Anderson, P. W. (1958). Absence of Diffusion in Certain Random Lattices. *Phys. Rev.*, 109(5), 1492–1505. i, 2, 13, 19, 60, 75

[Aspect & Inguscio, 2009] Aspect, A. & Inguscio, M. (2009). Anderson localization of ultracold atoms. *Physics Today*, 62(8), 080000–+. 92

[Aubry & André, 1980] Aubry, S. & André, G. (1980). Analyticity breaking and Anderson localization in incommensurate lattices. *Ann. Israel Phys. Soc.*, 3, 133. 18, 19

[Bagnato & Kleppner, 1991] Bagnato, V. & Kleppner, D. (1991). Bose-Einstein condensation in low-dimensional traps. *Phys. Rev. A*, 44(11), 7439–7441. 12

[Bar-Gill et al., 2006] Bar-Gill, N., Pugatch, R., Rowen, E., Katz, N., & Davidson, N. (2006). Quantum Phases of Ultra Cold Bosons in Incommensurate 1D Optical Lattices. *arXiv:0603.513v7 [cond-mat]*. 75

[Batrouni et al., 1990] Batrouni, G. G., Scalettar, R. T., & Zimanyi, G. T. (1990). Quantum critical phenomena in one-dimensional Bose systems. *Phys. Rev. Lett.*, 65(14), 1765–1768. 26, 61

[Berezinskiĭ, 1972] Berezinskiĭ, V. L. (1972). Destruction of Long-range Order in One-dimensional and Two-dimensional Systems Possessing a Continuous Symmetry Group. II. Quantum Systems. *Soviet Journal of Experimental and Theoretical Physics*, 34, 610. 24, 99

[Bilas & Pavloff, 2006] Bilas, N. & Pavloff, N. (2006). Anderson localization of elementary excitations in a one-dimensional Bose-Einstein condensate. *Eur. Phys. J. D*, 40, 387–397. 57, 58, 59

[Billy et al., 2008] Billy, J., Josse, V., Zuo, Z., Bernard, A., Hambrecht, B., Lugan, P., Clément, D., Sanchez-Palencia, L., Bouyer, P., & Aspect, A. (2008). Direct observation of Anderson localization of matter waves in a controlled disorder. *Nature*, 453, 891. ii, 2, 13, 19, 26, 57

[Bloch et al., 2008] Bloch, I., Dalibard, J., & Zwerger, W. (2008). Many-body physics with ultracold gases. *Rev. Mod. Phys.*, 80(3), 885–964. 7, 8, 20, 34

[Bogoliubov, 1947] Bogoliubov, N. (1947). The microscopic theory of superfluidity. *J. Phys. USSR*, 11, 23. 2, 4, 5, 34

[Bogoliubov, 1960] Bogoliubov, N. N. (1960). *Physica*, 26, 51. 9

[Carrasquilla et al., 2010] Carrasquilla, J., Becca, F., Trombettoni, A., & Fabrizio, M. (2010). Characterization of the Bose-glass phase in low-dimensional lattices. *Phys. Rev. B*, 81(19), 195129. iv

[Carusotto & Castin, 2001] Carusotto, I. & Castin, Y. (2001). An exact stochastic field method for the interacting Bose gas at thermal equilibrium. *Journal of Physics B: Atomic, Molecular and Optical Physics*, 34(23), 4589. 30, 40

[Carusotto & Castin, 2004] Carusotto, I. & Castin, Y. (2004). Superfluidity of the 1D Bose gas. *Comptes Rendus Physique*, 5(1). 62

[Castin, 2004] Castin, Y. (2004). Simple theoretical tools for low dimension Bose gases. *J. Phys. IV*, 116, 89. 9, 32, 39, 42, 63, 81

[Castin & Dum, 1998] Castin, Y. & Dum, R. (1998). Low-temperature Bose-Einstein condensates in time-dependent traps: Beyond the $U(1)$ symmetry-breaking approach. *Phys. Rev. A*, 57(4), 3008–3021. 27, 31, 32, 40, 103

[Castin et al., 2000] Castin, Y., Dum, R., Mandonnet, E., Minguzzi, A., & Carusotto, I. (2000). Coherence properties of a continuous atom laser. *Journal of Modern Optics*, 47, 2671–2695. 39

[Cazalilla et al., 2011] Cazalilla, M. A., Citro, R., Giamarchi, T., Orignac, E., & Rigol, M. (2011). One dimensional Bosons: From Condensed Matter Systems to Ultracold Gases. *arXiv:1101.5337 [cond-mat.str-el]*. 20, 23

[Cerimele et al., 2000] Cerimele, M. M., Chiofalo, M. L., Pistella, F., Succi, S., & Tosi, M. P. (2000). Numerical solution of the Gross-Pitaevskii equation using an explicit finite-difference scheme: An application to trapped Bose-Einstein condensates. *Phys. Rev. E*, 62(1), 1382–1389. 105

[Cetoli & Lundh, 2010] Cetoli, A. & Lundh, E. (2010). Correlations and superfluidity of a one-dimensional Bose gas in a quasiperiodic potential. *Phys. Rev. A*, 81(6), 063635. 47, 73, 74

[Chen et al., 2008] Chen, Y. P., Hitchcock, J., Dries, D., Junker, M., Welford, C., & Hulet, R. G. (2008). Phase coherence and superfluid-insulator transition in a disordered Bose-Einstein condensate. *Phys. Rev. A*, 77(3), 033632. iii, 14, 16, 42, 85

[Chiofalo et al., 2000] Chiofalo, M. L., Succi, S., & Tosi, M. P. (2000). Ground state of trapped interacting Bose-Einstein condensates by an explicit imaginary-time algorithm. *Phys. Rev. E*, 62(5), 7438–7444. 105

[Clément et al., 2008] Clément, D., Bouyer, P., Aspect, A., & Sanchez-Palencia, L. (2008). Density modulations in an elongated Bose-Einstein condensate released from a disordered potential. *Phys. Rev. A*, 77(3), 033631. iii, 16, 42, 85

[Clément et al., 2006] Clément, D., Varón, A. F., Retter, J. A., Sanchez-Palencia, L., Aspect, A., & Bouyer, P. (2006). Experimental study of the transport of coherent interacting matter-waves in a 1d random potential induced by laser speckle. *New Journal of Physics*, 8(8), 165. 16, 17

[Crooker et al., 1983] Crooker, B. C., Hebral, B., Smith, E. N., Takano, Y., & Reppy, J. D. (1983). Superfluidity in a Dilute Bose Gas. *Phys. Rev. Lett.*, 51(8), 666–669. 19

[Damski et al., 2003] Damski, B., Zakrzewski, J., Santos, L., Zoller, P., & Lewenstein, M. (2003). Atomic Bose and Anderson Glasses in Optical Lattices. *Phys. Rev. Lett.*, 91(8), 080403. iv, 25

[Davis et al., 1995] Davis, K. B., Mewes, M. O., Andrews, M. R., van Druten, N. J., Durfee, D. S., Kurn, D. M., & Ketterle, W. (1995). Bose-Einstein Condensation in a Gas of Sodium Atoms. *Phys. Rev. Lett.*, 75(22), 3969–3973. i, 1

[De Gennes, 1966] De Gennes, P. G. (1966). *Superconductivity of Metals and Alloys.* Benjamin, New York. 5

[Deissler et al., 2011] Deissler, B., Lucioni, E., Modugno, M., Roati, G., Tanzi, L., Zaccanti, M., Inguscio, M., & Modugno, G. (2011). Correlation function of weakly interacting bosons in a disordered lattice. *New Journal of Physics*, 13(2), 023020. 26

[Deissler et al., 2010] Deissler, B., Zaccanti, M., Roati, G., D'Errico, C., Fattori, M., Modugno, M., Modugno, G., & Inguscio, M. (2010). Delocalization of a disordered bosonic system by repulsive interactions. *Nat. Phys.*, 6(2), 354. iii, iv, 26, 42, 74, 75, 85

[Delande & Zakrzewski, 2009] Delande, D. & Zakrzewski, J. (2009). Compression as a Tool to Detect Bose Glass in a Cold Atomic Gas. *Phys. Rev. Lett.*, 102(8), 085301. iv

[Deng et al., 2008] Deng, X., Citro, R., Minguzzi, A., & Orignac, E. (2008). Phase diagram and momentum distribution of an interacting Bose gas in a bichromatic lattice. *Phys. Rev. A*, 78(1), 013625. 71, 75

[Diener et al., 2001] Diener, R. B., Georgakis, G. A., Zhong, J., Raizen, M., & Niu, Q. (2001). Transition between extended and localized states in a one-dimensional incommensurate optical lattice. *Phys. Rev. A*, 64(3), 033416. 17

[Dries et al., 2010] Dries, D., Pollack, S. E., Hitchcock, J. M., & Hulet, R. G. (2010). Dissipative transport of a Bose-Einstein condensate. *Phys. Rev. A*, 82(3), 033603. 16, 85, 90

[Falco et al., 2009a] Falco, G. M., Nattermann, T., & Pokrovsky, V. L. (2009a). Localized states and interaction-induced delocalization in Bose gases with quenched disorder. *EPL (Europhysics Letters)*, 85(3), 30002. 26, 77

[Falco et al., 2009b] Falco, G. M., Nattermann, T., & Pokrovsky, V. L. (2009b). Weakly interacting Bose gas in a random environment. *Phys. Rev. B*, 80(10), 104515. 26, 66, 71

[Fallani et al., 2007] Fallani, L., Lye, J. E., Guarrera, V., Fort, C., & Inguscio, M. (2007). Ultracold Atoms in a Disordered Crystal of Light: Towards a Bose Glass. *Phys. Rev. Lett.*, 98(13), 130404. iii

[Fetter, 1972] Fetter, A. L. (1972). Nonuniform states of an imperfect bose gas. *Annals of Physics*, 70, 67–101. 4

[Fisher et al., 1973] Fisher, M. E., Barber, M. N., & Jasnow, D. (1973). Helicity Modulus, Superfluidity, and Scaling in Isotropic Systems. *Phys. Rev. A*, 8(2), 1111–1124. 60, 61, 81

[Fisher et al., 1989] Fisher, M. P. A., Weichman, P. B., Grinstein, G., & Fisher, D. S. (1989). Boson localization and the superfluid-insulator transition. *Phys. Rev. B*, 40, 546–570. ii, iii, 14, 20, 22, 23, 24, 25, 46, 47, 54, 56, 57, 71

[Fontanesi et al., 2010] Fontanesi, L., Wouters, M., & Savona, V. (2010). Mean-field phase diagram of the one-dimensional Bose gas in a disorder potential. *Phys. Rev. A*, 81(5), 053603. 63, 81

[Fort et al., 2005] Fort, C., Fallani, L., Guarrera, V., Lye, J. E., Modugno, M., Wiersma, D. S., & Inguscio, M. (2005). Effect of Optical Disorder and Single Defects on the Expansion of a Bose-Einstein Condensate in a One-Dimensional Waveguide. *Phys. Rev. Lett.*, 95(17), 170410. 17, 74

[Freericks & Monien, 1994] Freericks, J. K. & Monien, H. (1994). Phase diagram of the Bose-Hubbard Model. *Europhysics Letters*, 26(7), 545. 22

[Freericks & Monien, 1996] Freericks, J. K. & Monien, H. (1996). Strong-coupling expansions for the pure and disordered Bose-Hubbard model. *Phys. Rev. B*, 53(5), 2691–2700. 22, 24

[Gati & Oberthaler, 2007] Gati, R. & Oberthaler, M. K. (2007). A bosonic Josephson junction. *Journal of Physics B: Atomic, Molecular and Optical Physics*, 40(10), R61. 53, 55

[Gaul & Müller, 2011] Gaul, C. & Müller, C. A. (2011). Bogoliubov excitations of disordered Bose-Einstein condensates. *Phys. Rev. A*, 83(6), 063629. 57

[Gaul et al., 2009] Gaul, C., Renner, N., & Müller, C. A. (2009). Speed of sound in disordered Bose-Einstein condensates. *Phys. Rev. A*, 80(5), 053620. 54

[Giamarchi, 2004] Giamarchi, T. (2004). *Quantum Physics in One Dimension*. Oxford University Press, New York. 7

[Giamarchi & Schulz, 1987] Giamarchi, T. & Schulz, H. J. (1987). Localization and Interaction in One-Dimensional Quantum Fluids. *EPL*, 3(12), 1287. 11, 22, 23, 24, 71

[Giamarchi & Schulz, 1988] Giamarchi, T. & Schulz, H. J. (1988). Anderson localization and interactions in one-dimensional metals. *Phys. Rev. B*, 37(1), 325–340. ii, 22, 23, 25, 26, 56, 67, 71, 72

[Girardeau, 1960] Girardeau, M. (1960). Relationship between Systems of Impenetrable Bosons and Fermions in One Dimension. *Journal of Mathematical Physics*, 1, 516–523. 10, 28

[Glauber, 1963] Glauber, R. J. (1963). The Quantum Theory of Optical Coherence. *Phys. Rev.*, 130(6), 2529–2539. 46

[Goodman, 2007] Goodman, J. W. (2007). *Speckle Phenomena in Optics: Theory and Applications*. Roberts and Company Publishers, Greenwood Village, Colorado. 17

[Greiner et al., 2002] Greiner, M., Mandel, O., Esslinger, T., Hänsch, T. W., & Bloch, I. (2002). Quantum phase transition from a superfluid to a Mott insulator in a gas of ultracold atoms. *Nature*, 415, 39–44. ii, 25

[Griffiths, 1969] Griffiths, R. B. (1969). Nonanalytic Behavior Above the Critical Point in a Random Ising Ferromagnet. *Phys. Rev. Lett.*, 23(1), 17–19. 25

[Grimm et al., 2000] Grimm, R., Weidemuller, M., & Ovchinnikov, Y. B. (2000). Optical dipole traps for neutral atoms. volume 42 of *Advances In Atomic, Molecular, and Optical Physics* (pp. 95 – 170). Academic Press. 16

[Gross, 1963] Gross, E. P. (1963). Hydrodynamics of a Superfluid Condensate. *Journal of Mathematical Physics*, 4(2), 195. 5

[Guarrera et al., 2007] Guarrera, V., Fallani, L., Lye, J. E., Fort, C., & Inguscio, M. (2007). Inhomogeneous broadening of a mott insulator spectrum. *New Journal of Physics*, 9(4), 107. 18

[Gurarie & Altland, 2005] Gurarie, V. & Altland, A. (2005). Phonons in Random Elastic Media and the Boson Peak. *Phys. Rev. Lett.*, 94(24), 245502. 54

[Gurarie et al., 2009] Gurarie, V., Pollet, L., Prokof'ev, N. V., Svistunov, B. V., & Troyer, M. (2009). Phase diagram of the disordered Bose-Hubbard model. *Phys. Rev. B*, 80(21), 214519. 25, 71

[Gurarie et al., 2008] Gurarie, V., Refael, G., & Chalker, J. T. (2008). Excitations of One-Dimensional Bose-Einstein Condensates in a Random Potential. *Phys. Rev. Lett.*, 101(17), 170407. iv, 24, 57, 58

[Hadzibabic et al., 2006] Hadzibabic, Z., Krüger, P., Cheneau, M., Battelier, B., & Dalibard, J. (2006). Berezinskii-Kosterlitz-Thouless crossover in a trapped atomic gas. *Nature*, 441, 1118–1121. i

[Haldane, 1981] Haldane, F. D. M. (1981). Demonstration of the "Luttinger liquid" character of Bethe-ansatz-soluble models of 1-D quantum fluids. *Physics Letters A*, 81, 153–155. 11

[Haldane, 1981] Haldane, F. D. M. (1981). Effective Harmonic-Fluid Approach to Low-Energy Properties of One-Dimensional Quantum Fluids. *Phys. Rev. Lett.*, 47(25), 1840–1843. 23, 46

[Halperin, 1965] Halperin, B. I. (1965). Green's Functions for a Particle in a One-Dimensional Random Potential. *Phys. Rev.*, 139(1A), A104–A117. 14

[Harper, 1955] Harper, P. G. (1955). Single band motion of conduction electrons in a uniform magnetic field. *Proc. Phys. Soc. A*, 68, 874. 18

[Hertz et al., 1979] Hertz, J. A., Fleishman, L., & Anderson, P. W. (1979). Marginal Fluctuations in a Bose Glass. *Phys. Rev. Lett.*, 43(13), 942–946. 59

[Hess & Fairbank, 1967] Hess, G. B. & Fairbank, W. M. (1967). Measurements of Angular Momentum in Superfluid Helium. *Phys. Rev. Lett.*, 19(5), 216–218. 60

[Hohenberg, 1967] Hohenberg, P. C. (1967). Existence of Long-Range Order in One and Two Dimensions. *Phys. Rev.*, 158(2), 383–386. 9

[Horak et al., 1998] Horak, P., Courtois, J.-Y., & Grynberg, G. (1998). Atom cooling and trapping by disorder. *Phys. Rev. A*, 58(5), 3953–3962. 17

[Huber et al., 2007] Huber, S. D., Altman, E., Büchler, H. P., & Blatter, G. (2007). Dynamical properties of ultracold bosons in an optical lattice. *Phys. Rev. B*, 75(8), 085106. 56

[Hulet, 2011] Hulet, R. (2011). Private Communication. 85, 90

[Huntley, 1989] Huntley, J. M. (1989). Speckle photography fringe analysis: assessment of current algorithms. *Appl. Opt.*, 28, 4316. 17

[Jaksch et al., 1998] Jaksch, D., Bruder, C., Cirac, J. I., Gardiner, C. W., & Zoller, P. (1998). Cold Bosonic Atoms in Optical Lattices. *Phys. Rev. Lett.*, 81(15), 3108–3111. 20

[Jaksch et al., 2008] Jaksch, D., Bruder, C., Cirac, J. I., Gardiner, C. W., & Zoller, P. (2008). Dirty bosons: twenty years later. *Mod. Phys. Lett. B*, 22, 2623. 20, 22, 25

[Kagan et al., 2000] Kagan, Y., Kashurnikov, V. A., Krasavin, A. V., Prokof'ev, N. V., & Svistunov, B. (2000). Quasicondensation in a two-dimensional interacting Bose gas. *Phys. Rev. A*, 61(4), 043608. 99

[Kane & Kadanoff, 1967] Kane, J. W. & Kadanoff, L. P. (1967). Long-Range Order in Superfluid Helium. *Phys. Rev.*, 155(1), 80–83. 6, 35

[Ketterle & van Druten, 1996] Ketterle, W. & van Druten, N. J. (1996). Bose-Einstein condensation of a finite number of particles trapped in one or three dimensions. *Phys. Rev. A*, 54(1), 656–660. 12

[Kosterlitz & Thouless, 1973] Kosterlitz, J. M. & Thouless, D. J. (1973). Ordering, metastability and phase transitions in two-dimensional systems. *Journal of Physics C Solid State Physics*, 6, 1181–1203. 24, 99

[Kramer & MacKinnon, 1993] Kramer, B. & MacKinnon, A. (1993). Localization: theory and experiment. *Rep. Prog. Phys.*, 56, 1469–1564. 58, 75

[Krauth et al., 1991] Krauth, W., Trivedi, N., & Ceperley, D. (1991). Superfluid-insulator transition in disordered boson systems. *Phys. Rev. Lett.*, 67(17), 2307–2310. 22

[Lee & Gunn, 1990] Lee, D. K. K. & Gunn, J. M. F. (1990). Bosons in a random potential: condensation and screening in a dense limit. *Journal of Physics: Condensed Matter*, 2(38), 7753. 54

[Lee & Gunn, 1992] Lee, D. K. K. & Gunn, J. M. F. (1992). The fate of the Lifshitz tail for condensed bosons. *Journal of Physics Condensed Matter*, 4, 1729–1742. 54

[Leggett, 1973] Leggett, A. J. (1973). *Physica Fennica*, 8, 125. 8, 60

[Leggett, 1998] Leggett, A. J. (1998). On the Superfluid Fraction of an Arbitrary Many-Body System at $T = 0$. *Journal of Statistical Physics*, 93, 927. 60

[Leggett, 2001] Leggett, A. J. (2001). Bose-Einstein condensation in the alkali gases: Some fundamental concepts. *Rev. Mod. Phys.*, 73(2), 307–356. 2, 8, 61, 62

[Lewenstein & You, 1996] Lewenstein, M. & You, L. (1996). Quantum Phase Diffusion of a Bose-Einstein Condensate. *Phys. Rev. Lett.*, 77(17), 3489–3493. 31

[Lieb & Liniger, 1963] Lieb, E. H. & Liniger, W. (1963). Exact Analysis of an Interacting Bose Gas. I. The General Solution and the Ground State. *Phys. Rev.*, 130(4), 1605–1616. iii, 10, 11, 28, 29, 35

[Lieb et al., 2002] Lieb, E. H., Seiringer, R., & Yngvason, J. (2002). Superfluidity in dilute trapped Bose gases. *Phys. Rev. B*, 66(13), 134529. 60, 61, 62

[Lifshitz, 1963] Lifshitz, I. M. (1963). Structure of the energy spectrum of impurity bands in disordered solid solutions. *Sov. Phys. JETP*, 17, 1159. 54

[Lifshitz, 1964] Lifshitz, I. M. (1964). The energy spectrum of disordered systems. *Adv. Phys.*, 13, 483. 54

[Lifshitz et al., 1988] Lifshitz, M. A., Gredeskul, S. A., & Pastur, L. A. (1988). *Introduction to the theory of disordered systems*. Wiley, New York. 13

[Lim et al., 2008] Lim, L.-K., Smith, C. M., & Stoof, H. T. C. (2008). Correlation effects in ultracold two-dimensional Bose gases. *Phys. Rev. A*, 78(1), 013634. 99

[Lugan, 2010] Lugan, P. (2010). *Ultracold Bose gases in random potentials: collective excitations and localization effects*. PhD thesis, Ecole Polytechnique, Palaiseau. 26, 73, 74

[Lugan et al., 2007a] Lugan, P., Clément, D., Bouyer, P., Aspect, A., Lewenstein, M., & Sanchez-Palencia, L. (2007a). Ultracold Bose Gases in 1D Disorder: From Lifshits Glass to Bose-Einstein Condensate. *Phys. Rev. Lett.*, 98(17), 170403. iii, iv, 26, 40, 67, 73, 77

[Lugan et al., 2007b] Lugan, P., Clément, D., Bouyer, P., Aspect, A., & Sanchez-Palencia, L. (2007b). Anderson Localization of Bogolyubov Quasiparticles in Interacting Bose-Einstein Condensates. *Phys. Rev. Lett.*, 99(18), 180402. 57

[Ma et al., 1993] Ma, M., Nisamaneephong, P., & Zhang, L. (1993). Ground state and excitations of disordered boson systems. *Journal of Low Temperature Physics*, 93, 957. 54, 56

[Mermin & Wagner, 1966] Mermin, N. D. & Wagner, H. (1966). Absence of Ferromagnetism or Antiferromagnetism in One- or Two-Dimensional Isotropic Heisenberg Models. *Phys. Rev. Lett.*, 17(22), 1133–1136. 1, 9

[Modugno, 2010] Modugno, G. (2010). Anderson localization in bose–einstein condensates. *Reports on Progress in Physics*, 73(10), 102401. ii, 18

[Modugno, 2009] Modugno, M. (2009). Exponential localization in one-dimensional quasi-periodic optical lattices. *New Journal of Physics*, 11(3), 033023. 18

[Mora, 2006] Mora, C. (2006). *Gaz de bosons et de fermions condensès : phases de Fulde-Ferrell-Larkin-Ovchinnikov et quasicondensats.* PhD thesis, Laboratoire de Physique Statistique de l'ENS, Paris VI. 27, 40

[Mora & Castin, 2003] Mora, C. & Castin, Y. (2003). Extension of Bogoliubov theory to quasicondensates. *Phys. Rev. A*, 67(5), 053615. iii, 10, 27, 29, 30, 31, 32, 33, 35, 39, 47, 103

[Mueller et al., 2006] Mueller, E. J., Ho, T.-L., Ueda, M., & Baym, G. (2006). Fragmentation of Bose-Einstein condensates. *Phys. Rev. A*, 74(3), 033612. 78, 79

[Muruganandam & Adhikari, 2009] Muruganandam, P. & Adhikari, S. (2009). Fortran programs for the time-dependent gross-pitaevskii equation in a fully anisotropic trap. *Computer Physics Communications*, 180(10), 1888 – 1912. 105

[Nattermann & Pokrovsky, 2008] Nattermann, T. & Pokrovsky, V. L. (2008). Bose-Einstein Condensates in Strongly Disordered Traps. *Phys. Rev. Lett.*, 100(6), 060402. iii, 26

[Nelson & Kosterlitz, 1977] Nelson, D. R. & Kosterlitz, J. M. (1977). Universal Jump in the Superfluid Density of Two-Dimensional Superfluids. *Phys. Rev. Lett.*, 39(19), 1201–1205. 24, 25, 64

[Nisamaneephong et al., 1993] Nisamaneephong, P., Zhang, L., & Ma, M. (1993). Gaussian theory of superfluid–Bose-glass phase transition. *Phys. Rev. Lett.*, 71(23), 3830–3833. 54

[Nozières, 1995] Nozières, P. (1995). *in Bose-Einstein condensation*, chapter Some comments in BEC. Cambridge University Press, Cambridge. iv, 78

[Nozières, P. & Saint James, D., 1982] Nozières, P. & Saint James, D. (1982). Particle vs. pair condensation in attractive Bose liquids. *J. Phys. France*, 43(7), 1133–1148. 78

[Pai et al., 1996] Pai, R. V., Pandit, R., Krishnamurthy, H. R., & Ramasesha, S. (1996). One-Dimensional Disordered Bosonic Hubbard Model: A Density-Matrix Renormalization Group Study. *Phys. Rev. Lett.*, 76(16), 2937–2940. 71

[Paramekanti et al., 1998] Paramekanti, A., Trivedi, N., & Randeria, M. (1998). Upper bounds on the superfluid stiffness of disordered systems. *Phys. Rev. B*, 57(18), 11639–11647. 62

[Paraoanu et al., 2001] Paraoanu, G. S., Kohler, S., Sols, F., & Leggett, A. J. (2001). The Josephson plasmon as a Bogoliubov quasiparticle. *J. Phys. B*, 34(23), 4689–4696. 55

[Pasienski et al., 2010] Pasienski, M., McKay, D., White, M., & DeMarco, B. (2010). A disordered insulator in an optical lattice. *Nat. Phys.*, 6, 677. iii, 25

[Peierls, 1935] Peierls, R. E. (1935). *Ann. Inst. Henri. Poincare*, 5, 177. 9

[Penrose & Onsager, 1956] Penrose, O. & Onsager, L. (1956). Bose-Einstein Condensation and Liquid Helium. *Phys. Rev.*, 104(3), 576–584. 2, 46

[Petrov et al., 2000] Petrov, D. S., Shlyapnikov, G. V., & Walraven, J. T. M. (2000). Regimes of Quantum Degeneracy in Trapped 1D Gases. *Phys. Rev. Lett.*, 85(18), 3745–3749. 12, 95

[Pilati et al., 2008] Pilati, S., Giorgini, S., & Prokof'ev, N. (2008). Critical Temperature of Interacting Bose Gases in Two and Three Dimensions. *Phys. Rev. Lett.*, 100(14), 140405. 99

[Pitaevskii, 1961] Pitaevskii, L. (1961). Vortex lines in an imperfect Bose gas. *Sov. Phys. JETP*, 13, 451. 5

[Pitaevskii & Stringari, 1991] Pitaevskii, L. & Stringari, S. (1991). Uncertainty principle, quantum fluctuations, and broken symmetries. *Journal of Low Temperature Physics*, 85, 377–388. 9

[Pitaevskii & Stringari, 2003] Pitaevskii, L. & Stringari, S. (2003). *Bose-Einstein Condensation*. Clarendon Press, Oxford. 7, 29

[Pollack et al., 2009] Pollack, S. E., Dries, D., Junker, M., Chen, Y. P., Corcovilos, T. A., & Hulet, R. G. (2009). Extreme Tunability of Interactions in a ^{7}Li Bose-Einstein Condensate. *Physical Review Letters*, 102(9), 090402. 11, 90

[Pollet et al., 2009] Pollet, L., Prokof'ev, N. V., Svistunov, B. V., & Troyer, M. (2009). Absence of a Direct Superfluid to Mott Insulator Transition in Disordered Bose Systems. *Phys. Rev. Lett.*, 103(14), 140402. 24

[Popov, 1972] Popov, V. N. (1972). On the theory of the superfluidity of two- and one-dimensional Bose systems. *Theor. and Math. Phys.*, 11, 565–573. 1, 29, 46

[Popov, 1972] Popov, V. N. (1972). On the theory of the superfluidity of two- and one-dimensional bose systems. *Theoretical and Mathematical Physics*, 11, 565–573. 7, 8

[Popov, 1980] Popov, V. N. (1980). Long-wave asymptotic form of the many-body Green's functions of a one-dimensional Bose gas. *JETP Lett.*, 31, 526. 35, 46, 47

[Popov, 1983] Popov, V. N. (1983). *Functional integrals in quantum field theory and statistical physics.* Reidel. 9, 35

[Prokof'ev et al., 2001] Prokof'ev, N., Ruebenacker, O., & Svistunov, B. (2001). Critical Point of a Weakly Interacting Two-Dimensional Bose Gas. *Phys. Rev. Lett.*, 87(27), 270402. 24

[Prokof'ev & Svistunov, 2004] Prokof'ev, N. & Svistunov, B. (2004). Superfluid-Insulator Transition in Commensurate Disordered Bosonic Systems: Large-Scale Worm Algorithm Simulations. *Phys. Rev. Lett.*, 92(1), 015703. 22

[Prokof'ev & Svistunov, 1998] Prokof'ev, N. V. & Svistunov, B. V. (1998). Comment on "One-Dimensional Disordered Bosonic Hubbard Model: A Density-Matrix Renormalization Group Study". *Phys. Rev. Lett.*, 80(19), 4355. ii, 24, 71, 72

[Prokof'ev & Svistunov, 2000] Prokof'ev, N. V. & Svistunov, B. V. (2000). Two definitions of superfluid density. *Phys. Rev. B*, 61(17), 11282–11284. 61

[Rapsch et al., 1999] Rapsch, S., Schollwöck, U., & Zwerger, W. (1999). Density matrix renormalization group for disordered bosons in one dimension. *Europhys. Lett.*, 46(5), 559–564. ii, 24, 61, 71, 72

[Roati et al., 2008] Roati, G., D'Errico, C., Fallani, L., Fattori, M., Fort, C., Zaccanti, M., Modugno, G., Modugno, M., & Inguscio, M. (2008). Anderson localization of a non-interacting Bose-Einstein condensate. *Nature*, 453, 895. ii, 2, 13, 19, 26, 57

[Roscilde, 2008] Roscilde, T. (2008). Bosons in one-dimensional incommensurate super-lattices. *Phys. Rev. A*, 77(6), 063605. 25

[Roth & Burnett, 2003a] Roth, R. & Burnett, K. (2003a). Phase diagram of bosonic atoms in two-color superlattices. *Phys. Rev. A*, 68(2), 023604. 60, 61, 62, 71, 75

[Roth & Burnett, 2003b] Roth, R. & Burnett, K. (2003b). Ultracold bosonic atoms in two-colour superlattices. *Journal of Optics B: Quantum and Semiclassical Optics*, 5(2), S50. 25

[Roux et al., 2008] Roux, G., Barthel, T., McCulloch, I. P., Kollath, C., Schollwöck, U., & Giamarchi, T. (2008). Quasiperiodic Bose-Hubbard model and localization in one-dimensional cold atomic gases. *Phys. Rev. A*, 78(2), 023628. 18, 25, 74, 75

[Sachdev, 1999] Sachdev, S. (1999). *Quantum Phase Transitions*. Cambridge University Press. 20, 25

[Sanchez-Palencia, 2006] Sanchez-Palencia, L. (2006). Smoothing effect and delocalization of interacting Bose-Einstein condensates in random potentials. *Phys. Rev. A*, 74(5), 053625. 67, 77, 82

[Sanchez-Palencia et al., 2007] Sanchez-Palencia, L., Clément, D., Lugan, P., Bouyer, P., Shlyapnikov, G. V., & Aspect, A. (2007). Anderson Localization of Expanding Bose-Einstein Condensates in Random Potentials. *Phys. Rev. Lett.*, 98(21), 210401. 17, 57

[Sanchez-Palencia & Lewenstein, 2010] Sanchez-Palencia, L. & Lewenstein, M. (2010). Disordered quantum gases under control. *Nat. Phys.*, 6, 87. ii, 19

[Scalettar et al., 1991] Scalettar, R. T., Batrouni, G. G., & Zimanyi, G. T. (1991). Localization in interacting, disordered, Bose systems. *Phys. Rev. Lett.*, 66(24), 3144–3147. 22, 26, 49, 56, 57, 72

[Schmitt et al., 2010] Schmitt, F., Hild, M., & Roth, R. (2010). Ab initio phase diagram of ultracold ^{87}rb in a one-dimensional two-colour superlattice. *Journal of Physics B: Atomic, Molecular and Optical Physics*, 43(23), 235301. 25

[Schwartz, 1977] Schwartz, M. (1977). Off-diagonal long-range behavior of interacting Bose systems. *Phys. Rev. B*, 15(3), 1399–1403. 35, 46

[Schweikhard et al., 2007] Schweikhard, V., Tung, S., & Cornell, E. A. (2007). Vortex Proliferation in the Berezinskii-Kosterlitz-Thouless Regime on a Two-Dimensional Lattice of Bose-Einstein Condensates. *Physical Review Letters*, 99(3), 030401. i

[Shevchenko, 1992] Shevchenko, S. (1992). On the theory of a Bose gas in a nonuniform field. *Sov. J. Low Temp. Phys.*, 18, 223. 10, 29

[Singh & Rokhsar, 1994] Singh, K. G. & Rokhsar, D. S. (1994). Disordered bosons: Condensate and excitations. *Phys. Rev. B*, 49(13), 9013–9023. 59, 60, 61

[Spekkens & Sipe, 1998] Spekkens, R. W. & Sipe, J. E. (1998). Some Remarks on the Fragmentation of Bose Condensates. *Progr. Phys.*, 46, 873. 80

[Spekkens & Sipe, 1999] Spekkens, R. W. & Sipe, J. E. (1999). Spatial fragmentation of a Bose-Einstein condensate in a double-well potential. *Phys. Rev. A*, 59(5), 3868–3877. 80

[Spielman et al., 2007] Spielman, I. B., Phillips, W. D., & Porto, J. V. (2007). Mott-Insulator Transition in a Two-Dimensional Atomic Bose Gas. *Phys. Rev. Lett.*, 98(8), 080404. ii, 25

[Spielman et al., 2008] Spielman, I. B., Phillips, W. D., & Porto, J. V. (2008). Condensate Fraction in a 2D Bose Gas Measured across the Mott-Insulator Transition. *Phys. Rev. Lett.*, 100(12), 120402. 25

[Stöferle et al., 2004] Stöferle, T., Moritz, H., Schori, C., Köhl, M., & Esslinger, T. (2004). Transition from a Strongly Interacting 1D Superfluid to a Mott Insulator. *Phys. Rev. Lett.*, 92(13), 130403. ii, 25

[Stoof & Bijlsma, 1993] Stoof, H. T. C. & Bijlsma, M. (1993). Kosterlitz-Thouless transition in a dilute Bose gas. *Phys. Rev. E*, 47(2), 939–947. 99

[Streltsov et al., 2004] Streltsov, A. I., Cederbaum, L. S., & Moiseyev, N. (2004). Ground-state fragmentation of repulsive Bose-Einstein condensates in double-trap potentials. *Phys. Rev. A*, 70(5), 053607. 80

[Vosk & Altman, 2011] Vosk, R. & Altman, E. (2011). The superfluid insulator transition of ultra-cold bosons in disordered 1D traps. *arXiv:1104.2063 [cond-mat.dis-nn]*. 26, 63

[Wu & Griffin, 1996] Wu, W.-C. & Griffin, A. (1996). Quantized hydrodynamic model and the dynamic structure factor for a trapped Bose gas. *Phys. Rev. A*, 54(5), 4204–4212. 29

[Yang & Yang, 1969] Yang, C. N. & Yang, C. P. (1969). Thermodynamics of a One-Dimensional System of Bosons with Repulsive Delta-Function Interaction. *J. Math. Phys.*, 10, 1115. 8, 28

[Ziman, 1982] Ziman, T. A. L. (1982). Localization and Spectral Singularities in Random Chains. *Phys. Rev. Lett.*, 49(5), 337–340. iii, 52, 54

List of Abbreviations

BdG	Bogoliubov-de Gennes
BEC	Bose-Einstein condensation
BG	Bose-glass
BKT	Berezinskii-Kosterlitz-Thouless
DoS	Density of states
GP	Gross-Pitaevskii
IPR	Inverse Participation Ratio
MI	Mott-insulator
ODLRO	Off-diagonal long-range order
PDD	Probability Distribution of the Density
QC	Quasi-condensate
SF	Superfluid
TF	Thomas-Fermi
WN	White-noise

ACKNOWLEDGMENTS

This thesis would not exist if it was not for my supervisor, Vincenzo Savona. I want to truly thank him for his support, his enthusiasm and his confidence in giving me the possibility to explore unknown areas of physics. I owe a lot also to Michiel Wouters as an infinite source of ideas and answers: his contribution was crucial in the achievement of the results presented in this work. I thank the members of the jury, T. Esslinger, T. Giamarchi, S. Giorgini and O. Schneider for accepting to read and review my thesis and for the interesting comments and questions that led to the present version of this manuscript. I'm particularly indebt to Pierre Lugan for several discussions that led to a very proficuous scientific interplay. I want to acknowledge fruitful collaborations with experimental groups, in particular with B. Deissler and R. Hulet that enriched my comprehension of the real-world limitations. I even want to thank Gora Shlyapnikov for his precious *baptême du feu* and for stimulating an intense analysis in the interpretation of our results.

Many other people contributed with some bricks to the build-up of this work. Among others, I want to acknowledge I. Aleiner, E. Altman, B. Altshuler, G. Bertaina, I. Carusotto, A. Cetoli, B. Das, J. Keeling, M. Köhl, E. Lucioni, G. Modugno, M. Modugno, C. A. Müller, S. Pollack, N. Prokofiev, G. Roati, E. Runge, L. Sanchez-Palencia, C. Salomon, D. Sarchi, R. Vosk, R. Zimmermann.

For what concerns the non-scientific part of these four years... My main "thank you" goes to my parents for their continuous support during these four years. I'd like to thank the colleagues of the ITP, in particular Guillaume, who shared these years inside and outside the EPFL. A huge thanks goes to my flatmates. In primis to Leo, as a colleague and a friend, for pointing out that studying one-dimensional systems at zero temperature with infinite density is not less unreal than studying theories with 10 or more dimensions. To Elsa, the subject of my future PhD in behavioural psychology, and to the new arrival, Floriano. Christopher for the pleasure I had in sharing the office with him. I want to thank Emanuele, for his faith in my future career in politics. My life has benefited from collaboration with experimentalists, such as the wise old man from Pavia, alias il Manni, and GiGi, that forced me to disprove a different philosophy every week. Some people in Reggio Emilia too: 20u and *The Ant*, Cervi, Agu, Alle, Anto and all the others that successfully did their best to make my italian stays as much fun. I thank Martina for having shared half of this adventure. Thanks a lot also to –in random order– Alessandro, Federico, Simone, Stefano, Tim.

Quella che sarà probabilmente la parte più letta della tesi merita una traduzione nella mia lingua madre. Il mio "grazie" principale va di certo ad Ivonne ed Ivano per non aver mai osteggiato le mie scelte ed anzi per avermi sostenuto ed incoraggiato. Una miriade di persone ed eventi – che la memoria non arriva a contare – hanno contribuito a rendere Losanna un posto migliore ed un'esperienza indimenticabile. *Guillaume* con cui ho avuto la fortuna di condividere quattro anni di dottorato tra vette di montagna, pareti d'arrampicata, campi da squash, tour in bicicletta, pause caffè e group meeting. La mia *famiglia* di Av. de Tivoli. In primis *Leo*, per aver condiviso qualsiasi cosa in questi anni, ma soprattutto per avermi fatto notare che studiare sistemi unidimensionali a temperatura zero con infinite particelle non è meno paradossale che studiare teorie a 10 o più dimensioni. A seguire, la mia cavia *Elsa*, oggetto del mio futuro dottorato in psicologia comportamentale ed al contempo severa insegnante di quella strana lingua che si è rivelata essere il francese. Non c'è Elsa senza Floriano, ma forse qui sono loro che dovrebbero ringraziare me. L'*ingegner Facchinetti* per aver a cuore il mio futuro e per la sua fiducia nella mia carriera di politico. Ringrazio gli sperimentali che hanno allietato la mia permanenza all'EPFL, mi riferisco in particolare al saggio pavese con la camicia, alias il *Manni*, per la confusione che porta nel corridoio dell'ITP senza farne parte e *GiGi*, il personal trainer fissato che mi ha costretto a confutare una filosofia nuova ogni settimana a Zelig.

La natura dicotomica di questo mio dottorato mi consente di ricordare anche la gente che mi segue da Reggio Emilia. I miei nonni, da cui ho imparato tutto. Il *20u* e la Formica, perché sono una sicurezza. *Matte*, *Alle*, *Agu*, *Anto* e tutti gli altri che hanno reso i miei rientri in Italia altrettanto piacevoli. Ringrazio *Martina* per aver condiviso metà di questa avventura. Voglio anche ringraziare – in ordine sparso – *Alessandro*, *Federico*, *Simone*, *Stefano*, *Tim* e tutte le persone che hanno arricchito la mia vita insegnandomi ad apprezzare *la birra* –tra Zelig e SAT– *il cibo* –di qua e di là dalle Alpi– *il Jazz* – tra Montreaux, Cully e Perugia– *la musica* –tra festa di Radio, Paléo, Street Parade, la Ruche, Balelec– *la parte migliore delle persone* –tramite Couchsurfing– e *la fisica* e le sue sfaccettature tra Cargese, l'India, la Galizia, Parigi, Roma, Firenze e l'EPFL.

Grazie di cuore a tutti e in particolare a te, lettore, che hai preso il tempo di leggere una parte o anche solo una frase di questa mia tesi.

Luca
Losanna, 27 Ottobre 2011

ADDRESS
Av. de Tivoli 4. 1007, Lausanne

CONTACT
luca.fontanesi@gmail.com

+41 76 2657990
+39 338 1701922

LUCA FONTANESI

Date and Place of Birth: 5 March 1982. Montecchio Emilia (RE), Italy

EDUCATION

Nov. 2007 – Present	**PhD in Theoretical Physics** Swiss Institute of Technology (EPFL). Lausanne, CH
Nov. 2004 – May 2007	**Master Degree in Physics (Condensed Matter)** University of Pisa. Italy
Oct. 2001 – Sept. 2004	**Bachelor Degree in Physics** University of Parma, Italy
May 2004 – Jun. 2004	Internship at Laue-Langevin Institute. Neutron Source. Grenoble, FR

LANGUAGES

Italian	Mother tongue
English	Fluent. C1 level
French	Fluent. C1 level

COURSES

Teaching Assistant	General Physics at Civil Engineering Statistical Physics 1 Statistical Physics 2 Statistical Physics 3
Examiner	Mathematical Physics Statistical Physics

INTERESTS

Cinema, Photography, Running, Travels.

Oral Presentations

- **June 2011**
  Disordered Systems: From Condensed-Matter Physics to Ultracold Atomic Gases.
  Cargése, France.
  CONTRIBUTED TALK

- **January 2011**
  Research Frontiers in Ultra-Cold Atomic and Molecular Gases. Goa, India.
  CONTRIBUTED TALK

- **July 2010**
  LENS, European Laboratory for Non-Linear Spectroscopy. Florence, Italy.
  INVITED TALK

- **April 2010**
  Nonlinear phenomena in quantum degenerate gases. Ourense, Spain.
  CONTRIBUTED TALK

- **November 2009**
  Université de Paris-Sud. Palaiseau, France.
  INVITED TALK

Publications

- L. FONTANESI, M. WOUTERS AND V. SAVONA, *Fragmentation and the Bose-glass phase transition of the disordered one-dimensional Bose gas*, Phys. Rev. A, **83**, 033626 (2011).

- F. MANNI, K. G. LAGOUDAKIS, B. PIETKA, L. FONTANESI, M. WOUTERS, V. SAVONA, R. ANDRÉ, AND B. DEVEAUD-PLÉDRAN, *Polariton Condensation in a One-Dimensional Disordered Potential*, Phys. Rev. Lett., **106**, 176401 (2011).

- L. FONTANESI, M. WOUTERS AND V. SAVONA, *Mean-field phase diagram of the one-dimensional Bose gas in a disorder potential*, Phys. Rev. A, **81**, 053603 (2010).

- L. FONTANESI, M. WOUTERS AND V. SAVONA, *Superfluid to Bose-Glass Transition in a 1D Weakly Interacting Bose Gas*, Phys. Rev. Lett., **103**, 030403 (2009).

- L. MAZZA, L. FONTANESI AND G. LA ROCCA, *Organic-based microcavities with vibronic progressions: Photoluminescence*, Phys. Rev. B, **80**, 235314 (2009).

- L. FONTANESI, L. MAZZA AND G. LA ROCCA, *Organic-based microcavities with vibronic progressions: Linear spectroscopy*, Phys. Rev. B, **80**, 235313 (2009).